Supported by

An Illustrated Handbook of LNAPL Transport and Fate in the Subsurface

CL:AIRE

ISBN 978-1-905046-24-9 © CL:AIRE 2014

Published by Contaminated Land: Applications in Real Environments (CL:AIRE), 32 Bloomsbury Street, London WC1B 3QJL.

Acknowledgements
Shell Global Solutions (UK) Ltd is gratefully acknowledged for their generous funding of the collation of the underpinning research and synthesis and production of the illustrated handbook. The editor and authors thank staff from Shell Global Solutions (UK) Ltd, Shell Global Solutions US Inc. and the Environment Agency for their technical discussions and formative reviews of the handbook. CL:AIRE would like to thank members of its Technology and Research Group, Phil Morgan, Sirius Geotechnical and Environmental Ltd and Richard Moss, AkzoNobel for their reviews of the document.

Editor
Michael O. Rivett, University of Birmingham, UK

Authors
Derek W. Tomlinson, Geosyntec Consultants (Philadelphia, USA)
Steven F. Thornton, University of Sheffield, UK
Alan O. Thomas, ERM, UK
Stephen A. Leharne, University of Greenwich, UK
Gary P. Wealthall, Geosyntec Consultants (Toronto, Canada)

Steering Board
Sanjay Garg, Shell Global Solutions US Inc.
Alwyn J. Hart, Environment Agency, UK
Jonathan W.N. Smith, Shell Global Solutions (UK) Ltd
Rob Sweeney, CL:AIRE, UK
Peter Zeeb, Geosyntec Consultants (Boston, USA)

Report citation
It is recommended citation to this report is made as follows:
CL:AIRE, 2014. An illustrated handbook of LNAPL transport and fate in the subsurface. CL:AIRE, London. ISBN 978-1-905046-24-9. Download at www.claire.co.uk/LNAPL

Executive Summary

This illustrated handbook presents best-practice guidance for the assessment and remediation of light non-aqueous phase liquids (LNAPLs) in the subsurface. LNAPLs notably include fuels and oils, for example petrol (gasoline), diesel and heating oils, and are amongst the most commonly encountered organic contaminants in the subsurface environment due to their ubiquitous use, accidental release and, perhaps, poor (historical) disposal. Central to this handbook and the management of risks posed is the development of conceptual models of LNAPL behaviour in common hydrogeological systems.

LNAPLs typically comprise a complex mixture of predominantly hydrocarbon organic chemicals with a wide range of physical-chemical and toxicological properties that may influence their environmental fate and risks posed (*Section 2*). Their subsurface transport is complex, being a multi-phase (LNAPL-water-air) flow problem, but nevertheless is often characterised by an accumulation of buoyant hydrophobic LNAPL in the vicinity of the water table interface that has potential to migrate laterally (perhaps seeping to surface water receptors) or redistribute vertically due to natural or human-induced water table fluctuations (*Section 3*). Further risks to groundwater resources and wells may often arise from the wider migration of a dissolved-phase plume that may develop from the subsurface LNAPL source, although these may be mitigated by natural attenuation processes, notably biodegradation (*Section 4.1*). Also, risks to receptors at ground surface, for example building inhabitants, may arise from volatile LNAPL constituents that form subsurface vapour plumes (*Section 4.2*). The above sections underpin the development of conceptual models of LNAPL transport and fate across a comprehensive range of common hydrogeological systems (*Section 5*). This is considered the handbook hub from which local conceptual site models may be developed that fundamentally support both the characterisation and investigation of sites (*Section 6*) and the management and remediation of sites designed to address unacceptable risks posed (*Section 7*).

The handbook provides an illustrated blend of technical detail and real world conceptualisation of the LNAPL problem and appropriate methods to investigate and manage it. The handbook also facilitates access to a wealth of detailed research, guidance and case study literature within the various topics covered. It will be useful to the practitioner and research communities, and also provide a valuable educational resource to others having a less direct interest or specialised knowledge.

Contents

Acronyms

API	American Petroleum Institute
ASTM	American Society for Testing and Materials
BTEX	Benzene, toluene, ethylbenzene and xylenes
CL:AIRE	Contaminated Land: Applications in Real Environments
COPC	Contaminants of potential concern
CPT	Cone penetrometer testing
CSM	Conceptual site model
Defra	Department for Environment, Food and Rural Affairs
DNAPL	Dense non-aqueous phase liquid
EA	Environment Agency
ETBE	Ethyl tertiary-butyl ether
FID	Flame ionisation detection/detector
GC	Gas chromatograph/chromatography
GTL	Gas-to-liquid
ISCO	*In situ* chemical oxidation
ITRC	Interstate Technology and Regulatory Council
LIF	Laser-induced fluorescence
LNAPL	Light non-aqueous phase liquid
MIP	Membrane interface probe
MNA	Monitored natural attenuation
MTBE	Methyl tertiary-butyl ether
NAPL	Non-aqueous phase liquid
NFEC	Naval Facilities Engineering Command
NSZD	Natural source zone depletion
PAH	Polycyclic aromatic hydrocarbons
PID	Photoionisation detection/detector
PITT	Partitioning interwell tracer testing
PRB	Permeable reactive barrier
SPE	Solid phase extraction
SVE	Soil vapour extraction
TAME	Tertiary-amyl methyl ether
TBA	Tert-butyl alcohol
TCEQ	Texas Commission on Environmental Quality
TEX	Toluene, ethylbenzene and xylenes
TPH	Total petroleum hydrocarbons
TPHCWG	Total Petroleum Hydrocarbon Criteria Working Group
TPH-D	Diesel range total petroleum hydrocarbons
TPH-G	Gasoline range total petroleum hydrocarbons
USEPA	United States Environmental Protection Agency
UST	Underground storage tank
VER	Vacuum enhanced recovery
VI	Vapour intrusion
VOC	Volatile organic compound

1. Introduction

This illustrated handbook presents best-practice guidance for the assessment and remediation of light non-aqueous phase liquids (LNAPLs) in the subsurface. The document is anticipated to be of benefit to not only practitioner and supporting research communities, but also serve as an educational resource to those having a more peripheral interest (noting a glossary of key technical terms is provided). It aims to provide a mix of technical detail and practical conceptualisation of the problem that is relevant to real world scenarios. It also serves to provide a convenient interface to a wealth of modern and established research, guidance and case study literature.

LNAPLs are hydrophobic liquid organic chemicals that are immiscible with water and are less dense than water. A LNAPL hence exists as a separate organic liquid phase when in contact with water and is able to 'float' upon that aqueous-phase liquid. They are amongst the most frequently encountered organic contaminants in the subsurface environment. They include a wide range of substances, but the most common types are fuels and oils, such as petrol (gasoline), diesel, heating oils and jet fuel (kerosene). LNAPL releases to ground can result from a range of release mechanisms. As illustrated in Fig. 1.1, these include accidental leakage from above ground and underground storage tanks (USTs) and associated pipelines as well as accidental release during handling, storage or transfer at fuel manufacturing facilities, refineries, bulk-product terminals, petrol filling stations, airports, military bases, and from smaller scale storage at domestic properties, industrial facilities and farms (CL:AIRE, 2002; Molins *et al*., 2010; USEPA, 2009; USGS, 1998). Whilst the vast majority of LNAPL releases originate from (near) ground surface, occasionally LNAPL sources may occur at depth below the water table and pose risks of buoyant LNAPL rise into an overlying groundwater resource. This may include natural LNAPL seeps from deep strata, but also risks of anthropogenic origin. For example, risks posed by potential release of LNAPL from degraded Intermediate Level (nuclear) Waste stored in an engineered geological disposal facility at depth where LNAPL fate in the near-field hydrogeological environment requires consideration (Benbow *et al*., 2014; Wealthall, 2002).

Figure 1.1. Example of LNAPL releases showing a leaky underground storage tank (left) and LNAPL impact to a surface-water receptor (right) (Courtesy of N. Clarke and M.O. Rivett respectively).

Unlike dense non-aqueous phase liquids (DNAPLs) that sink in water, LNAPLs are less dense than water and when released to the subsurface they migrate through partially (water) saturated strata until they reach the water table, which impedes (but not completely prevents) their migration deeper due to both increasing water content and associated buoyancy forces arising from the LNAPL-water fluid density contrast. Lateral spread of LNAPL near the water table is determined principally by the subsurface geology, size of the LNAPL release, as well as physical-chemical properties of the LNAPL.

Mobility of the LNAPL is influenced by the size of the release and the fluid's viscosity. Low viscosity LNAPL releases (such as petrol) may stabilise within weeks to months, whereas high viscosity LNAPLs (such as heating oil or crude oil) flow more slowly for longer periods and may require months to years for the LNAPL to gradually stabilise. The LNAPL distribution that accumulates in the subsurface is typically termed the 'source zone' of contamination. It comprises both immobile residual LNAPL, which is trapped in pore space by capillary forces, and potentially mobile LNAPL which exists as a continuous liquid across interconnected pores and is able to migrate when subjected to a sufficient driving head. The latter often manifests as a layer of LNAPL (e.g., oil or fuel) distributed across the water table-capillary fringe interface due to the LNAPL buoyant nature. Some penetration of LNAPL below that interface is, however, possible (Fig. 1.2).

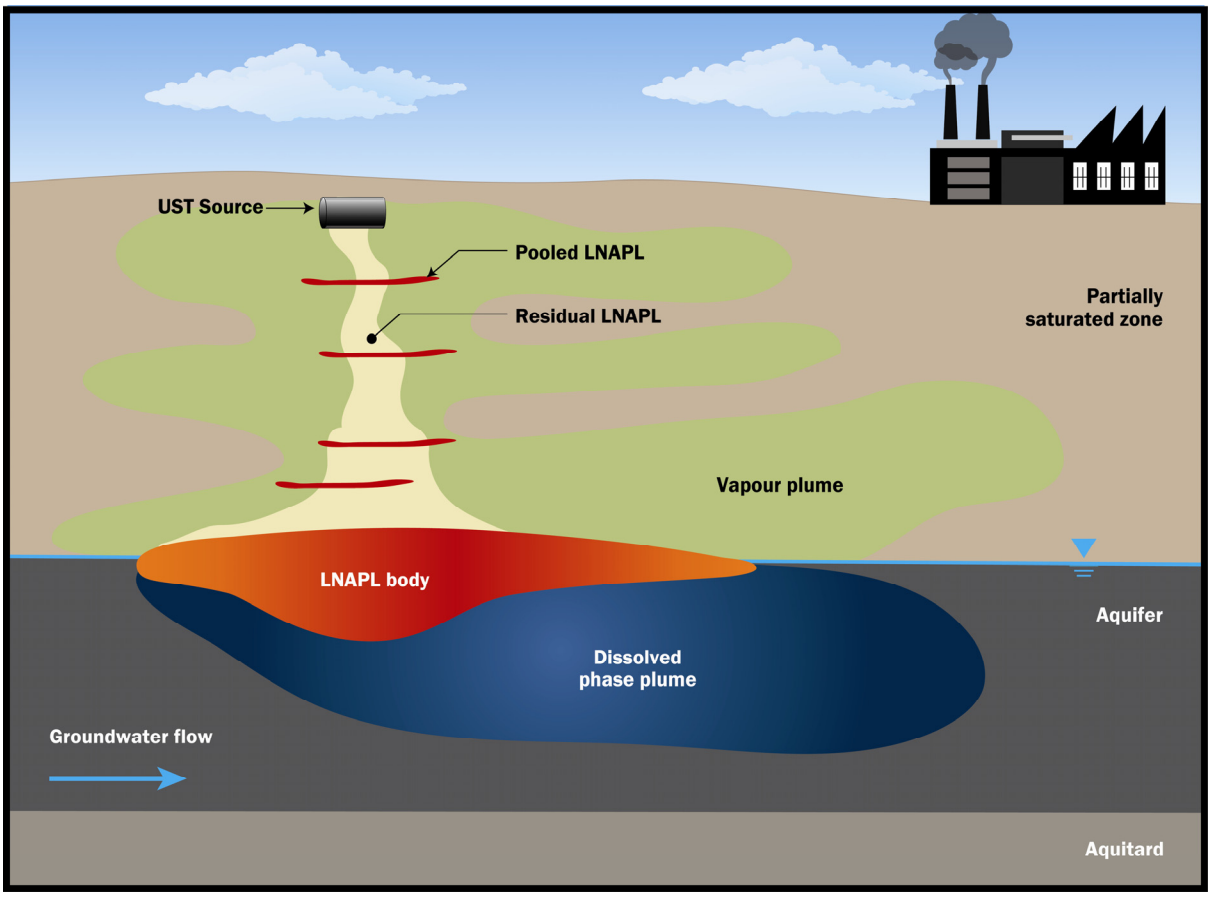

Figure 1.2. Illustrative conceptual model of a LNAPL release to the subsurface.

The physical-chemical properties of individual compounds within the contaminant mixture control rates of partitioning (mass transfer) from the LNAPL to the gas and aqueous phases. This transfer leads to the development of vapour-phase plumes in the unsaturated (vadose, or more accurately partially saturated) zone above the water table and shallow dissolved-phase plumes in groundwater laterally flowing beneath the water table. These processes are conceptualised in Fig. 1.2.

This document aims to provide an accessible overview of LNAPL behaviour in soil and groundwater, including a series of illustrative conceptual models of LNAPL in different hydrogeological environments, to establish:

- better conceptual understanding of LNAPL transport and fate in the subsurface, on which risk-management strategies can be developed;
- more effective site characterisation and robust risk prediction;
- risk-based management of LNAPL releases that is more sustainable; and
- improved understanding of where and/or when specific LNAPL remedial techniques are likely to be effective in performance and cost.

2. Types of LNAPL and their properties

2.1. Introduction

The term LNAPL describes a class of liquid organic chemicals that are characterised by:

- immiscibility with water (hydrophobicity);
- densities which are less than that of water; and
- complex chemical compositions in most cases.

These defining characteristics have a direct impact upon their behaviour in the geological subsurface when released at sites. The most frequently encountered LNAPLs are complex mixtures of organic compounds, such as fuels and oils. Such LNAPLs are compositionally complex containing aliphatic and aromatic hydrocarbons in varying ratios. They may be further formulated with a range of additives that enhance and extend their performance as fuels or lubricants. This section provides details of the types and uses of commonly encountered LNAPLs, elaborating on the key physical-chemical properties - such as density, viscosity, interfacial tension (against water), composition, aqueous solubility, vapour pressure and wetting behaviour - that influence their environmental fate. The variability in properties of some typical LNAPLs is illustrated in Table 2.1. The diversity in LNAPL properties occurring across the wide range of fuels and oils leads to contrasting fate and transport in the subsurface. It is hence important to obtain available literature property data in making an assessment; such data may be found, for example, in Mercer and Cohen (1990), the API Interactive LNAPL Guide (API, 2006a), and the API Parameters Database (API, 2006b).

Table 2.1. Typical fuel LNAPLs: uses and physical properties (at 15°C) (NFEC, 2010).

Fuel type	Fuel use	Density (g/cm^3)	Viscosity (cP)	Boiling point range (°C)	Interfacial tension (mN/m)
Petrol	Road vehicle fuel	0.67-0.8	0.62	38-204	52
AVGAS	Aviation spirit for piston engines	0.71	2.3	33-170	37
Jet A-1	Civil aviation jet fuel	0.804	2-3	145-300	-
JP-4	Military jet fuel	0.75	1.0	60-270	50
JP-5	Military jet fuel	0.82	2.0	176	-
JP-8	Military jet fuel	0.78-0.84	2.0	205-300	-
Kerosene	Paraffin - used for heating and lighting	0.81	2.3	151-301	47-49
Diesel	Transport fuel	0.87	2.7	150-370	50
Bunker C	Fuel oil used for ship propulsion	0.9-1.1	45,030	>177	40
Tar / bitumen	Tarmac, road surfacing	1.15	-	-	-

Water is a polar compound that is in marked contrast with typical hydrocarbon components encountered in non-aqueous phase liquids (NAPLs) that are non-polar. This difference in polarity characteristically results in low hydrocarbon solubilities in water. Generally aqueous-phase solubility decreases with increasing molecular mass (and size) of the hydrocarbon molecule. Aromatic compounds are more soluble than the less polar alkanes or alicyclic hydrocarbons of comparable molecular mass. Indeed the monoaromatic (single ring) hydrocarbons, benzene, toluene, ethylbenzene and xylene (BTEX), which are commonly encountered fuel constituents, are some of the more water soluble hydrocarbons. However, the most water-soluble components frequently encountered in LNAPL fuel mixtures tend to be ether oxygenates such as methyl tertiary-butyl ether (MTBE) (of solubility 50,000 mg/L) or alcohols, such as ethanol. The latter is completely miscible with water and partitions from the LNAPL to the water phase rapidly.

There are important consequences of LNAPL fuels comprising a mixture of compounds, a so-called 'multi-component LNAPL'. As outlined in Section 4.1, the 'effective solubility' of the aromatic components from multi-component LNAPL fuels is much reduced compared to their pure-phase solubility (the maximum dissolved-phase concentration obtained in water in contact with a single component LNAPL). This is illustrated in Table 2.2 that compares pure-phase (single component LNAPL) solubility concentrations with effective solubility concentrations predicted (Section 4.1) for a 'typical European petrol' composition that comprises around 1% benzene, 10% toluene, 2% ethylbenzene and 10% xylenes. Although the pure-phase solubility of benzene alone is 1790 mg/L, the effective solubility from this fuel will be around 1% of that value, around 18 mg/L, which would represent the maximum groundwater concentration to be expected adjacent to a release of such a LNAPL fuel. Even though the effective solubility of benzene (and other aromatics) from LNAPL fuels are much reduced compared to its pure-phase solubility, concentrations will still be orders of magnitude greater than concentrations permitted in drinking water (0.005 mg/L per the United States Environmental Protection Agency (USEPA) or 0.001 mg/L per the EU Drinking Water Directive). Although less common, releases of single component LNAPLs may still be encountered. For example, benzene is an intermediate for manufacture of other aromatic compounds. Toluene and hexane are common industrial and laboratory solvents.

Table 2.2. Comparison of individual pure-phase solubilities of BTEX compounds with effective solubility value estimated for a 'typical European petrol' fuel composition assumed to comprise 1% benzene (B), 10% toluene (T), 2% ethylbenzene (E) and 10% xylenes (X) (percent mole fractions within the LNAPL fuel).

LNAPL	Benzene (mg/L)	Toluene (mg/L)	Ethylbenzene (mg/L)	Xylenes (mg/L)
Pure-phase solubility (100% Single component)	1790	470	152	175
'Typical European petrol' 1% B, 10% T, 2% E, 10% X	18	47	3	18

2.2. Hydrocarbon fuels and oils

Crude oil is generally used as the feedstock for LNAPL product formulation though a range of hydrocarbon products is also obtained from vegetable oils, animal fats, liquefied gases, and tars and bitumen. Historically, coal sources may be the hydrocarbon feedstock and lead to chemical industry development associated with colliery-coking works complexes. Crude oil is a mixture of linear, branched, cyclic and aromatic hydrocarbons as well as asphaltenes and resins that are high molecular mass components. In refineries, crude oil is distilled in order to separate the components into fractions characterised by having a common boiling point range (Table 2.3). These fractions often undergo further treatment. Petrol (gasoline) has a comparatively low boiling point range. Even so it is still compositionally complex. Other important petroleum fractions include kerosene (jet fuel), diesel and paraffin (which is used for heating). Diesel has a higher boiling point range than petrol, and contains larger molecules and a higher percentage of alkanes. Diesel is normally derived from crude oil, but increasingly biodiesel is available which includes components derived from vegetable oils, and diesel can also be synthesised from gas. Gas-to-liquid (GTL) fuels have very low aromatic content. Hence even refined petroleum fuel and oil products may contain a multitude of compounds as illustrated by gas chromatograph (GC) traces that exhibit characteristic profiles (fingerprints) for the various fuel/oil types allowing their identification in environmental samples (unless significantly degraded) (Fig. 2.1).

Table 2.3. Hydrocarbon fractions obtained from the distillation of crude oil (TPH is Total Petroleum Hydrocarbons). The boiling point range corresponds to the fractional distillation ranges at the refinery (Table 2.1 data apply to final fuel oil products that are likely to be blends and hence boiling point ranges may not necessarily correspond between tables).

Fraction name	Typical number of carbon atoms	Boiling point range (°C)	Uses (examples)
Refinery Gas	3-4	< 30	Bottled Gas (propane or butane)
TPH-G	6-10	-	Gasoline range organics
Petrol	6-10	100-150	Fuel for spark-ignition engines (e.g., cars, motorbikes, vans)
TPH-D	12-28	-	Diesel range organics
Naphtha	6-11	70-200	Solvents and used in petrol
Kerosene (paraffin)	10-12	150-200	Fuel for jet engines and stoves
Diesel Oil	12-18	200-300	Fuel for compression ignition engines (e.g., road vehicles, boats and trains)
Lubricating Oil	18-25	300-400	Lubricant for machinery
Fuel Oil	20-27	350-450	Fuel for ships and heating
Greases and Wax	25-30	400-500	Lubricants and candles.
Bitumen	>35	>500	Road surfacing

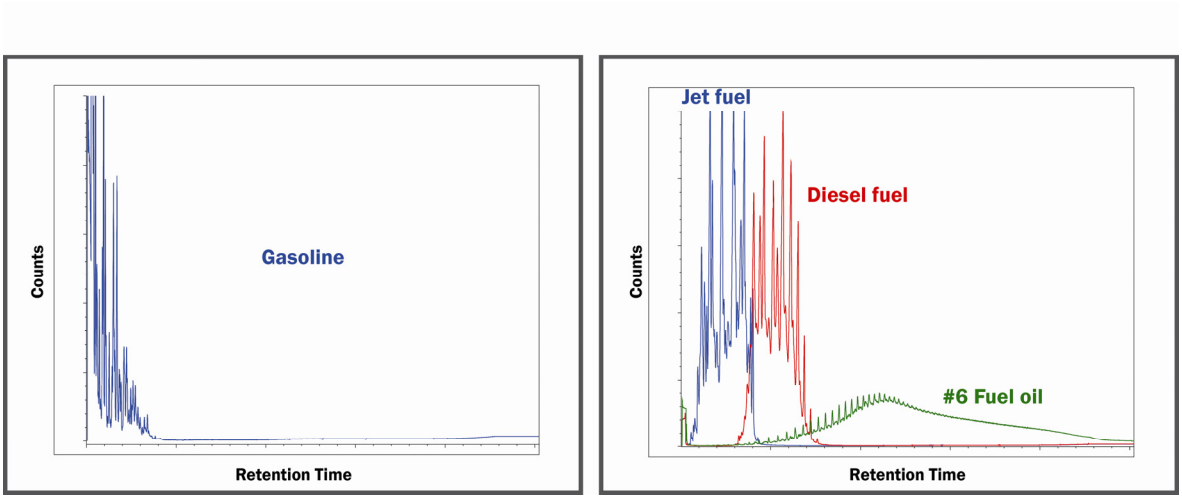

Figure 2.1. Exemplar chromatograms obtained for a number of hydrocarbon fuels. The reader's attention is drawn to (i) the multi-component complexity of the fuel samples and (ii) the boiling point range of the samples which is related to their retention times.

2.3. Physical properties and molecular characteristics

The physical properties of LNAPL components are influenced by molecular size. For example, solubility decreases and viscosity increases with molecular mass. For aliphatic hydrocarbons this viscosity increase is not that large; however, in biodiesels the viscosity range of fatty acid derived compounds is often greater than that of the various hydrocarbons that comprise petroleum-derived diesel.

Surface tension is determined by molecular size and molecular interactions. Generally as the size increases so does the degree of molecular attraction, for example heptane (C_7H_{16}) has a surface tension of 20.5 mN/m compared to 28.1 mN/m for hexadecane ($C_{16}H_{34}$). Both surface and interfacial tension arise from unfavourable molecular interactions at the contact interface between two immiscible fluids. Tensions involving water as one of the immiscible fluids are often very high, due to the high polarity of water and low polarity of the organic liquid. Aliphatic hydrocarbons in contact with water have interfacial tensions of the order of 50 mN/m, whereas slightly more polar aromatic hydrocarbons, such as benzene have interfacial tensions of around 35 mN/m.

Wetting describes the ability of a liquid to spread over a solid (e.g., mineral) surface in competition with another immiscible liquid, which exerts a key control upon LNAPL behaviour. The contact angle is used to characterise wetting behaviour and is the angle between a line drawn tangential to the NAPL-water interface starting from the three phase contact line and solid surface (Fig. 2.2). By convention the contact angle is measured through the aqueous phase. Contact angles between 0 and 70° indicate water wetting conditions, 70 to 110° neutral wetting, and 110 to 180° oil wetting. For many LNAPL spills under normal geological conditions, water is wetting with respect to LNAPL that, in turn, is wetting relative to air. Research has shown that repeated LNAPL contact with soils or aquifer minerals can result in the LNAPL becoming less non-wetting with time.

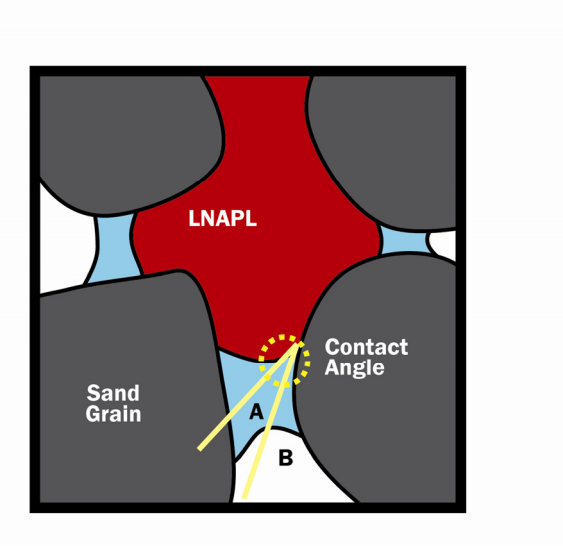

Figure 2.2. Schematic showing non-wetting LNAPL and its contact angle with mineral surfaces in the presence of water that preferentially wets the geological solid surface ('A' is located in the water phase and 'B' in the air phase at the pore throat of interest).

2.4. Capillary forces

LNAPLs are encountered in porous media soils/rocks as droplets held in pores and as contiguous bodies of liquid 'ganglia' joined through two or more pores. They are held in the pores by capillary forces that arise from the presence of a pressure drop across the curved interface between two immiscible fluids. In Fig. 2.2, LNAPL is held in the pore by the surrounding water. The curvature of the interface at A indicates that the pressure in the LNAPL (concave) side of the interface (P_L) is greater than the pressure immediately adjacent in the water phase (P_W). The pressure drop is defined as the capillary pressure with the threshold capillary pressure (or entry pressure) for a non-wetting fluid (typically LNAPL) to enter a wetting fluid (typically water) given by:

$$P_L - P_W = \frac{2\,\sigma_{LW}\cos(\theta)}{r} \qquad \text{Eq. 2.1}$$

The entry pressure is hence directly proportional to the interfacial tension (σ_{LW}) between the LNAPL and water and cosine of the contact angle (θ) and inversely proportional to the pore throat radius (r). Fig. 2.2 also shows the expected curvature of trapped non-wetting NAPL droplets in a water-saturated porous medium. The effect of these capillary forces upon fluid distribution is shown in Fig 2.3. Water is held in the form of lenses at grain contacts and in small pores. Air and LNAPL fluids are held in larger pore spaces entrapped by water lenses in very narrow pore throats unable to overcome high entry pressures.

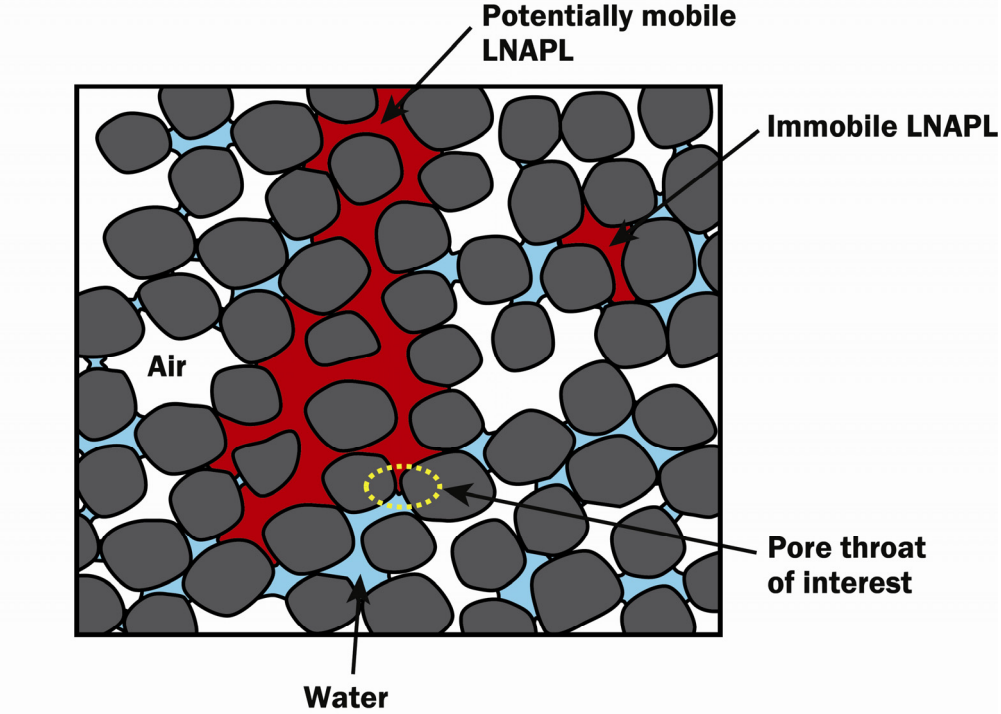

Figure 2.3. Fluid distribution in the partially saturated zone. The large LNAPL body is prevented from entering the identified pore throat by the large entry pressure due to the pore throat's small aperture.

2.5. Capillary forces influenced by formulated components

Petrol, although hydrocarbon based, may be formulated with a range of additional organic compounds. Ether oxygenates are often added to unleaded petrol to improve fuel octane rating and combustion efficiency and reduce atmospheric emissions. Typical ether oxygenates include MTBE, ethyl tertiary-butyl ether (ETBE) and tertiary-amyl methyl ether (TAME). Additives (<1% of the fuel composition) include corrosion inhibitors, metal deactivators, anti-foaming agents, and surfactants. The adsorption of these organic compounds at the LNAPL-water interface results in reductions in the interfacial tension leading to a reduction in the entry pressure. Moreover adsorption of surfactants – this includes the corrosion inhibitors – at soil surfaces can alter the wetting properties of the solid surfaces usually by increasing the contact angle, and as a consequence again reducing the entry pressure. Such changes may potentially facilitate migration.

Petrol may be blended with ethanol, or higher alcohols such as propanol and butanol. E85 fuel comprises 85% ethanol blended with 15% petrol. Greater fuel alcohol contents lead to reduced hydrophobicity of the fuel and increased alcohol partitioning to the aqueous phase. This may cause reductions in the surface tension of water, drainage of capillary-held water, reductions in height of the capillary fringe leading to increased mobility of the LNAPL body. Enhanced vapour intrusion to buildings at ground surface may occur due to the reductions in capillarity and increased potential for methanogenesis (methane production). Alcohols in water may also act as a cosolvent for hydrocarbons and hence E85 releases may lead to enhanced transfer of LNAPL components to the mobile groundwater. Rapid aerobic ethanol biodegradation may result in oxygen depletion and rapid establishment of anaerobic conditions. Biodegradation rates of petroleum hydrocarbons are typically decreased under anaerobic conditions.

2.6. Spreading coefficient

An important consideration in the partially saturated zone where LNAPL comes into simultaneous contact with water and air is the spreading coefficient (*S*):

$$S = \sigma_{WA} - (\sigma_{LW} + \sigma_{LA}) \qquad \text{Eq. 2.2}$$

where σ_{WA} is the surface tension of water, σ_{LW} is the interfacial tension between the LNAPL and water and σ_{LA} is the surface tension of the LNAPL. The spreading coefficient represents the spreading of one liquid over a unit area of another and is equal to the surface tension of the stationary liquid less the sum of the surface tension of the spreading liquid and the interfacial tension between the liquids. When *S* is positive, LNAPL spreads over water films surrounding soils grains and water lenses encountered at soil grain contact areas (Keller and Chen, 2003). This is most prevalent in the propagation of sheens and less so for the LNAPL body as a whole. This will tend to increase the amount of LNAPL mass held at soil grains in the partially saturated zone. The presence of additives that reduce σ_{LW} and σ_{LA} will lead to an increase in spreading pressure and may increase, further, the mass held by grains. Unfortunately, additive transfer to the water phase, which will lead to a reduction in σ_{WA} will consequently give rise to a reduction in the spreading pressure. Indeed the spreading pressure may become negative leading to LNAPL drainage. The degree of lateral LNAPL migration is greater for lower density and lower viscosity LNAPLs such as petrol and diesel fuels, and less for higher density and higher viscosity LNAPLs such as fuel oil and coal tar. Similarly, the amount of spread of the LNAPL is greater for LNAPLs with lower interfacial tension ratios of LNAPL-air and LNAPL-water such as petrol, compared to higher interfacial tensions within higher distillate oils and crude oil.

2.7. Dynamic LNAPL composition and properties

LNAPL composition may be dynamic with time due to varying component losses from vapourisation and dissolution (solubilisation). Evolving LNAPL composition may also induce change in physical properties such as LNAPL viscosity and density leading to perhaps dynamically variable transport properties and LNAPL mobility potential. This is particularly important when it is considered that such transient composition, dynamic property LNAPLs are typically present in greatest volume close to the water table that intrinsically provides a dynamic water-air environment.

3. LNAPL transport and distribution

3.1. Fundamental concepts

The mobility of the various fluids present (water, LNAPL and perhaps air) in a porous/fractured geological medium is governed in part by their relative fluid saturations of the pore space (saturation being the percentage of pore space occupied by a fluid). An invading LNAPL needs to displace an equivalent volume of the resident fluids (air and or water) and requires a specific threshold capillary pressure (or entry pressure) to do so (Eq. 2.1). In a water-saturated medium, invading LNAPL will lead to water drainage from the pores until localised films of the wetting water fluid remain that cannot be displaced; this is the residual (or irreducible) water content. The reverse, imbibition, process may occur for instance during water table fluctuation whereby water re-enters the medium gradually displacing the LNAPL. Again, not all of the LNAPL drains and a residual saturation of LNAPL remains held in the pores due to retentive capillary forces. The capillary pressure curves for the above cycle (Fig. 3.1a) illustrate that primary drainage and primary imbibition curves follow different pathways. A further cycle of water drainage would likewise produce a secondary drainage curve non-coincident with the primary due to the differing starting position, i.e., the process is hysteretic. The maximum capillary-held residual LNAPL saturation hence varies due to both the hysteresis process and the amount of LNAPL initially released into the porous domain (Fig. 3.1b). Saturations of LNAPL above the capillary-held residual threshold are considered mobile and may continue to migrate, or are considered potentially recoverable by remediation (Section 7).

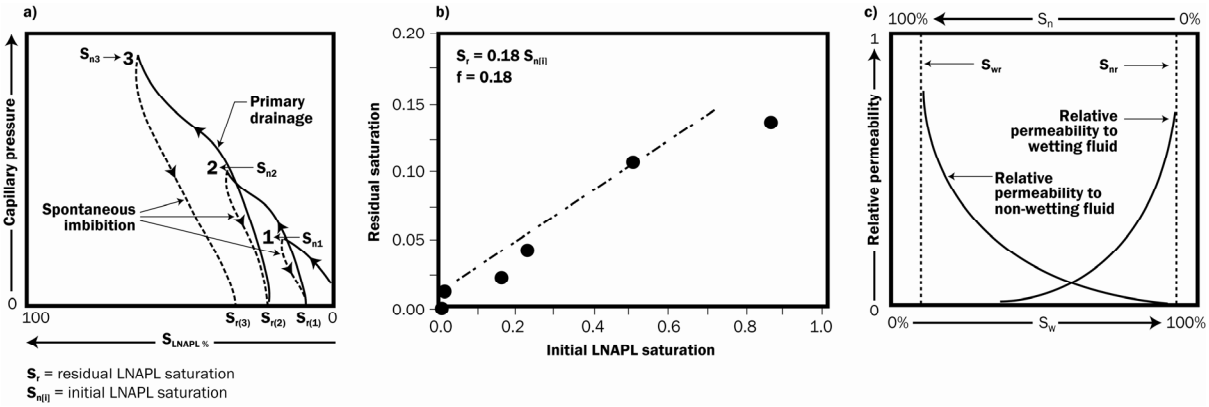

Figure 3.1. (a) Schematic depicting three hysteresis loops with progressively higher maximum pressures of 1, 2, and 3 (shown as initial LNAPL saturation, $S_{n[i]}$) and the corresponding residual saturations ($S_{r[i]}$). (b) Residual saturation and initial saturation example of Borden sand, CFB Borden, Ontario, Canada. The correlation was that the residual saturation (S_r) was approximately 18% of the initial saturation ($S_{n[i]}$) or a slope (f) of 0.18 (Kueper *et al.*, 1993). (c) Typical relationship between relative permeability and fluid saturation for a two-phase system under drainage, shown is the water saturation (S_w), residual water saturation (S_{wr}), LNAPL saturation (S_n) and residual LNAPL saturation (S_{nr}).

The mobility of a specific fluid, say LNAPL, is dependent upon its saturation of the pore space relative to the other fluids, water and/or air present. If a specific fluid is at or below its residual saturation, that fluid is unable to move. The fluid needs to exceed the lower

threshold of residual saturation for it to form a contiguous phase that is mobile, overcoming retentive capillary forces. As the saturation of that specific fluid increases, the (so-called) relative permeability of the rock with respect to that fluid also (non-linearly) increases (Fig. 3.1c). A number of relationships have been developed to quantitatively relate relative fluid permeability to relative fluid saturation, for example the Brooks-Corey/Burdine and van Genuchten/Mualem relationships. The concepts briefly outlined above and in Fig. 3.1 provide the fundamental cornerstone for understanding LNAPL migration in porous or fractured media (Lenhard and Parker, 1988; Mercer and Cohen, 1990). Appendix 1 provides several illustrative calculations that may be used to evaluate LNAPL transport.

3.2. LNAPL migration in porous media

LNAPL migration immediately following release typically entails vertical transport under the influence of gravity, accompanied by lateral spreading due to geologic heterogeneity (Fig. 1.2) (Mercer and Cohen, 1990). If only a small amount of LNAPL is released, the migration will cease within the partially saturated zone as mass is immobilised within soil pores due to retentive capillary forces. For larger releases with sufficient volume to overcome the residual soil retention capacity, the LNAPL will continue to migrate downwards toward the underlying water table.

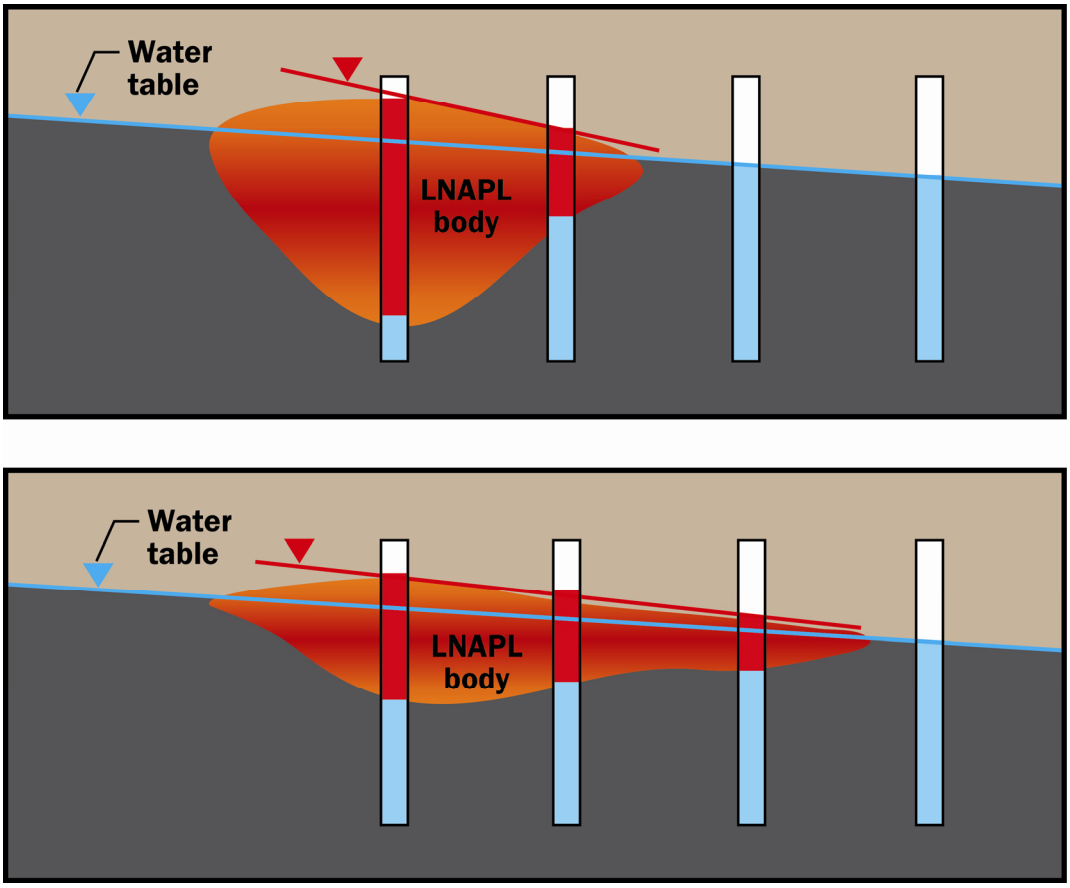

Figure 3.2. Evolution of a LNAPL spill with time showing downward migration through the unsaturated zone, penetration below the water table, buoyancy driven rebound upwards, and lateral movement under a LNAPL head gradient. Eventually the LNAPL footprint may stabilise (as shown later in Fig. 6.2).

Once in contact with the saturated zone, the vertical migration of the LNAPL continues until buoyancy and increasing water content (and thus increased capillary pressure (Eq. 2.1), impede vertical migration. LNAPL begins to spread laterally at the capillary fringe unless sufficient LNAPL elevation head (potential energy) exists for it to displace water and penetrate below the water table (Fig. 1.2). In such a case, vertical LNAPL penetration will continue until the pressure head is balanced by the upwards forces of buoyancy and capillary pressure, which are together referred to as either LNAPL pore entry pressure or water displacement pressure (Eq. 2.1; Mercer and Cohen, 1990). The resulting LNAPL body will then continue to migrate laterally following the water table down hydraulic gradient and radially due to LNAPL mounding above the water table (creating a LNAPL head gradient) in response to the resisting forces (Fig. 3.2).

LNAPL passage leaves behind a trail of residual LNAPL in the form of disconnected ganglia and droplets (Fig. 3.3). Residual, immobile, saturations of LNAPL form due to hydrodynamic instabilities at the pore scale and represent the maximum amount of LNAPL that can be held in place by capillary forces that arise from tensional states at LNAPL-water and LNAPL-air interfaces. Residual saturation values depend upon the geological media properties, LNAPL type and history of LNAPL exposure exhibiting hysteretic behaviour (Fig. 3.1). As shown in Fig. 3.1b, the residual saturation varies with the initial saturation, and also varies with the type of soil in which the LNAPL release occurred. Field investigations often show saturations below residual saturation due to removal of some of the original capillary-held LNAPL by natural source zone depletion (NSZD) mechanisms of volatilisation and dissolution, particularly at older sites (Section 7.5.6). Field measurements significantly above anticipated residual saturation values are indicative of mobile LNAPL presence, which has the potential to migrate.

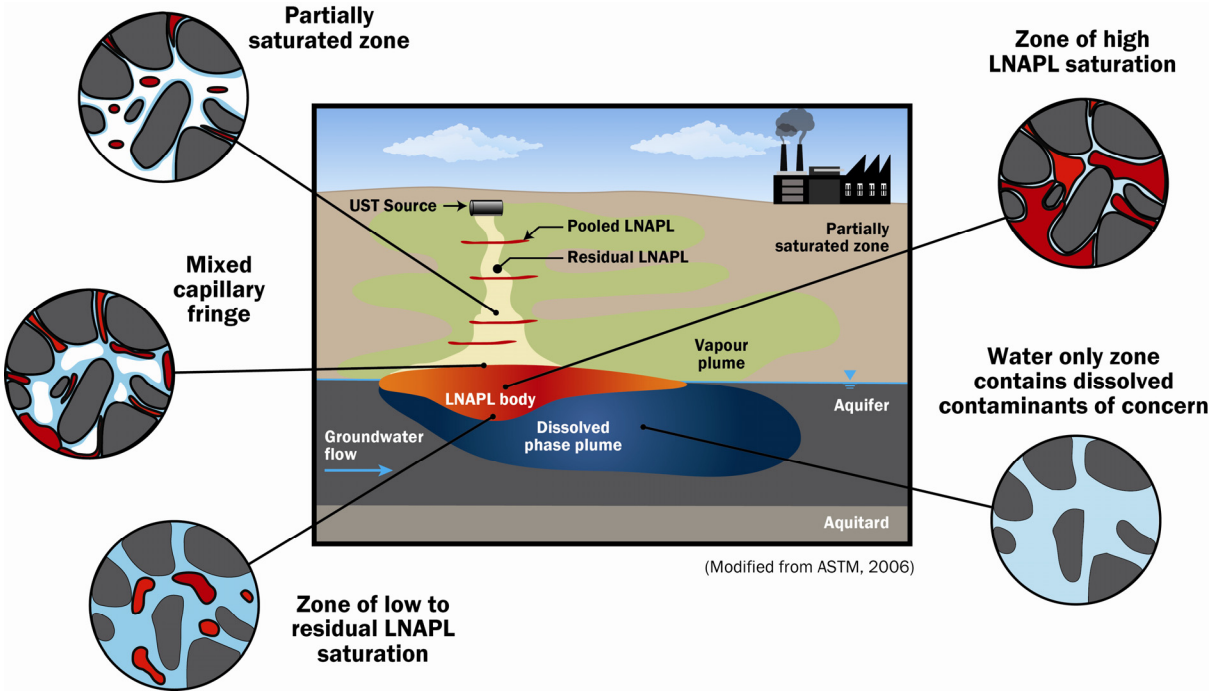

Figure 3.3. Variation in multi-phase system type observed through a typical LNAPL body profile. Three-phase systems exist within the partially saturated zone and upper portions of the capillary fringe, with two-phase systems within the lower portions of the capillary fringe and saturated zone.

Source zone development is significantly influenced by lateral LNAPL migration at the water table where LNAPL can more easily push the water from the formation into the capillary fringe. LNAPL will mound in response to resistance from buoyancy and pore entry pressures. Lateral migration will occur in response to the gravitational forces for this mounded LNAPL enhancing the gradient laterally; the resistive forces laterally are lower than those for continued vertical migration. The lateral migration and growth of the LNAPL body will continue until the driving force from the release dissipates or is balanced by the formation capillary pressures and thus LNAPL pore entry pressure or water displacement pressure at the leading edges. At the leading edges, LNAPL reaches residual saturation, becomes discontinuous and is immobilised by capillary forces under ambient groundwater flow conditions leading to dispersed LNAPL ganglia (Fig. 3.3). The LNAPL source zone is only quasi-stable. Dissolution and volatilisation cause gradual NSZD (Section 4.3) accelerated by local dissolved-phase plume biodegradation. Local dynamic redistribution of the LNAPL body will also occur due to water table fluctuations, or even LNAPL seepage to adjoining river, wetland or coastline receptors.

3.3. Influences on LNAPL distribution

Subsurface variations in LNAPL distribution depend upon a combination of wettability (fluid pressures of each phase) and capillary forces (i.e., pore size distribution) through the process of imbibition (Section 3.1). LNAPL movement is resisted by capillary forces (the LNAPL pore entry pressure or water displacement pressure, with smaller pore throats leading to greater capillary forces (Eq. 2.1)). Water preferentially favours smaller pores and LNAPL and air, larger pores. Since soils (geological solids) are usually water wet, LNAPL entry requires sufficient driving force to exceed the capillary forces of water within the smaller pore throats. Already large capillary forces in fine-grained clays or silts are further increased by wetting water being pushed into the finer pores by the advancing non-wetting LNAPL. LNAPL hence exhibits a tortuous path preferentially following the path of least resistance resulting in an irregular, heterogeneous distribution of disconnected ganglia following drainage of the LNAPL from pores.

LNAPL type and release mode may influence LNAPL distribution. For a catastrophic release such as a tank rupture, LNAPL elevation heads will initially be large and gradually decline. Whereas, for an on-going leaking pipeline, there may be a constant elevation head to the resulting LNAPL body. For large catastrophic releases of LNAPL, the LNAPL elevation head dissipates quickly, resulting in less penetration below the water table with lateral spread driven by the gradient difference which will dissipate and become self-limiting (Fig. 3.2). A longer term release with a constant LNAPL elevation head will continue to overcome the resistance of buoyancy and capillary pressure at the water table, and drive the LNAPL deeper below the water table with less lateral spread for a similar volume of released LNAPL.

LNAPL viscosity also affects timeframes for its stability. For a limited volume release, a LNAPL of low viscosity such as petrol will travel downward rapidly and reach hydrostatic equilibrium typically in the range of days to months. LNAPL viscosity increase leads to slower LNAPL migration and increased timeframes for that LNAPL to reach hydrostatic equilibrium. Highly viscous LNAPLs such as heavy crude oil, fuel oils and bunker oils may move very slowly through the subsurface and take years to reach equilibrium (Oostrom *et*

al., 2006). The greater the density difference between LNAPL and water, the stronger the buoyancy forces and less vertical penetration of the LNAPL and greater lateral spread.

3.4. Shark fins rather than pancakes

Early understanding of the LNAPL migration in porous media conceptualised the LNAPL body as a continuous 'pancake' layer floating on the water table. This conceptualisation incorrectly assumed LNAPL migration to the water table and lateral spread along the capillary fringe forming a continuous layer of complete saturation of the pore space by LNAPL. The LNAPL body was assumed to float on the water table as a separate continuous layer, and correlated directly to the thickness observed in monitoring wells (or some fraction of this observed LNAPL thickness in wells with several theoretical and semi-empirical relations developed relating this difference). This earlier understanding failed to fully recognise the controls of capillary forces and could greatly over-predict both the amount of LNAPL within the subsurface (particularly in fine-grained strata (Huntley and Beckett, 2002)), as well as the amount of potentially recoverable LNAPL.

A closer approximation of the LNAPL saturation distribution is afforded from considering the capillary pressures of the various liquid phases and the development of functions that relate fluid contents of the porous media to capillary pressures (extending concepts in Fig. 3.1; Farr *et al*., 1990; Lenhard and Parker, 1990a,b). The LNAPL saturation profile at the water table interface is predicted to assume the shape of a shark fin within a homogeneous isotropic unconfined aquifer under equilibrium conditions when capillary pressure considerations are invoked (Fig. 3.4).

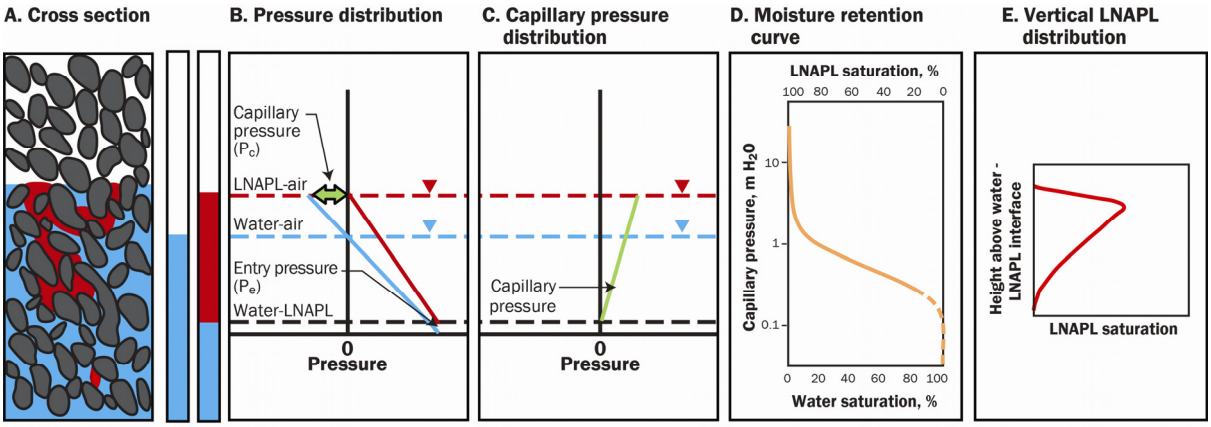

Figure 3.4. Idealised vertical equilibrium distribution of LNAPL saturation for a homogeneous unconfined aquifer: a) a simple homogeneous LNAPL distribution with two monitoring wells, one with no LNAPL present (on left) and one with LNAPL present; b) the pressure distribution of the two phases of water and LNAPL (note that LNAPL is more buoyant and thus has less lateral pressure and a higher gauge pressure (pressure relative to the local atmospheric or ambient pressure)); c) the difference between the LNAPL and water pressures is the capillary pressure; d) the moisture retention curve is the saturation of water and LNAPL through the capillary fringe. The addition of the capillary pressure with the saturation distribution results in: e) the idealised 'shark fin' distribution of LNAPL saturation (ITRC, 2009a).

With increasingly complex conditions, LNAPL saturations will depart from the rather idealised shark fin description and may become highly variable with depth as LNAPL distributions are influenced by both soil heterogeneity and water table variability over time (Fig 3.5; Beckett and Lundegard, 1997). Fig. 3.5 illustrates that within a heterogeneous formation, the soil properties will affect the level of (residual) saturation and cause variability within the LNAPL profile that may or may not retain characteristics of the shark fin ideal (Huntley *et al.*, 1994a,b).

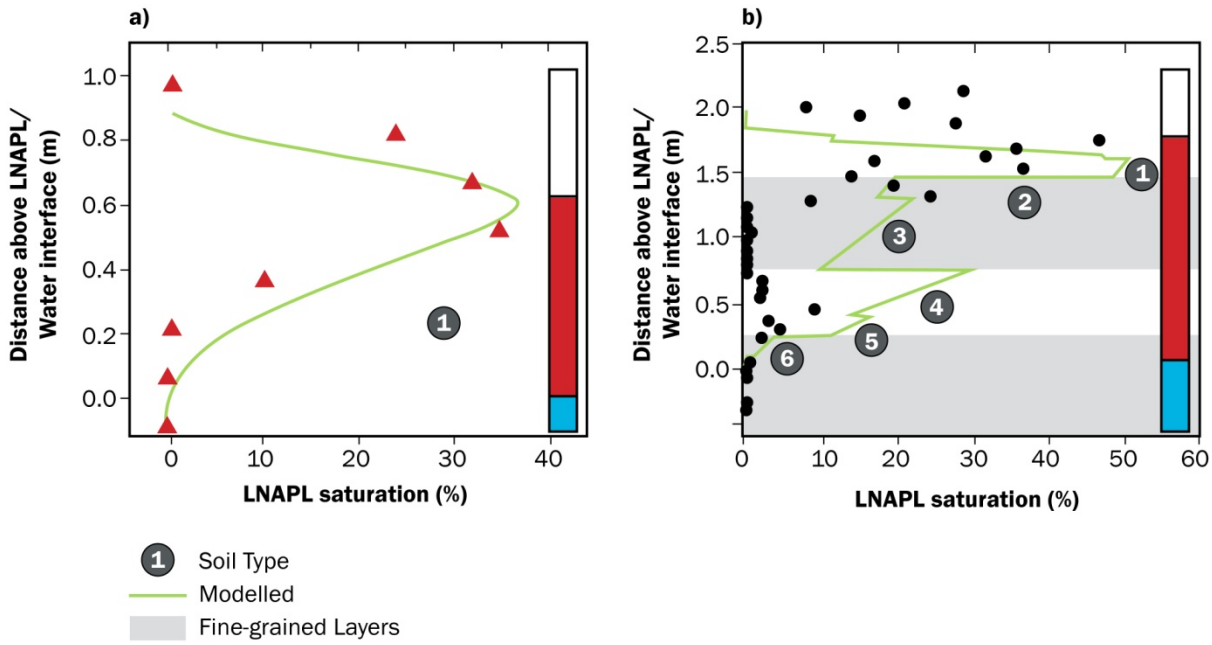

Figure 3.5. LNAPL saturation near the water table showing observed (symbols) LNAPL saturation compared to vertical equilibrium model simulation predictions (lines). The observed in-well LNAPL thickness is shown for: a) homogeneous (Beckett and Lundegard, 1997); b) a heterogeneous case with finer grained layers (2, 3 and 6) and coarser grained layers (1, 4 and 5) (Huntley *et al.*, 1994a,b).

3.5. Water table fluctuations and LNAPL redistribution

Water table fluctuations due to seasonality or abstraction may influence the occurrence of LNAPL in the aquifer and wells as conceptualised in Fig. 3.6. (ITRC, 2009a; Kemblowski and Chiang, 1990). Typical annual water table fluctuations vary from 1 m or so for fairly porous sands and gravels or sandstones (porosity ~25%) to over 10 m in, say, chalk or limestone aquifers where the fracture porosity (a few percent) largely represents the volume available for transient water storage. Common monitoring well observations are (Marinelli and Durnford, 1996):

- wells can contain no observable LNAPL, even though soil sampling indicates significant LNAPL in the adjacent formation;
- for unconfined aquifers, LNAPL thickness in wells tends to decrease with water table rise and increase with water table fall;
- for confined aquifers, LNAPL thickness in wells tends to rise with water table rise and decrease with water table fall;

- sudden appearance or disappearance of LNAPL in wells; and
- if water table drops below its previous range of fluctuation, LNAPL may disappear from wells.

These observations are due to the balancing of forces and level of LNAPL saturation. Assuming a defined volume of LNAPL in the aquifer, the LNAPL observed in a well is the observations of LNAPL above residual saturation.

Observed decreases in LNAPL thickness in an unconfined aquifer well with a rising water table (and vice versa) are due to distribution and re-distribution of mobile LNAPL within the LNAPL body (Huntley *et al*., 1994a,b). For an unconfined homogeneous aquifer, Fig. 3.6a shows an initial vertical equilibrium shark-fin distribution. During the initial water table fall, the LNAPL body drains due to gravity and smears forming a low three-phase (water-LNAPL-air) residual LNAPL saturation above the LNAPL body within the expanded vadose zone (Fig. 3.6b) through the process of imbibition (Fig. 3.1). With water level increase, the buoyant LNAPL will rise; however, LNAPL will be trapped as an increased two-phase residual LNAPL saturation due to capillary forces (Fig 3.6c). At the water table maximum, LNAPL may become entirely (or partially) entrapped in the formation and show no (or a lower) thickness in the well (Fig 3.6d). Upon water table decline again, the entrapped LNAPL will once again drain allowing the thickness of LNAPL to build in the well (Fig 3.6e). Variation from this ideal conceptualisation may occur depending on heterogeneity and water table position during the initial spill release.

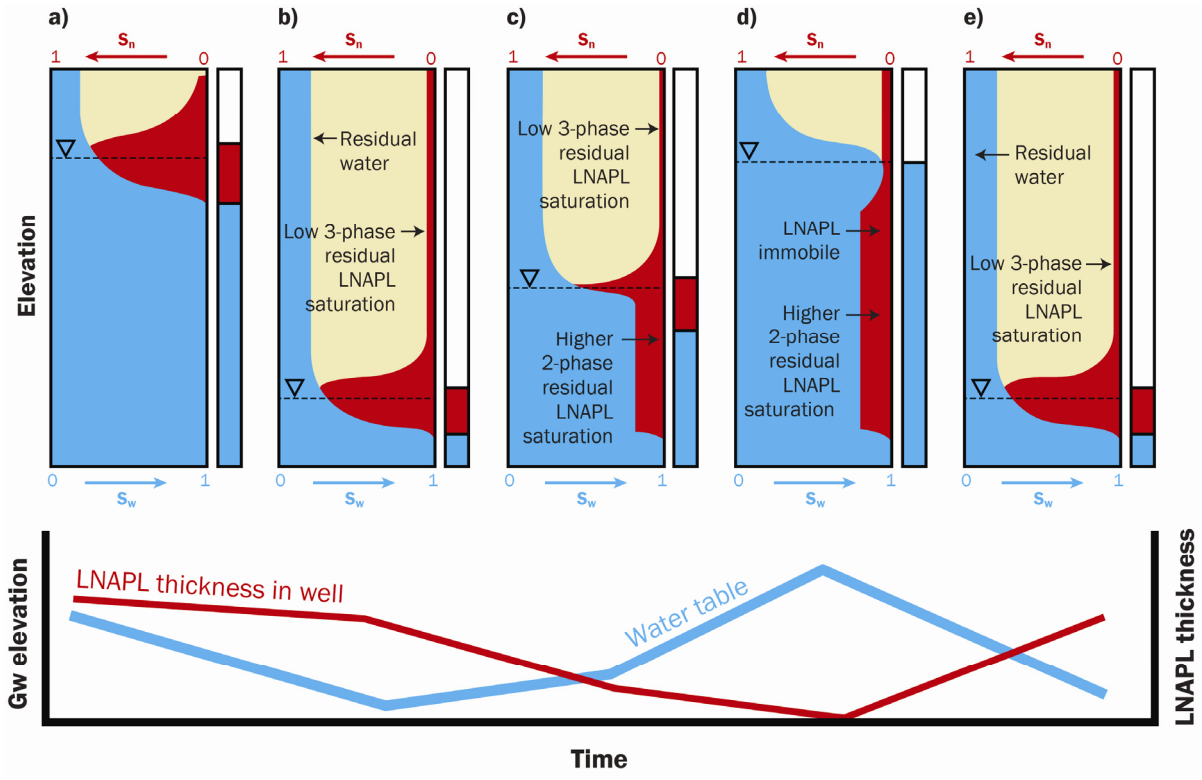

Figure 3.6. Conceptualised variation of LNAPL observed within formation and within monitoring wells (a - e) during a water table cycle with varying water table and LNAPL thickness (shown on bottom graph) (after ITRC, 2009a). S_n is saturation (of pore space) of NAPL, S_w is saturation of water.

3.6. LNAPL migration in fractured rock

Fractures provide discrete planar discontinuities within which LNAPL may preferentially migrate and accumulate (Hardisty *et al*., 1998). The matrix rock may or may not have significant porosity and potentially some permeability; however, its fracture system will typically exert the dominant control. Within the partially saturated zone, LNAPL will move downwards through vertical and sub-vertical fractures under the influence of gravity (Fig. 3.7; Hardisty *et al*., 1998; Johnston, 2010). The steeper the fracture dip, the greater the influence of gravity and the lower the LNAPL retention (residual saturation). LNAPL flow also increases as fluid viscosity decreases and as fracture aperture increases. With greater LNAPL-water density contrast, vertical driving forces are increasingly resisted by LNAPL buoyancy that promotes lateral spread of the LNAPL at the water table during release and after water table fluctuations (Johnston, 2010). Significant lateral LNAPL migration may also occur along dipping fractures in the partially saturated zone.

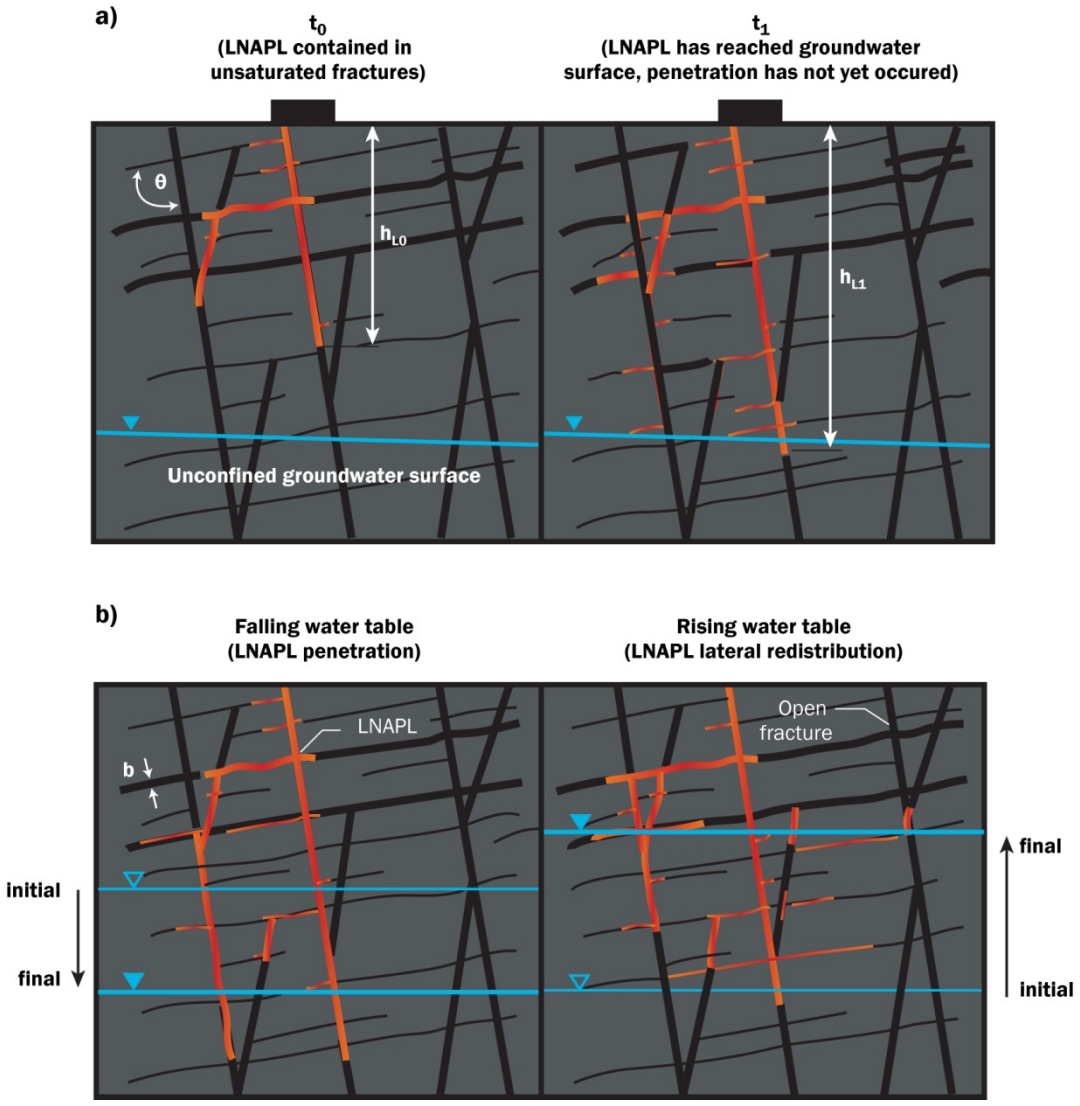

Figure 3.7. a) Conceptual representation of LNAPL migration in the partially saturated zone with a continuous source (after Hardisty *et al*., (1998); Johnston, 2010). b) LNAPL entrapment by a fluctuating groundwater surface (after Hardisty *et al*., (1998)).

Controls on LNAPL distribution within the porous matrix of the rock body between fractures exhibit similarity to those already described for porous media, with LNAPL entry being controlled by the variation in permeability of the rock matrix (Huntley *et al*., 1994a,b). Where the matrix is of high porosity, but low permeability (i.e., small pore size) or else of very low porosity, the LNAPL will be largely restricted to the fractures and may potentially migrate further. In this case gravity will be the primary driving force, with completely vertical fractures (i.e., in the direction of gravity) having the greatest penetration of LNAPL, with less penetration from sub-vertical to horizontal orientation. In fully horizontal fractures, the driving pressure head is zero, and LNAPL is immobilised, unless it remains connected to LNAPL in other non-horizontal fractures that aid in driving the LNAPL laterally with some influence due to groundwater flow (Hardisty *et al*., 1998).

Once at the water table, the LNAPL's accumulated weight will begin to depress the LNAPL-water interface within the fracture (Fig. 3.8). In a water-wet system, LNAPL will enter a given fracture only if the LNAPL-water capillary pressure at the fracture entrance is greater than the fracture entry pressure (Kueper and McWhorter, 1991). Fracture aperture controls the ability of LNAPL to displace resident fluids (water and air) and enter the fracture. Typically fractures are rough walled, variable aperture and may contain porous materials as a result of chemical alteration of the fracture face or transport of fines (Johnston, 2010). The entry of LNAPL into a fracture is controlled by the entry pressure (P_e), which may be estimated by the Laplace Equation of capillarity (Corey, 1990):

$$P_e = \frac{2\sigma\cos\theta}{b} \qquad \text{Eq. 3.1}$$

where P_e is the entry pressure (P_L-P_W in Eq. 2.1), b is the fracture aperture, and θ is the contact angle with the wetting fluid (i.e., replacing r in Eq. 2.1 with b).

The pressure is balanced by the buoyancy of the LNAPL provided by penetration beneath the water table and the fracture entry pressure (Hardisty *et al*., 1998). Other fractures connected to the LNAPL-bearing fracture beneath the groundwater surface could also be invaded by LNAPL, depending on their aperture and orientation. The restriction of the LNAPL to the fractures and generally low bulk lateral transmissivity (due to small cross sectional area of the fracture within the rock volume) means that fluid pressure driving the infiltration of the LNAPL may be maintained deep into the partially saturated zone. Maintaining high LNAPL (and hence capillary) pressures will enhance both lateral migration and vertical penetration of the LNAPL below the water table (Johnston, 2010). This is in contrast to porous media, where capillary effects tend to dominate and LNAPL is not physically constrained. Hence LNAPL may penetrate to greater depths below the water table within fractured media (Hardisty *et al*., 1998, 2003).

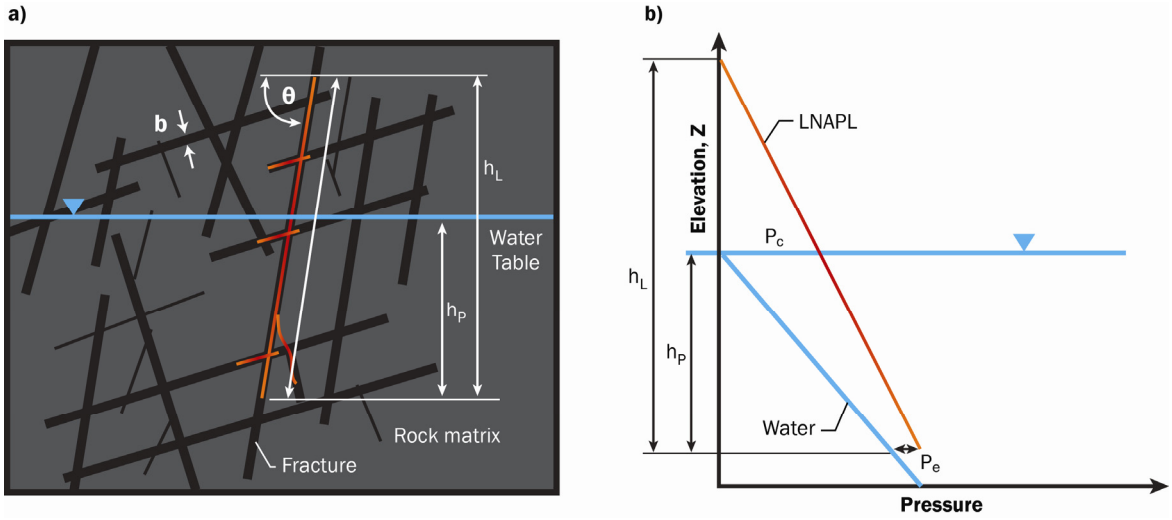

Figure 3.8. a) LNAPL penetration beneath the groundwater surface on left is a function of the buoyancy and pore entry pressure which is a function of dip angle θ, height of LNAPL h_L, LNAPL penetration depth h_P, aperture width, fluid density and gravitational force. b) Pressure-elevation relationship of LNAPL in a vertical fracture at the groundwater surface, with a fracture aperture b, capillary pressure P_c and entry pressure P_e (based on Hardisty *et al*., 2003).

3.7. Water table fluctuation in fractured rock

Water table fluctuations within fractured rock may significantly influence LNAPL entrapment and migration (Hardisty *et al*., 1998, 2003). Depending on the capillary pressure characteristics of the matrix, the LNAPL will follow a declining water table almost immediately through larger aperture vertical fractures (Fig. 3.7). Lateral migration of LNAPL into newly-unsaturated fractures may then occur via less steeply dipping fractures. With water table rise, LNAPL within steeply dipping fractures will be most able to follow; however, LNAPL will also enter the less steeply dipping fractures via buoyancy with the rising water level within this previously water-filled fracture. In this way, a fluctuating groundwater surface can essentially "pump" LNAPL laterally, with LNAPL entering new fractures with each cycle of rise and fall leading to a more dispersed LNAPL source zone.

3.8. LNAPL transmissivity

LNAPL transmissivity (Fig. 3.9) provides a useful concept to quantitatively assess the hydraulic recoverability of a LNAPL body, including that accumulated at the water table and potentially removable via LNAPL pumped recovery (Section 7). Transmissivity is the only metric that exhibits a consistent proportional relationship to LNAPL recovery (ASTM, 2011). Akin to groundwater transmissivity, the LNAPL transmissivity (T_n) is a proportionality coefficient describing the ability of a permeable medium to transmit LNAPL and represents the volume of LNAPL through a unit width of aquifer per unit time per unit drawdown. A permeable coarse sand will transmit more LNAPL than a fine-grained clay for a given LNAPL well thickness or induced gradient on LNAPL within the geological formation.

The relative permeability of a fluid, including LNAPL, is a function of its saturation of the pore space (Fig. 3.1); similarly, NAPL conductivity K_n (estimated from baildown tests; Section 6.4.5) is a function of saturation $K_n(S_n)$. T_n is given by the summed product of K_n and NAPL

thickness, b_n (Fig. 3.9). The LNAPL transmissivity will vary over the observed thickness range in a well for the homogeneous case, the predominant transmissive portion of the LNAPL body will be at the peak of the observed saturation (Fig. 3.9). In heterogeneous formations, there may be greater LNAPL contributions from the more geologically permeable horizons, particularly if LNAPL saturations there are also high. A LNAPL transmissivity of approximately 9.3×10^{-3} to 7.4×10^{-2} m^2/day is considered the lower range for recovery of LNAPL by pumping from wells (see hydraulic recovery in Section 7.5.3) (ITRC, 2009a).

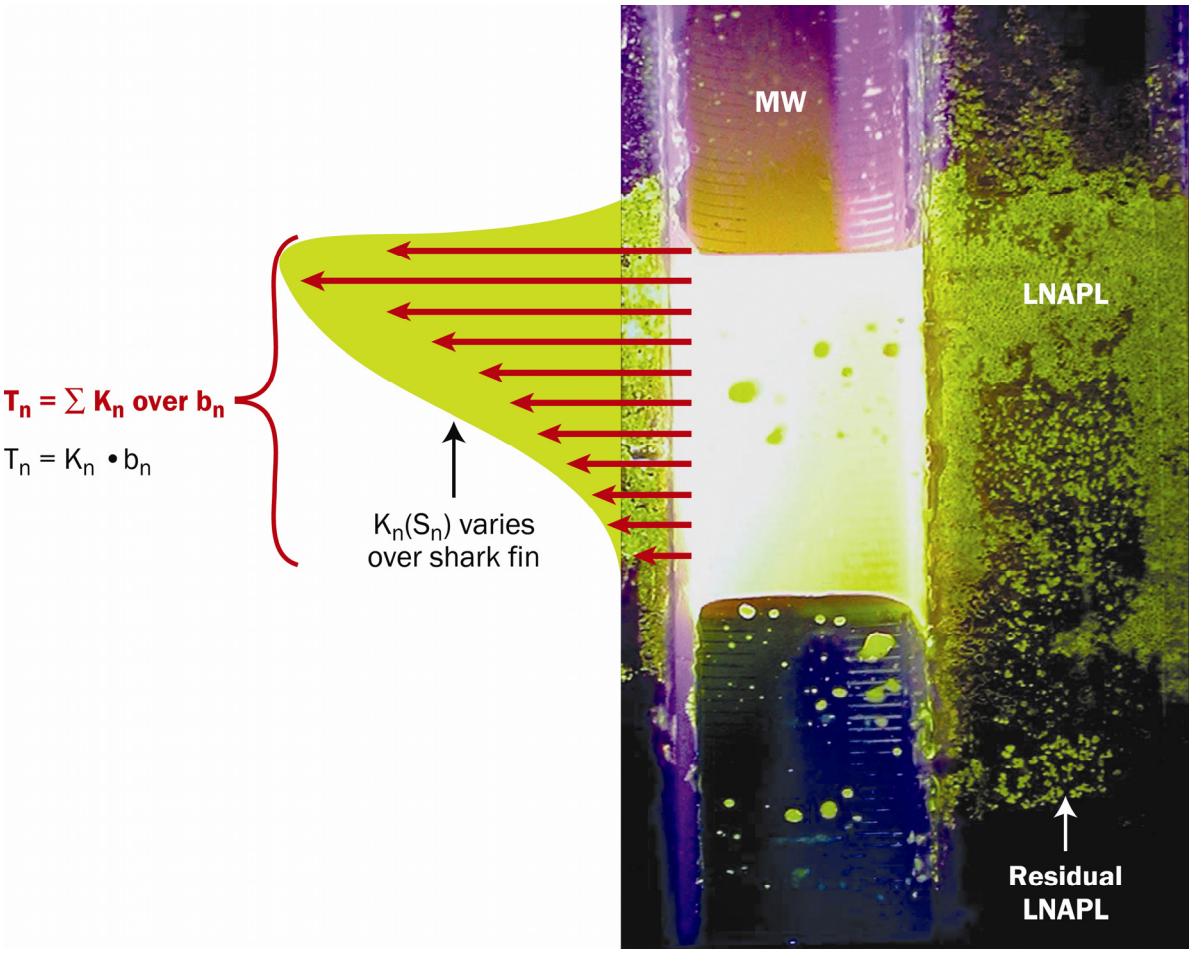

Figure 3.9. Illustration of the relationship of LNAPL transmissivity to saturation (Photograph courtesy of Andrew Kirkman; ITRC, 2009a; ASTM, 2013a).

4. LNAPL mass transfer and plume fate

Contaminant mass transfer may occur from the LNAPL source zone to co-existing aqueous and/or gas phases. In the former, the process of dissolution creates a dissolved-phase plume in groundwater, whereas the latter creates a vapour-phase plume above the water table. This section examines these LNAPL mass transfer processes and the fate and transport of the respective plumes that are produced. This includes the role of natural attenuation in their management and risk mitigation.

4.1. LNAPL dissolution and dissolved plume fate

A conceptual model of the LNAPL dissolution process is shown in Fig. 1.2. Subsurface LNAPL trapped as ganglia, at or below residual saturation, or present as mobile pools above a capillary barrier (for example, a clay layer) and/or water table is a long-term source of groundwater contamination. Soluble components are leached from the LNAPL by flowing groundwater and a dissolved-phase plume develops. LNAPL dissolution rates and hence source zone longevity are influenced by LNAPL composition, distribution and saturation, LNAPL-water contact area, groundwater velocity, molecular diffusivity of the LNAPL chemicals in water, non-equilibrium dissolution effects and enhanced dissolution due to biodegradation of dissolved components (Garg and Rixey, 1999). Complete dissolution of the LNAPL may require many thousands of pore volumes of water to be flushed through a source, with significant variation in timescale possible due to variation in LNAPL composition and effective solubility of components (Thornton *et al*., 2013). LNAPL dissolution rates for petrol are an order of magnitude greater than diesel and two orders greater than the less soluble heavy fuel oils.

4.1.1. LNAPL dissolution

Most LNAPLs are multi-component mixtures of organic compounds, for which the equilibrium dissolved-phase concentration (effective solubility) of individual components may be approximated by Raoult's Law (solubility analogue):

$$S^e_i = X_i S_i \qquad \text{Eq. 4.1}$$

where S^e_i is the effective aqueous solubility of compound (component) i in the LNAPL mixture, X_i is the mole fraction in the LNAPL and S_i is the aqueous solubility of the pure-phase compound. For fresh and weathered petrols with a benzene mole fraction of 0.0076 and 0.0021 respectively, the predicted effective solubilities are 13.5 mg/L and 3.78 mg/L. These are much less than the pure-phase solubility of benzene of 1790 mg/L. Where NAPLs contain high molecular mass compounds, such as polycyclic aromatic hydrocarbons (PAHs), that would actually be present individually as solids under the relevant environmental temperature and pressure conditions, those components require the use of hypothetical supercooled liquid solubilities for the S_i term, in recognition of their liquid state within the NAPL mixture (Vadas *et al*., 1991).

Most fuels/oils contain a significant proportion of unidentified components and an estimated molecular mass of the unidentified LNAPL mass fraction may be used to obtain X_i. Mean molecular mass estimates of bands of quantified hydrocarbon ranges may likewise be used.

Where observed site concentrations approach the pure phase solubility of a chemical or significantly exceed the expected effective solubility of typical fuel compositions, this would strongly indicate a release of the pure chemical rather than a fuel that comprises a complex mixture of many organic chemical components.

The effective solubility of LNAPL components varies with time as the more soluble components preferentially dissolve into water, causing the mole fractions to change (Eq. 4.1). Fig. 4.1 illustrates how the more soluble fuel oxygenate compounds in the LNAPL are dissolved quickly, leading to increased aromatic hydrocarbon dissolution later on as their mole fraction increases. The evolving LNAPL composition therefore leads to time-variant risk and remediation considerations. In typical petrol formulations, the light-end hydrocarbons and fuel oxygenate compounds such as MTBE will preferentially dissolve from the LNAPL source at relatively high concentration with, and followed by, dissolution of BTEX. Nonpolar hydrophobic hydrocarbons are often relatively significant and may include branched or straight chain alkanes, which are sparingly soluble and more persistent. Consequently LNAPL fuels progressively dissolve to leave a less soluble and persistent residue in the source.

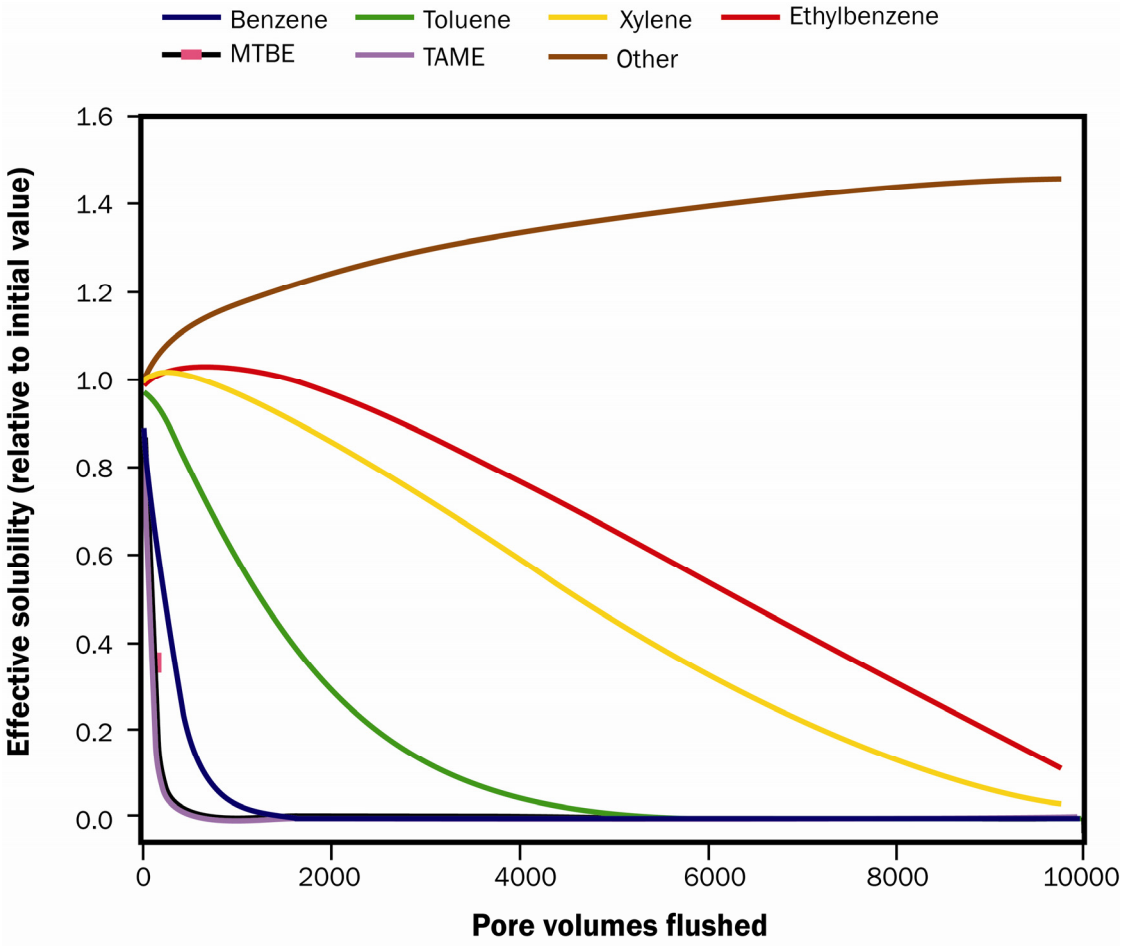

Figure 4.1. Prediction of time-variant effective solubility for petrol components, reflecting preferential partitioning of the more soluble components (Thornton *et al*., 2013). MTBE and TAME oxygenate profiles eclipse each other and decrease rapidly. The “other” fraction represents the significant mass of undifferentiated, less soluble, LNAPL components, the effective solubility of which rises above its initial value due to its increasing mole fraction with time.

Although estimates of effective solubility are most appropriate for ideal mixtures where the organic components are structurally similar in size and polarity, the Raoult's Law analogue is nevertheless a reasonable indicator of effective solubilities for most LNAPL mixtures. Hydrocarbon concentration ratios near the source (recognising that groundwater monitoring wells may often lead to some dilution) typically reflect the effective solubility ratio of components in the absence of other processes such as sorption or biodegradation. The latter may cause ratios to change markedly even within relatively short transport distances down gradient of the source.

4.1.2. Factors controlling LNAPL dissolution

The time (days) required to completely dissolve a LNAPL source may be approximated by:

$$t = \frac{m}{(v\, n_e\, C_w\, A)} \qquad \text{Eq. 4.2}$$

where m is the LNAPL mass (g), v is the groundwater velocity (m/day), n_e is effective porosity of the aquifer, A is the cross-sectional area containing LNAPL through which groundwater flows (m^2), and C_w is the dissolved concentration (mg/L). This, however, is considered a very simple approach in that it does not consider processes which lead to time-variant, typically declining, LNAPL dissolution (unless an algorithm for C_w based on Eq. 4.1 is adopted). Also, the presence of LNAPL reduces the permeability of the host porous material to the aqueous phase (Fig. 3.1), leading to a profile of groundwater velocity through a LNAPL source that varies with depth. The greatest groundwater velocity (within a reasonably homogeneous geological setting) occurs at the periphery of the LNAPL source where a low LNAPL saturation exists. The lowest groundwater velocity may occur through the central body of the LNAPL, the peak of 'shark-fin' saturation profile (Section 3.4), that typically occurs close to the water table-capillary fringe interface. Higher velocities may occur deeper below the water table and within the LNAPL smear zone produced by water table fluctuation. Dissolution will hence be greater at the periphery of a LNAPL body and through dispersed ganglia, which are more accessible to flowing groundwater than the central body of pooled LNAPL from which mass transfer will be low. Seasonal or other influences on the water table elevation may, however, allow this body of less water-accessible LNAPL to be dispersed vertically and be more easily dissolved.

The permeability field of the geological media also has a key influence on source zone dissolution. Increased groundwater flow in coarse-grained layers will induce more rapid dissolution of LNAPL present there, leaving more persistent LNAPL mass in the fine-grained layers, from which mass transfer may become increasingly diffusion controlled. Dissolution may become rate-limited and/or diffusion controlled when groundwater velocity is very high, LNAPL saturation is low, and/or the mole fraction of relatively soluble species in a LNAPL mixture is low (Thornton *et al*., 2013). The mass transfer during dissolution depends upon many physical parameters, including pore fluid velocity, LNAPL saturation (and interfacial surface area), pore-scale geometry and geological heterogeneity, which are not easily measured (even at the lab-scale). The effect of these controls is typically captured with lumped mass transfer coefficients (λ), which may be determined from (mostly DNAPL) lab or controlled field experiments.

Other factors, such as temperature variation, the presence of co-solvents (e.g., alcohols such as ethanol), salinity and dissolved organic matter tend to be of secondary importance.

The aqueous solubility of organic chemicals decreases somewhat with increasing salinity. Although dissolved organic matter (humic and fulvic acids) can enhance solubility, concentrations of these organic complexing agents are typically too low in most groundwaters to be a major concern. Overall, a modest increase (<20%) in the solubility of most organic chemicals is anticipated unless the aqueous-phase concentration of co-solvents exceeds 2% v/v (by volume) (Rao *et al*., 1991).

4.1.3. Natural attenuation of dissolved-phase plumes

The composition of the dissolved-phase plume that develops immediately down gradient of a LNAPL source is closely linked to the chemical composition of the LNAPL and its evolving dissolution (and vapourisation) characteristics. Depletion of the LNAPL source will continue naturally by a range of processes at the same time as dissolution supports the development a dissolved-phase plume in groundwater. The processes responsible for NSZD include dissolution, vapourisation and local biodegradation, supported by electron acceptor exchange with gas and water in the unsaturated and saturated zone. Collectively these processes may enhance mass transfer from the LNAPL (Fig. 1.2; ITRC, 2009b; Johnson *et al*., 2006; Lundegard and Johnson, 2006). It is emphasised that source zone depletion (either natural or enhanced by remediation efforts) relates to the LNAPL and is different from management approaches such as monitored natural attenuation (MNA), which focus on the down gradient dissolved-phase plume.

Preferential dissolution of the more soluble and volatile LNAPL components will lead to plumes from fuel releases that are often dominated by BTEX components and higher solubility fuel oxygenates. BTEX components are often key contaminants of potential concern (COPC) in the assessment of risks posed by petrol fuels (Bowers and Smith, 2014; Thornton *et al*., 2013). A complex plume organic chemistry evolves over time as different components are dissolved from the LNAPL. For example, Spence *et al*. (2005) illustrate within a fractured chalk aquifer setting the typical petroleum fuel spill scenario, whereby a MTBE plume initially develops in groundwater due to its higher effective solubility and lower attenuation. This is typically followed by a relatively extensive benzene plume. However, the less soluble and typically more biodegradable aromatic hydrocarbons such as toluene, ethylbenzene and xylenes often develop dissolved-phase plumes that are restricted to the LNAPL source area.

While LNAPL dissolution fundamentally controls the duration of inputs to dissolved-phase plumes, the plume size and composition is predominantly controlled by natural attenuation in the aquifer. Dispersion will dilute contaminant concentrations, but biodegradation and sorption, which respectively remove plume contaminant mass and can slow plume migration, are often more important attenuation processes than dispersion.

The significant interest over the past two decades in MNA as a management strategy for contaminated groundwater (API, 1998; ASTM, 1998; EA, 2000; USEPA, 2004a; Wiedemeier *et al*., 1995, 1997) has provided a comprehensive body of evidence on the theoretical basis and practical site implementation of this approach for dissolved plumes originating from LNAPL sources (Rivett and Thornton, 2008; Wiedemeier *et al*., 1999). A brief overview of biodegradation as the main natural attenuation process controlling the fate of plumes at many LNAPL release sites is provided below. It should also be recognised that sorption to the aquifer solids and porous matrix diffusion may be significant in determining the relative migration of the various compounds in the dissolved-phase plume. For example, highly

soluble LNAPL components such as MTBE and benzene may adsorb little to the aquifer solids, forming larger groundwater plumes compared with more hydrophobic, less soluble and higher molecular mass components whose migration is more strongly retarded.

4.1.4. Biodegradation

Many organic compounds in LNAPLs can be biodegraded by naturally-occurring subsurface microorganisms (Rivett and Thornton, 2008). Microbially-mediated oxidation-reduction (redox) reactions occur, whereby organic compounds are metabolised as a carbon substrate often to innocuous by-products, such as carbon dioxide, methane, water and organic metabolites. Electron acceptors (oxidants) used to support biodegradation include dissolved oxygen, nitrate and sulphate in pore water and mineral oxidants such as manganese and iron-oxides present as grain coatings. Once those electron acceptors are depleted, fermentation of organic compounds may occur with the ultimate production of methane. Aerobic biodegradation (using oxygen as an electron acceptor) and anaerobic biodegradation (using other electron acceptors) typically occurs concurrently in plumes as illustrated in the Fig. 4.2 case study example.

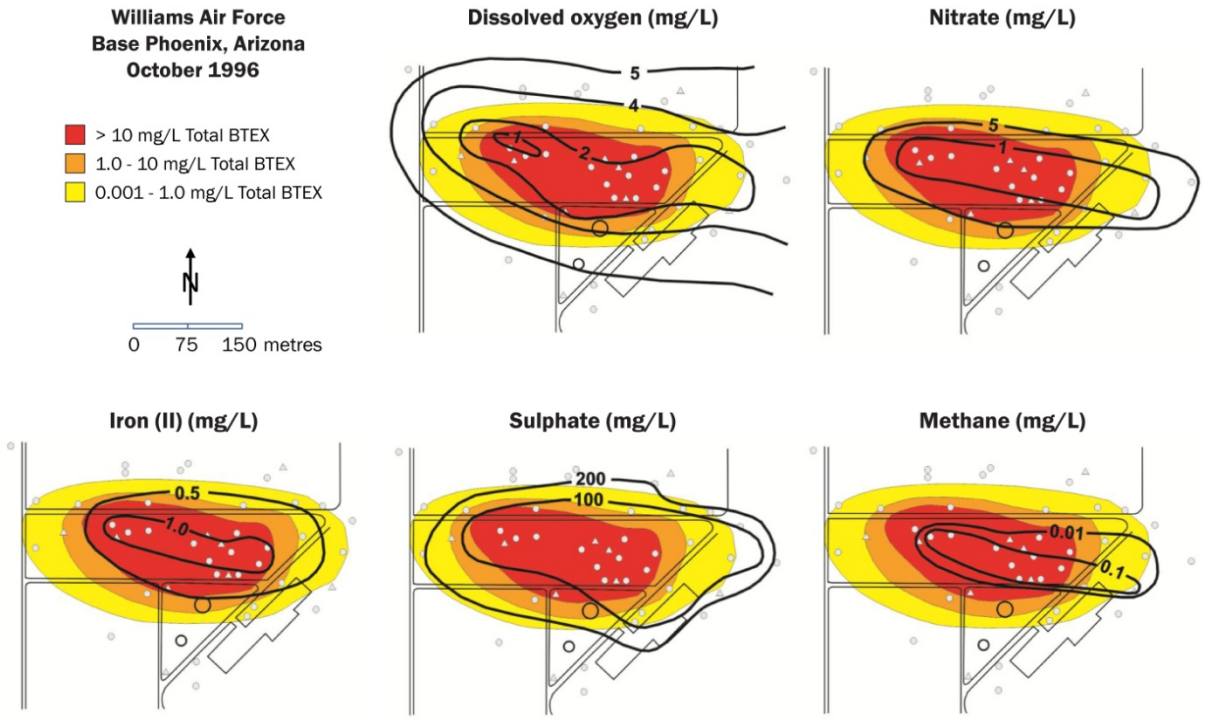

Figure 4.2. Concentration distribution of total BTEX, electron acceptors and biodegradation products in groundwater at the Williams Air Force Base, Phoenix, Arizona in October 1996 (Figure courtesy of Todd Wiedemeier).

Thermodynamically, as indicated by the Gibbs free energy of reaction (ΔG_r^o) for benzene biodegradation (Table 4.1), aerobic oxidation of most contaminants will occur preferentially due to a greater energy yield relative to anaerobic processes, with methanogenesis being the least energetically favourable. The Gibbs free energy of reaction for BTEX (Table 4.2) also predicts, thermodynamically, that ethylbenzene and xylenes will be preferentially oxidised before toluene, provided oxygen is not limiting. Aerobic respiration of benzene will

occur when these have been consumed. Therefore benzene is generally observed to be the most persistent mono-aromatic hydrocarbon at petroleum fuel release sites (Rivett and Thornton, 2008).

Calculations of ΔG_r^o values for anaerobic biodegradation using other electron acceptors will provide a similar result. This helps explain the common site observation that the transport of toluene, ethylbenzene and xylene (TEX) compounds in groundwater is frequently limited by biodegradation under both aerobic and anaerobic conditions developed in the aquifer and that benzene may produce a relatively larger plume. Although the free energy concept provides a theoretical predictive framework, other factors, such as the presence of microorganisms available to facilitate a specific reaction, competitive effects between microbial populations and inhibition of biodegradation processes by contaminants can also occur (Thornton *et al*., 2011). Therefore, this must be considered a qualitative interpretation and cannot be linked directly to the rate at which a reaction will necessarily occur.

Table 4.1. Gibbs free energy of reaction for benzene biodegradation processes.

Full reaction	Process	Electron acceptor used	ΔG_r^o (KJ/mol)
$C_6H_6 + 7.5O_2 \rightarrow 6CO_2 + 3H_2O$	Aerobic respiration	O_2	-3202
$C_6H_6 + 6NO_3^- + 6H^+ \rightarrow 6CO_2 + 6H_2O + 3N_2$	Denitrification	NO_3^-	-2998
$C_6H_6 + 30Fe(OH)_3 + 60H^+ \rightarrow 6CO_2 + 78H_2O + 30Fe^{2+}$	Fe-reduction	Fe(III)	-2822
$C_6H_6 + 15MnO_2 + 30H^+ \rightarrow 6CO_2 + 18H_2O + 15Mn^{2+}$	Mn-reduction	Mn(IV)	-1964
$C_6H_6 + 3.75SO_4^{2-} \rightarrow 6CO_2 + 3H_2O + 3.75S^{2-}$	SO_4-reduction	SO_4^{2-}	-210
$C_6H_6 + 4H_2O \rightarrow 2.25CO_2 + 3.75CH_4$	Methanogenesis	CO_2	-135

Table 4.2. Gibbs free energy of reaction for aerobic biodegradation of BTEX compounds.

Compound	Full reaction	ΔG_r^o (KJ/mol)
Benzene (B)	$C_6H_6 + 7.5O_2 \rightarrow 6CO_2 + 3H_2O$	-3202
Toluene (T)	$C_7H_8 + 9O_2 \rightarrow 7CO_2 + 4H_2O$	-3823
Ethylbenzene (E)	$C_8H_{10} + 10.5O_2 \rightarrow 8CO_2 + 5H_2O$	-4461
m-Xylene (X)	$C_8H_{10} + 10.5O_2 \rightarrow 8CO_2 + 5H_2O$	-4449

Dissolved oxygen in groundwater reaches a maximum concentration of only ~10 mg/L in equilibrium with air. Such concentrations would be rapidly consumed within the plume core (due to the high contaminant concentrations) and only replenished very slowly at the plume fringe where it is rapidly consumed by aerobic biodegradation. Other oxidants are then used under anaerobic conditions, leading to a spatially distributed sequence of redox zones (Fig. 4.2). These comprise aerobic respiration at the leading edge and plume fringe, moving successively up gradient through zones where nitrate-reduction, Mn/Fe-reduction, sulphate reduction and finally methanogenesis closest to the plume source typically occur, subject to

the relevant respiratory substrates being present. Developing a site-specific conceptual model which combines the distribution of redox processes with organic contaminants represents an important tool for the interpretation of contaminant fate and site-specific risk assessment, for example within an assessment for MNA.

Anaerobic biodegradation may be slower than aerobic for many components but can account for most plume mass metabolised at LNAPL-release sites, due to the higher quantities of dissolved sulphate and Mn/Fe-oxide electron acceptors often available in aquifers. Mn- and Fe-reducing zones can be spatially extensive due to very large reservoirs of these mineral oxides typically present in many aquifers. In dual porosity aquifers such as the UK Chalk where fracture flow is dominant, the high porosity matrix may still provide a significant reservoir of dissolved electron acceptors that can diffuse into the fractures to support biodegradation (Spence *et al*., 2005). These redox zones develop as long as there is an excess flux of electron donors (organic compounds) released into the plume from the LNAPL source. However, with time and (natural or engineered) source depletion, the flux of biodegradable organic compounds into the plume decreases and plumes will shrink and progressively more oxidising conditions become re-established.

The capacity of aquifers to attenuate organic contaminants by biodegradation varies and can be represented by their oxidation capacity (EA, 2000). Other lines of evidence include confirming the presence of geochemical conditions *in situ* that reflect plume biodegradation processes. As illustrated by Fig. 4.2, these conditions may typically be lower dissolved oxygen, nitrate and sulphate in the plume, together with increased concentrations of inorganic by-products (e.g., dissolved Mn(II), Fe(II), methane and carbon dioxide (and S^{2-} that often precipitates)) and various specific organic metabolites that arise from the biodegradation pathways. The qualitative and quantitative interpretation of these chemical distributions (Thornton *et al*., 2001; Wilson *et al.,* 2004) forms the technical basis for the performance assessment of MNA and bioremediation (EA, 2000; Wiedemeier *et al.,* 1999). The development life-cycle of plume growth, steady-state stabilisation (balanced rates of growth and decay) and eventual decay can only be deduced by groundwater quality monitoring at appropriate intervals. Several years of monitoring may be required to deduce the development stage for slow moving plumes or where biodegradation rates are low (EA, 2000).

Contaminant biodegradation rates are key to any quantitative (risk) assessment and may be estimated using laboratory biodegradation studies, literature values or, less commonly, from field data (Shah *et al.,* 2009; Wilson *et al.,* 2004). The first-order decay model is commonly and conveniently used to describe biodegradation in assessments and transport models to represent often complex biodegradation processes:

$$C = C_0 e^{-\lambda t} \qquad \text{Eq. 4.3}$$

where C is the concentration of the organic compound after biodegradation at time t (T), C_0 is the initial concentration of the organic compound, and λ is the first-order biodegradation rate constant (T^{-1}), with the corresponding half-life ($t_{0.5}$) being:

$$t_{0.5} = \frac{\ln(2)}{\lambda} = \frac{0.693}{\lambda} \qquad \text{Eq. 4.4}$$

The model assumes that the biodegradation rate is a function of the organic compound concentration only. Potential limitations include not accounting for site-specific conditions, such as electron acceptor availability and competitive effects between microbial populations, and that laboratory estimates of λ may not easily be transferred to field assessments. DeVaull (2011) has collated measured first-order biodegradation rate data for petroleum hydrocarbons in aerobic soils, which show a wide variation in values for individual aromatic and alkane hydrocarbons. As an example, Fig 4.3 compares plots of mean biodegradation rates taken from DeVaull (2011), expressed as half-lives. The data illustrate the relative ease with which aerobic biodegradation of the alkanes occurs (given by shorter half-lives) compared with the aromatic compounds and the persistence of benzene and trimethylbenzene within that latter group.

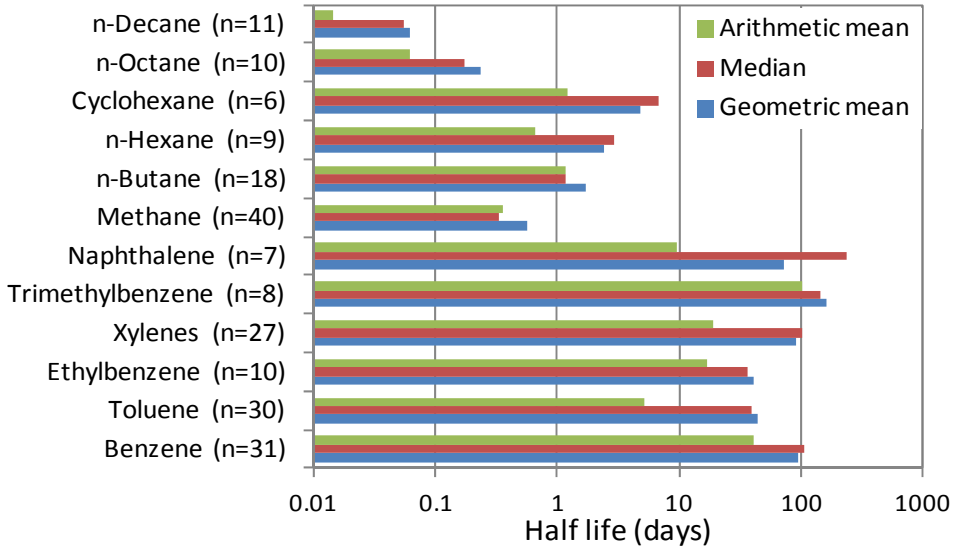

Figure 4.3. Mean half-life data for aerobic biodegradation of petroleum hydrocarbons in soils calculated from measured first-order biodegradation rates compiled in DeVaull (2011) (see DeVaull (2011) for the full dataset).

In terms of plume size and duration, for biodegradable compounds the plume expansion period is short compared with the duration of most LNAPL sources. Hence risks to receptors depend primarily on predicted maximum plume lengths rather than LNAPL source duration. Plume expansion continues until a quasi-stationary plume condition is reached, whereby the flux of dissolved components from the source is balanced by the mass removed through attenuation processes in the aquifer. The steady-state plume length can be linearly related to the groundwater velocity and is inversely proportional to the first-order biodegradation rate constant (Huntley and Beckett, 2002). A reduction in LNAPL saturation by remediation may not affect the maximum concentration at a receptor, but causes a more rapid decrease in that concentration as the source becomes depleted. Hence, the time a receptor may be exposed to unacceptable contaminant concentrations is reduced. For less biodegradable dissolved contaminants, plumes will expand further and result in larger plumes of those components. In this case dilution by dispersion may be more important for attenuation (Thornton *et al.,* 2013).

4.2. LNAPL vapourisation and vapour plume fate

Many LNAPLs contain volatile organic compounds (VOCs) that can vapourise during and after LNAPL migration in the subsurface, leading to the development of a vapour-phase plume in the partially saturated zone (Christophersen *et al.,* 2005; Molins *et al.,* 2010) (Fig. 4.4). Vapour plumes may expand rapidly beyond the source area, potentially in different directions to the groundwater plume. A decreased groundwater impact may occur where vapours migrate to the ground surface and are lost to the atmosphere. Conversely, early arrival and increased VOC contamination at the water table (with partitioning into groundwater) may also arise from downward vapour migration (Rivett *et al*., 2011).

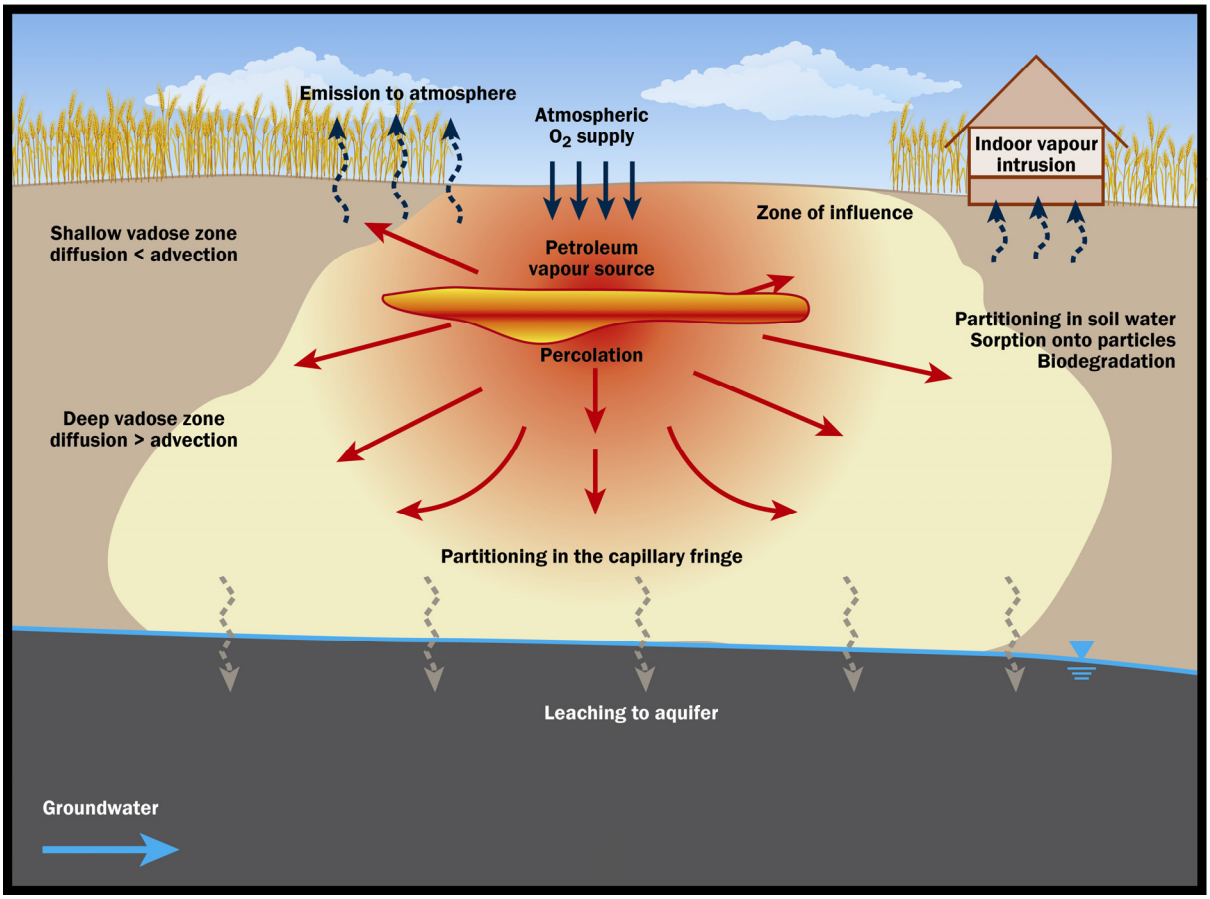

Figure 4.4. Conceptual model illustrating vapour transport from a LNAPL release.

4.2.1. LNAPL source zone vapourisation

LNAPL present in the partially saturated zone, supplemented by further smearing due to water table fluctuation, may vapourise into soil gas within the partially saturated zone. This mass transfer depends on the vapour pressure of a chemical. For individual chemical components in a multi-component LNAPL this is again approximated by Raoult's Law:

$$P_i = X_i P_i^o \qquad \text{Eq. 4.5}$$

where X_i is the NAPL mole fraction of chemical i, and P_i^o is its pure-phase vapour pressure. As with effective solubility (Section 4.1), preferential vapourisation of the most volatile NAPL components will occur. BTEX compounds in petroleum fuel vapourise in the order B > T > E

> X, based on their decreasing vapour pressures. Vapourisation is less important for diesel and heavier fuels/oils. Key controlling parameters – vapour pressure, Henry's Law constant and diffusion coefficient – are sensitive to temperature and increase with temperature. This causes vapour generation and migration to be sensitive to temperature profiles in the shallow subsurface (including near buildings) that may range over 40^{o}C between summer and winter in some countries.

4.2.2. Vapour plume fate – controls by physical processes

Local subsurface conditions will influence vapour transport. These include permeable backfilled conduits along service trenches, built structures and road or paved impermeable or semi-permeable (e.g., cracked) structures, which allow vapours to discharge at the ground surface or enter buildings. Key risks related to LNAPL vapour include volatilisation and migration into confined spaces or buildings that may lead to inhalation or fire/explosion risks. Vapour intrusion (VI) into buildings can be an important health risk driver and influence the remediation required, although risks associated with petroleum sources are usually considerably less than those for chlorinated solvents (USEPA, 2013).

Contaminants in a groundwater plume close to the water table may also diffuse across the capillary fringe and partition (in accordance with Henry's Law) into the air-filled porosity to create vapour risks remote from the LNAPL source (Davis *et al.,* 2006). Vapour risks from shallow groundwater plumes of petroleum hydrocarbons migrating under residential areas may be a concern (Lahvis, 2005; USEPA, 2012), although recent work on petroleum vapour biodegradation in the partially saturated zone indicates that it rarely manifests as an actual risk (Lahvis *et al*., 2013). This may not be the case for chlorinated solvent vapour impacts, since petroleum and chlorinated solvent VI risks are typically very different (USEPA, 2012).

BTEX and other VOC gas-phase diffusion coefficients are around four orders of magnitude greater than in water. Hence, diffusive migration of vapours driven by high concentration gradients near LNAPL sources may be significant and lead to a large spatial footprint of vapour contamination at sites. Appendix 2 provides a simple method to estimate the mass flux (loss) of VOCs due to volatilisation of LNAPL components and diffusion from a source at depth to ground surface.

Due to contrasting diffusion coefficients, vapour migration may be sensitive to infiltration that results in temporal variability of water content in the partially saturated zone (Davis *et al.,* 2004). Although capillary forces may often retain significant water content (particularly in fine-grained materials), a reduced water content under seasonally dry, arid/semi-arid field conditions or below buildings will promote more rapid diffusive VOC migration. Conversely, higher water contents due to precipitation infiltration, sewer leakage, or water-saturated low permeability clays, will restrict vapour diffusion, although some vapour displacement may be induced by rapidly infiltrating water. Drained macropores, due to fracturing of compacted clays or bedrock, or coarse-grained heterogeneities may, however, provide more permeable pathways for gas-phase diffusion, even under near-saturated conditions.

Diffusive VOC transfer across the largely immobile, water-saturated capillary fringe may be slow in either direction (Davis *et al.,* 2004; Werner and Höhener 2001). The capillary fringe may contain air-filled porosity, but air trapped in pore spaces may be physically disconnected and effectively restrict gas and vapour diffusion. Fluctuation in the water table may increase vertical mixing and can enhance volatilisation by increasing the contact area

between the contaminated groundwater and gas phase. Likewise, LNAPL redistribution caused by water table fluctuation may allow LNAPL to volatilise from a greater contact area exposed to the gas phase (Davis *et al.,* 2004; 2006). In general, vapour diffusive fluxes into the partially-saturated zone from either LNAPL or dissolved-phase groundwater plumes near the water table-capillary fringe interface will increase with the magnitude and periodicity of water table fluctuation (Werner and Höhener, 2001). Therefore, soil-gas concentration measurements used to estimate volatilisation rates and vapour migration should be completed over a sufficient period (e.g., at least an annual water table cycle) to account for these effects.

Advective vapour migration may be driven by subsurface pressure gradients arising from temperature changes, wind effects and barometric pressure changes, as well as relative vapour density differences between contaminated and uncontaminated soil gas (Davis *et al.,* 2004; USEPA, 2012). Vapour overpressure may develop during a fresh LNAPL release, causing lateral vapour plume advection until the pressure gradient has decreased. Advection can result in more rapid and extensive vapour migration, compared with diffusion only, but is of limited importance a few metres below ground due to restricted subsurface wind movement.

Barometric pressure changes may cause vapour migration over diurnal timescales and perhaps longer due to the induced pressure and temperature fluctuations, which will enhance lateral and vertical vapour movement in soil gas. Soil gas and hydrocarbon vapours can be advected into buildings as pressures upwind may exceed pressures downwind, leading to advection of soil gas beneath the building. Vapours will be drawn into the building/basements when the pressure inside is lower than the adjacent subsurface area. While advective flow due to density effects or high vapour pressure gradients may influence vapour migration, diffusion is generally the most important transport process at most LNAPL/hydrocarbon-contaminated sites (Davis *et al.,* 2004; 2006; Lahvis, 2005).

Temperature increases will have little influence at depths greater than a few metres but will nevertheless enhance vapour migration rates. This occurs due to the increased LNAPL source vapour pressures, diffusion rates and advection (greater convective air circulation) and decreased moisture content (greater air-filled porosity) that arise at higher temperatures (Rivett *et al.,* 2011).

4.2.3. Vapour plume natural attenuation

Vapour-phase contaminants are attenuated by physical-chemical mechanisms such as dilution, diffusion, atmospheric emission and partitioning into pore water, but also by sorption and biodegradation (Rivett *et al.,* 2011). For many petroleum constituents, biodegradation may lead to significant natural attenuation of (largely diffusive) vapour concentration profiles at sites (Grathwohl *et al*., 2001; Lahvis *et al.,* 2013; USEPA, 2013), as exemplified by studies on petroleum hydrocarbon LNAPLs (gasoline, diesel, kerosene, crude oil and others) (Christophersen *et al.,* 2005; Molins *et al.,* 2010).

The biodegradation potential of hydrocarbon vapours is controlled by their mass transport rates, rates of oxygen re-supply (where aerobic biodegradation is the attenuation mechanism). The stoichiometry of the biodegradation process plays a minor role in comparison to the influence of the specific hydrocarbon chemical structure (branched versus straight chain alkanes versus aromatics), which may influence aqueous-phase partitioning

properties and susceptibility to biodegradation. Chemical composition will vary with age of the source term and may lead to varying biodegradation potential as more recalcitrant, less volatile, components persist. Aerobic biodegradation to carbon dioxide of vapour-phase components from LNAPLs may readily occur in the presence of oxygen, with biodegradation half-lives as short as hours or days under certain conditions. Lahvis *et al*. (2013) have developed screening criteria for VI risk assessment based on observations of petroleum vapour aerobic biodegradation. Biodegradation is most rapid at the vapour plume periphery where oxygen re-supply occurs from the ground surface and lateral transport of aerobic soil gas that has been in recent contact with the atmosphere.

Subsurface gas sampling may provide important evidence of vapour plume attenuation via vertical concentration profiles (Fig. 4.5) (Clements *et al.,* 2009; Davis *et al.,* 2004; USEPA, 2012), as oxygen may be removed by other reactions (e.g., oxidation of natural organic matter, other co-contaminants or reduced inorganic species such as sulphides). Anaerobic conditions induced by these other processes can limit aerobic biodegradation of the vapour-phase contaminants (Davis *et al.,* 2005). The importance of aerobic biodegradation for the attenuation of petroleum hydrocarbon vapours is summarised by USEPA (2012) and was demonstrated by Roggemans *et al.* (2001), who provide conceptual models subdividing aerobic (>2% v/v oxygen) and anoxic zones (<2% v/v) that may generally apply to sites. Their study concluded that predictive models ignoring biodegradation could overestimate risks from vapour fluxes by one to four orders of magnitude at some sites.

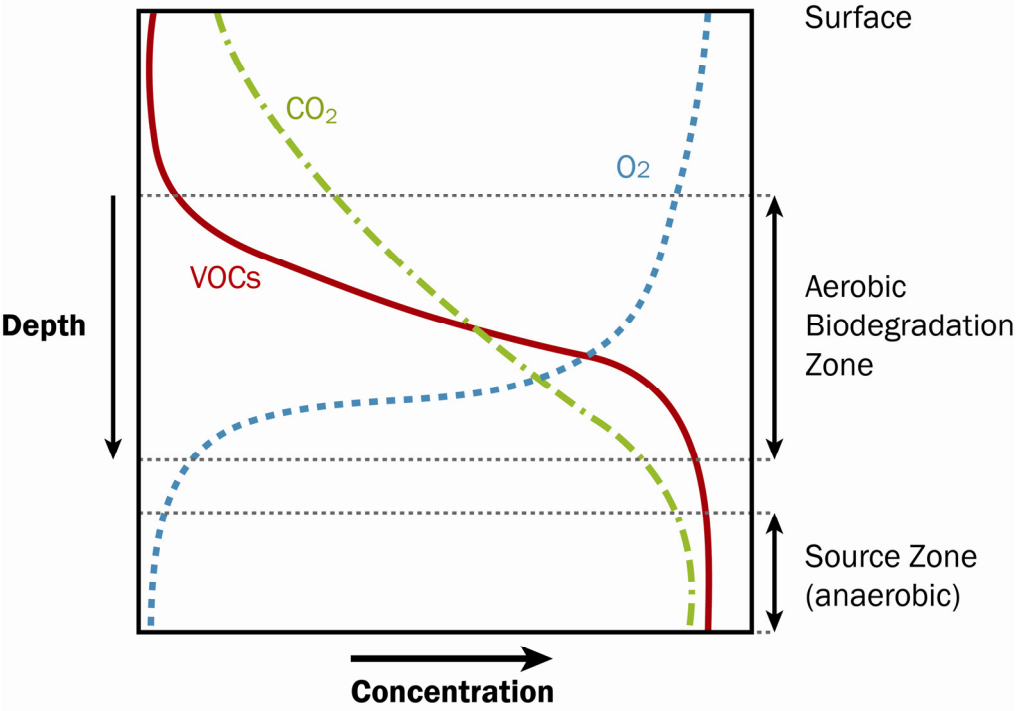

Figure 4.5. Vertical concentration profiles for aerobic biodegradation of oxidisable VOCs released from LNAPL in the partially saturated zone.

Under low oxygen supply and/or increased vapour concentration fluxes, the VOC reaction front (Fig. 4.5) moves upwards and, critically, may break through at ground surface, leading to potential exposure to receptors. Oxygen supply may be limited by sealed surfaces or low permeability units (Knight and Davis, 2013). Anaerobic biodegradation of hydrocarbon

vapours may still occur, using other oxidants in the pore water, but at slower rates (by up to ~100 fold), producing increased concentrations of carbon dioxide and methane (Verginelli and Baciocchi, 2011). Methane, a product of methanogenesis of labile fuel components, such as alcohols, is readily biodegraded aerobically (Ma *et al*., 2012) at the margin of a vapour plume, but creates additional oxygen demand.

Biodegradation rate and oxygen demand will vary for the different vapour plume contaminants, but with total oxygen demand being the sum of all compounds identified (assuming aerobic biodegradation). This oxygen demand should be estimated to deduce the biodegradation that can theoretically occur from the flux of atmospheric oxygen entering the subsurface naturally or via engineered remediation. Davis *et al.* (2009) provide a model (Appendix 3) which describes the aerobic biodegradation of petroleum vapour-phase contaminants for open ground conditions. The model balances the contaminant flux diffusing from a (water table) LNAPL source at depth with the atmospheric oxygen flux diffusing downwards from the ground surface, to estimate the depth at which the vapour-phase compounds and oxygen meet and the maximum depth of oxygen penetration for aerobic biodegradation. Using modelling-based predictions or direct on-site gas measurements, an attenuation factor (α) may also be conveniently defined to characterise vapour attenuation (Davis *et al.,* 2009). The value of α may be defined as the ratio of vapour concentration observed (C_{obs}) at the point of interest (e.g., indoor air, ground level soil) to the maximum vapour concentration found in the subsurface source zone (C_{max}):

$$\alpha = \frac{C_{obs}}{C_{max}} \qquad \text{Eq. 4.6}$$

A lower value of α indicates greater attenuation. For example, a LNAPL source zone vapour concentration (C_{max}) of 145,000 µg/m^3 and a near ground soil-gas concentration of 10 µg/m^3 produces a value of α of 7 x 10^{-5}. This is equivalent to a 10,000-fold concentration reduction. Due to heterogeneity in ground conditions, attenuation factors may vary by orders of magnitude over relatively short distances and this approach is considered highly simplified. The physical distribution of VOCs in soil gas upon which the attenuation factors are estimated, should therefore be verified by an appropriate sampling programme. EA (2002) reviews various modelling tools and their suitability for the assessment of vapour-phase transport and attenuation in partially saturated media, considering the underpinning conceptual model and site-specific data requirements.

Biodegrading vapour plumes will reach a relatively stable, steady-state size in which oxygen re-supply and contaminant biodegradation occurs at the same rate as vapourisation from the source. If the source is (partially) removed or naturally depletes, the vapour plume will shrink. The timescale of LNAPL depletion by vapourisation depends upon, for example, the original mass of LNAPL released, its surface area and geometry, vapour pressure, diffusion coefficients for constituent compounds, and distances to boundaries (e.g., ground surface).

4.2.4. Vapour intrusion into buildings

A significant body of literature exists on the risks of VI into buildings (Abreu and Johnson, 2005; 2006; DeVaull, 2007; ITRC, 2014; Johnson and Ettinger, 1991; Lahvis, 2005; Lahvis *et al.,* 2013; Ma *et al.,* 2012; USEPA, 2012). Mobile LNAPL or contaminated groundwater may be brought into proximity of a building foundation by a shallow, perched or rising water table. Cracks, pores or other openings in the foundation or unpaved floor may then allow VI,

or even LNAPL seepage, into the building. Where the air permeability of soils exceeds ~10-12 m^2, VI into buildings is usually controlled by the lower air pressure within the building relative to the adjacent porous media. A zone of influence may develop beneath the building, supporting advection of VOC vapours towards its substructure and through foundation cracks. Vapour-phase fluxes may then potentially exceed those from diffusion alone. Various models are available to predict VI into buildings for different scenarios (EA, 2002; Tillman and Weaver, 2005).

Buildings with a large footprint can also limit oxygen migration beneath the centre of the structure, which may lead to enhanced vapour transport under drier conditions (Knight and Davis, 2013). Establishing the potential for natural attenuation of vapours in the underlying subsurface is critical for the assessment of VI from LNAPL sources. Although many petrol filling stations are located in urban/residential areas, VI risks from fuel releases are often not found to be significant, due to the high aerobic biodegradability of petroleum hydrocarbon contaminants (Lahvis, 2005; Lahvis *et al.,* 2013; USEPA, 2012).

4.3. Natural source zone depletion

Natural source zone depletion (NSZD) simply recognises that source zones, including LNAPL in the subsurface, may deplete naturally. Key LNAPL depletion processes include: LNAPL dissolution into groundwater and biodegradation in the saturated zone; LNAPL vapourisation, volatilisation and biodegradation in the partially saturated zone, and direct biodegradation of LNAPL (ITRC, 2009b). NSZD is conceptualised in Fig. 4.6. The first two processes have largely been discussed above. Direct biodegradation of the LNAPL has received less study.

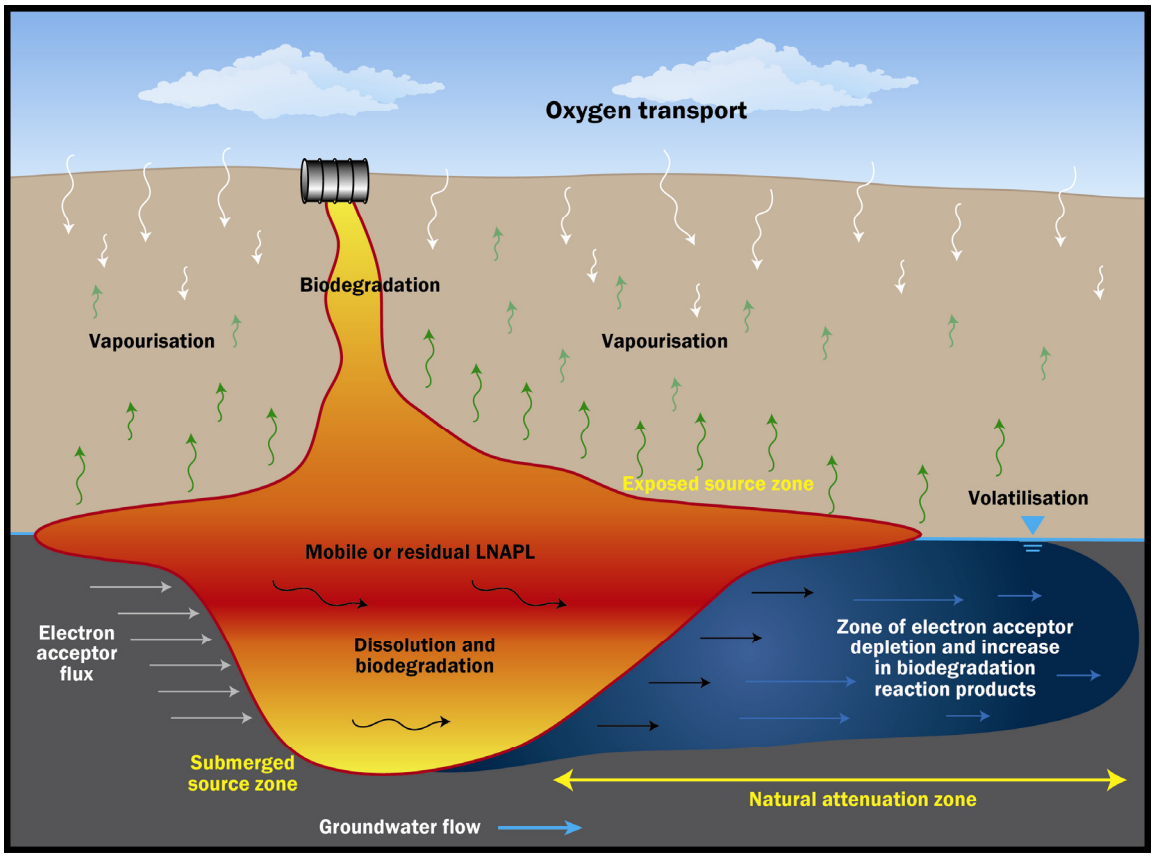

Figure 4.6. Conceptual model of LNAPL NSZD (adapted from ITRC (2009b)).

Although it is typically assumed that biodegradation processes in the source zone are limited by the mass transfer of organic compounds into the adjacent aqueous phase (dissolution), there is potential for bacteria to enhance this transfer, especially where NAPL constituents are not toxic to *in situ* microorganisms. Observations have been made of bacteria attachment to NAPL surfaces and also excretion of enzymes with the capacity to increase NAPL-to-water partitioning rates (Efroymson and Alexander, 1994a,b).

NSZD of LNAPL may therefore involve several processes that act together to physically redistribute LNAPL components to aqueous and gaseous phases and/or microbiologically break down source zone components (ITRC, 2009b). The rates of NSZD may be expected to vary with LNAPL composition and its physical/chemical properties which control the dissolution, vapourisation and potential for biodegradation of constituent compounds within the aerobic and anaerobic environments that may locally exist. Contrasting LNAPL distributions within diverse hydrogeological environments (Section 5) will likewise lead to contrasting rates of NSZD and dictate the need for specific site-by-site evaluations to rigorously assess NSZD potential (ITRC, 2009b). As many site spills are now perhaps decades old without on-going fresh releases (following departure of industry or implementation of more effective environmental controls), NSZD is anticipated to assume increasing importance in the long-term fate of LNAPL in the subsurface. Recent surveys over the last decade, for example the extensive review of sites in California by McHugh *et al*. (2012), illustrate a decline in plume size and contaminant concentrations over the long-term. This occurs for BTEX, MTBE and its principal biodegradation product, tert-butyl alcohol (TBA). These observations are attributed to (and illustrate the potential importance of) a combination of NSZD, natural attenuation of the plume, improved environmental controls and phasing out (or reduced product contents) of some of these components in fuel.

5. Conceptual models of LNAPL behaviour in common hydrogeological systems

5.1. Conceptual site models

A conceptual site model (CSM) of a LNAPL-impacted site is a representation or description of the site and the processes that control contaminant transport and fate. These processes need to be understood in order to identify hazards and assess the actual levels of risk. The CSM is used for identifying and assessing potential hazards, and for screening, characterising, assessing and managing risks posed (Gormley *et al*., 2011). It includes the physical-chemical state and distribution of the LNAPL and the dissolved and vapour-phase plumes produced. Within the CSM, these are linked to the plausible source-pathway-receptor linkage scenarios to evaluate how the LNAPL source may potentially impact receptors and underpin the estimation of associated risks. Key process-based components inherent to the CSM for LNAPL sites are illustrated in Fig. 1.2 and other detailed process-based conceptual figures in Sections 2 to 4.

CSMs are iteratively developed in conjunction with site investigation and assessment phases. The level of detail required is site-specific and related to the complexity of environmental conditions at a site, the regulatory framework, and site management objectives. Information typically required to develop a CSM for a LNAPL-impacted site may include (ASTM, 2007; EA, 2001; ITRC, 2009a):

- site setting (historical and current): land use, LNAPL use/storage (including amounts and periods) and release mechanisms, groundwater classification and use, receptor presence and proximity, etc.
- geological and hydrogeological information/setting;
- LNAPL physical (density, viscosity, interfacial tension, vapour pressure) and chemical (constituent chemistry, solubility and mole fractions) properties;
- LNAPL body spatial distribution (vertical and horizontal);
- LNAPL mobility and body stability information;
- LNAPL recoverability information;
- associated dissolved-phase and vapour-phase plume information; and
- LNAPL NSZD processes.

The CSM is a framework where the uncertainty in site understanding can be explored and the need for additional information against the improvement in certainty and cost can be evaluated. Ultimately, the judgment of the environmental professional must assess whether sufficient information has been gathered to make appropriate remediation decisions (Gormley *et al*., 2011; ITRC, 2009a).

5.2. Exemplar hydrogeological environments

Table 5.1 summarises the various exemplar hydrogeological environments that could exist based upon commonly encountered aquifer material and flow characteristics. These cover intergranular sediments and bedrocks of contrasting permeability and porosity types, and made (artificial) ground. Examples of these various environments are listed and are further developed as annotated CSMs. The examples provided are specific to the exemplar hydrogeological environments tabulated. However, further combinations of the environments are likely (e.g., superficial sediments over fractured bedrock) in which case, it is necessary to understand the LNAPL distribution within the overlying media, and use that as the source to the underlying media. Although the CSMs depict some of the more commonly expected behaviours, they cannot reflect all behaviours. Hence they should be applied with judgment and appropriate local extension to any actual case environment being considered. It should also be recognised that the conceptualisations are based upon the expected occurrence of LNAPL in the actual subsurface geological environment rather than the distribution of LNAPL that may be observed in monitoring wells. Based on the processes controlling LNAPL entry and behaviour in wells under transient conditions (Fig. 3.6), monitoring well observations alone are generally expected to be a poor basis for conceptualising the actual distribution of LNAPL present (Abdul *et al*., 1989). Rather, understanding the processes controlling the transport and fate of LNAPL in the porous or fractured hydrogeological domain of interest is key to producing representative CSMs.

Table 5.1. Exemplar hydrogeological environments.

Hydrogeological environment	Formation characteristics	Flow characteristics	Geological exemplars	Figure and Section Number
Intergranular superficial (drift) sediments	Low heterogeneity	High permeability	Beach Sands	Fig. 5.1 Section 5.3
		Low permeability	Marine Clays	Fig. 5.2 Section 5.4
	High heterogeneity	High permeability	Glacio-fluvial sands and gravel	Fig. 5.3 Section 5.5
		Low permeability	Glacial till	Fig. 5.4 Section 5.6
Bedrock	Low matrix porosity	Small aperture fractures	Granite / Igneous rock	Fig. 5.5 Section 5.7
		Large aperture fractures	Karst limestone	Fig. 5.6 Section 5.8
		Fracture and matrix	Cemented sandstone / gritstone	Fig. 5.7 Section 5.9
	High matrix porosity	Large aperture fractures	Chalk	Fig. 5.8 Section 5.10
		Small aperture fractures	Shale / Mudstone	Fig. 5.9 Section 5.11
		Fracture and matrix	Sandstone	Fig. 5.10 Section 5.12
Anthropogenic strata	High heterogeneity	Both low and High permeability	Made Ground, Backfill	Fig. 5.11 Section 5.13

5.3. LNAPL release into beach sands

LNAPL release within a beach sand environment may be influenced by some minor heterogeneity involving perhaps fine-scale layering or ripple structures and cross-bedding (Fig. 5.1). Most LNAPL will migrate vertically downwards under the influence of gravity with minimal lateral spread, although some fine-scale layering of residual saturations may be evident reflecting permeability variations. Low levels of LNAPL residual within the partially saturated zone may be expected. A well-defined vapour plume will radially develop, reflecting the sand's homogeneity. However, due to the sand's porous nature, oxygen easily penetrates and biodegradation may limit vapour migration to building receptors at surface.

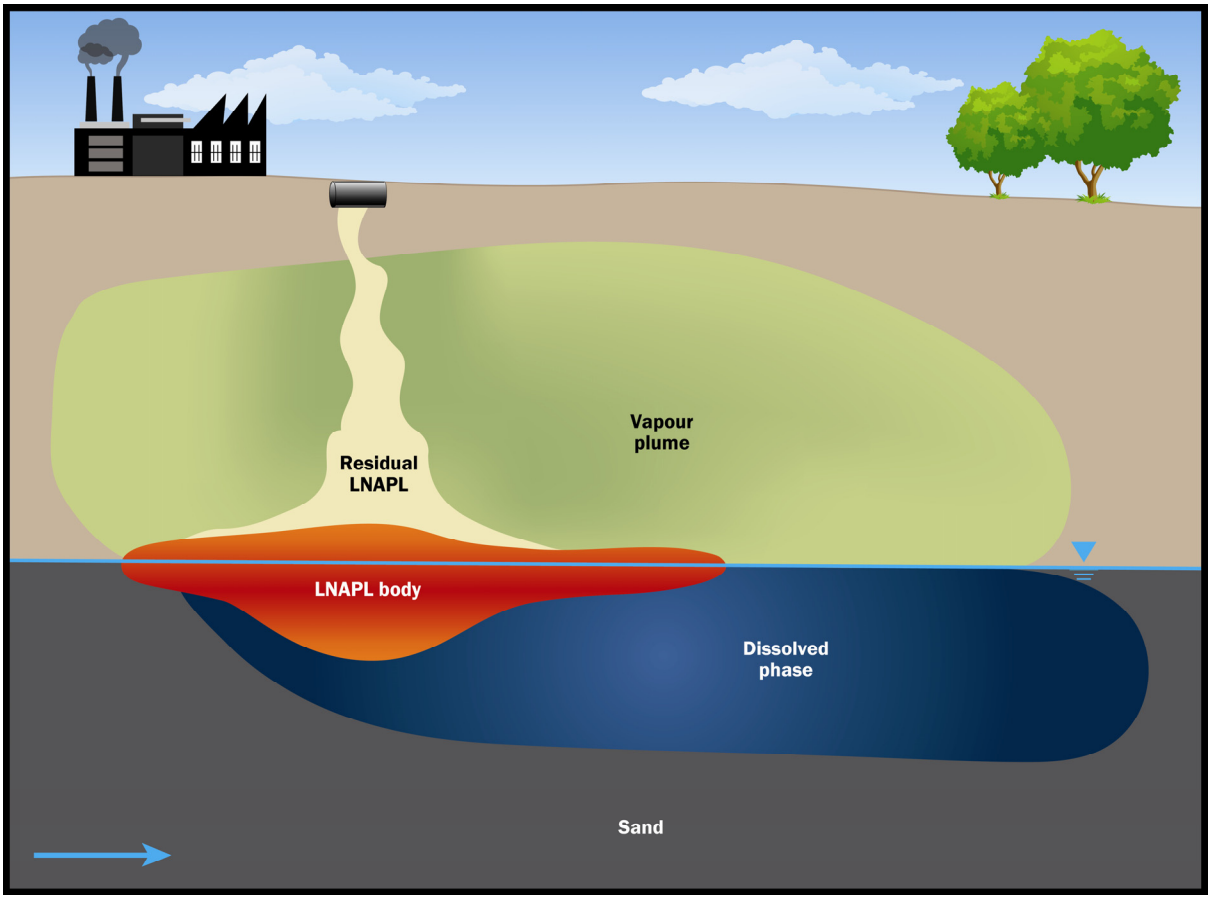

Figure 5.1. LNAPL release into beach sands.

Depending upon the LNAPL release volume and hence gravitational head, the LNAPL will be driven below the water table, mound and spread laterally as the LNAPL gradient and driving forces exceed pore entry pressures. These may be fairly low and uniform due to the sand's permeability and homogeneity and will facilitate spread of the LNAPL as it easily enters pores vertically and laterally with less driving force (height of LNAPL). The LNAPL spreads until the source area comes to equilibrium with the lateral pore entry pressures. The typical distribution is one of a greater vertical penetration below or near the release location, with radial lateral spreading biased down the water table gradient. The LNAPL source area is typically easy to define and locate within these types of geologies.

With respect to dissolved-phase and vapour-phase plume migration, these will form readily from the LNAPL source area. Dissolved-phase plumes tend to be longer in more porous inter-granular media; however, the plume will potentially reach a steady state-limited growth depending upon the fluxes of electron acceptor replenishment. Soon after hydrocarbon contamination enters the groundwater system, rapid depletion of dissolved oxygen caused by increased levels of aerobic microbial respiration results in the establishment of anaerobic conditions. The type of anaerobic degradation that dominates depends on the type of electron acceptor present, pH conditions, redox potential and microbial competition. Processes can vary temporally and throughout the plume. Typically, sulphate-reduction dominates followed by methanogenesis. Relatively easy oxygen penetration within the partially saturated zone vapour and recharge water will allow for fairly effective aerobic degradation of hydrocarbons down gradient.

5.4. LNAPL release into marine clays

Conceptualisation of LNAPL fate within a Marine Clay setting is illustrated in Fig. 5.2., showing both a continuous clay unit, and clay over an underlying more porous aquifer. Clay is water wet and will typically remain water wet even within the partially saturated zone. LNAPL will pool on competent clay in the partially saturated zone; however, clays may be fractured due to desiccation, weathering or root holes, affording the LNAPL and/or its dissolved-phase plumes the ability to locally penetrate the clay (White *et al*., 2008).

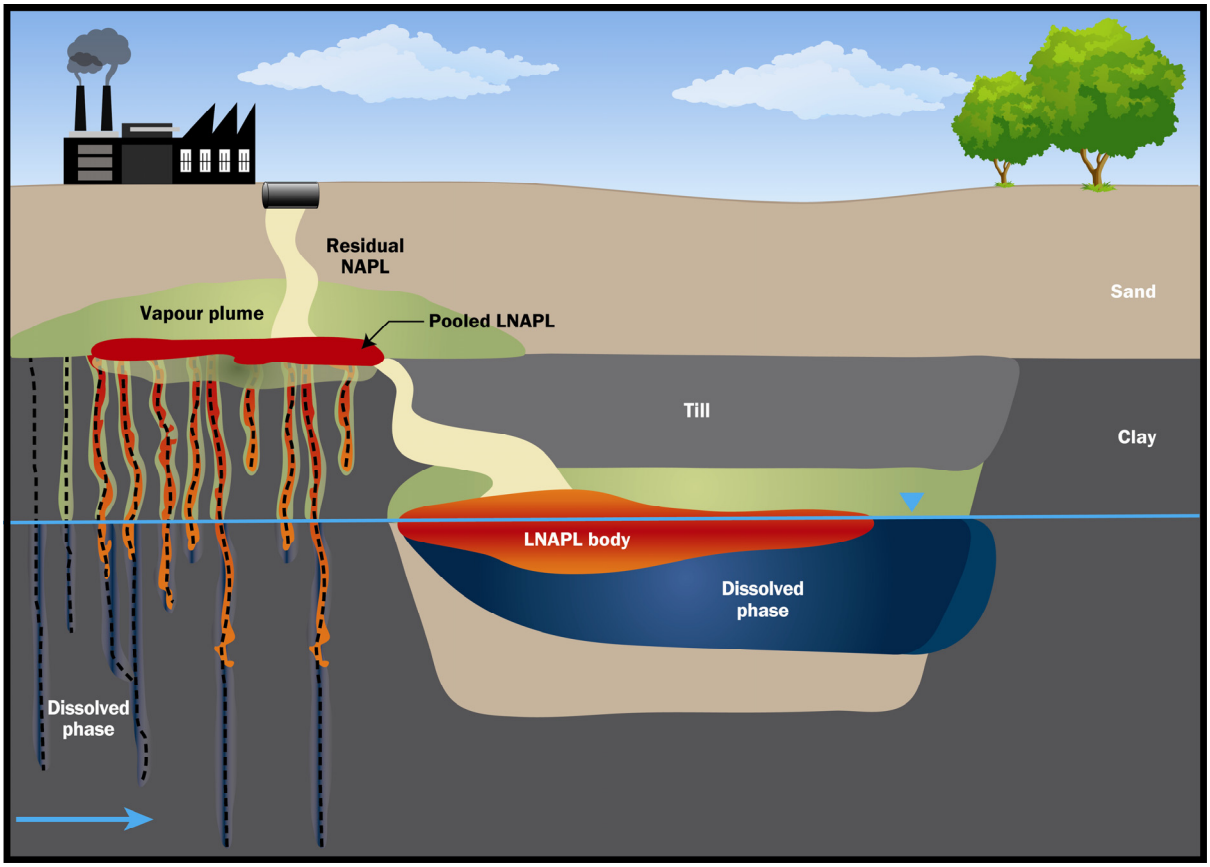

Figure 5.2. LNAPL release into marine clays.

The sparse nature of sand seams and macro-pores means that LNAPL migration pathways may not be found by site investigation. Given this elongated distribution within the more porous secondary porosity through the partially saturated zone, if a well penetrates one of these localities within the saturated zone the LNAPL thickness will be uncharacteristically great within the well, even though the saturation levels are not elevated within the clay unit and are likely less than 5%.

LNAPL will typically fail to overcome high pore-entry pressures in competent clays and so will pool. Within a layered stratigraphy, clay will cause further lateral LNAPL spread within the partially saturated zone due to migration under the influence of gravity. The edge of the clay or pathway through (stratigraphic window) may facilitate vertical LNAPL penetration.

Chemicals within the LNAPL will diffuse into and accumulate within the clay matrix as dissolved and sorbed phases. This mass stored within the clay matrix, due to concentration gradient reversal and slow back-diffusion at later time, may act as a longer term secondary source to dissolved- and vapour-phase plumes in any adjacent more permeable fracture zones or aquifer units. The clay matrix may limit biodegradation opportunities as the low permeability and small pore sizes limit microbial growth and mobility, as well as the replenishment of nutrients to maintain microbial activity.

Macropores will exaggerate the LNAPL thickness within a clay formation due to fracturing, root holes, and stratigraphic windows and may allow penetration through relatively thin clays (Adamski *et al*., 2005). The LNAPL saturation will be low within the clay formation even if metres of LNAPL are measured within the well column, which may inadvertently serve as a drainage collection point (sump) for the LNAPL. In the case of fluctuating water table levels, the LNAPL body within the lower aquifer shown in Fig. 5.2 could rise to the base of the overlying clay aquitard and cause a confined LNAPL condition (Kirkman *et al*., 2012). The confined LNAPL condition will be observed as rising measured LNAPL thickness within the well. As the potentiometric surface ("virtual water table" plane defined by wells that are completed in a (clay-)confined aquifer) rises into the clay unit above, the LNAPL upward movement is resisted and the monitoring well is a pressure release for the LNAPL. As the LNAPL is lighter than water and is non-wetting relative to water, the well preferentially is filled by LNAPL. A confined LNAPL condition can lead to over-estimation of the mass of LNAPL within the formation if not properly considered.

5.5. LNAPL release into glacio-fluvial sands and gravel

Fig. 5.3 illustrates a release of LNAPL into a glacio-fluvial deposit comprised predominantly of permeable sands and gravels. LNAPL has migrated laterally in all directions in response to the high heterogeneity of the stratification that results from the layered depositional nature of the formation. The LNAPL will follow a stratified flow pattern through the partially saturated zone following the bedding structure of the unconsolidated deposits. Depending on the thickness of the sequence above bedrock, the nature of the deposition of the glacio-fluvial deposits typically results in greater permeability with depth, allowing greater LNAPL migration. For LNAPLs with volatile components (e.g., petrol), a well-defined vapour plume will develop. Depending on the bedding structures, soil sampling to determine LNAPL presence may be a 'hit and miss' proposition because of the tortuous and sparse nature of migration pathways. A more efficient way of determining the lateral extent of the source zone

may be soil vapour or biodegradation off-gas measurement where the LNAPL gives rise to vapours and/or degradation signatures such as carbon dioxide.

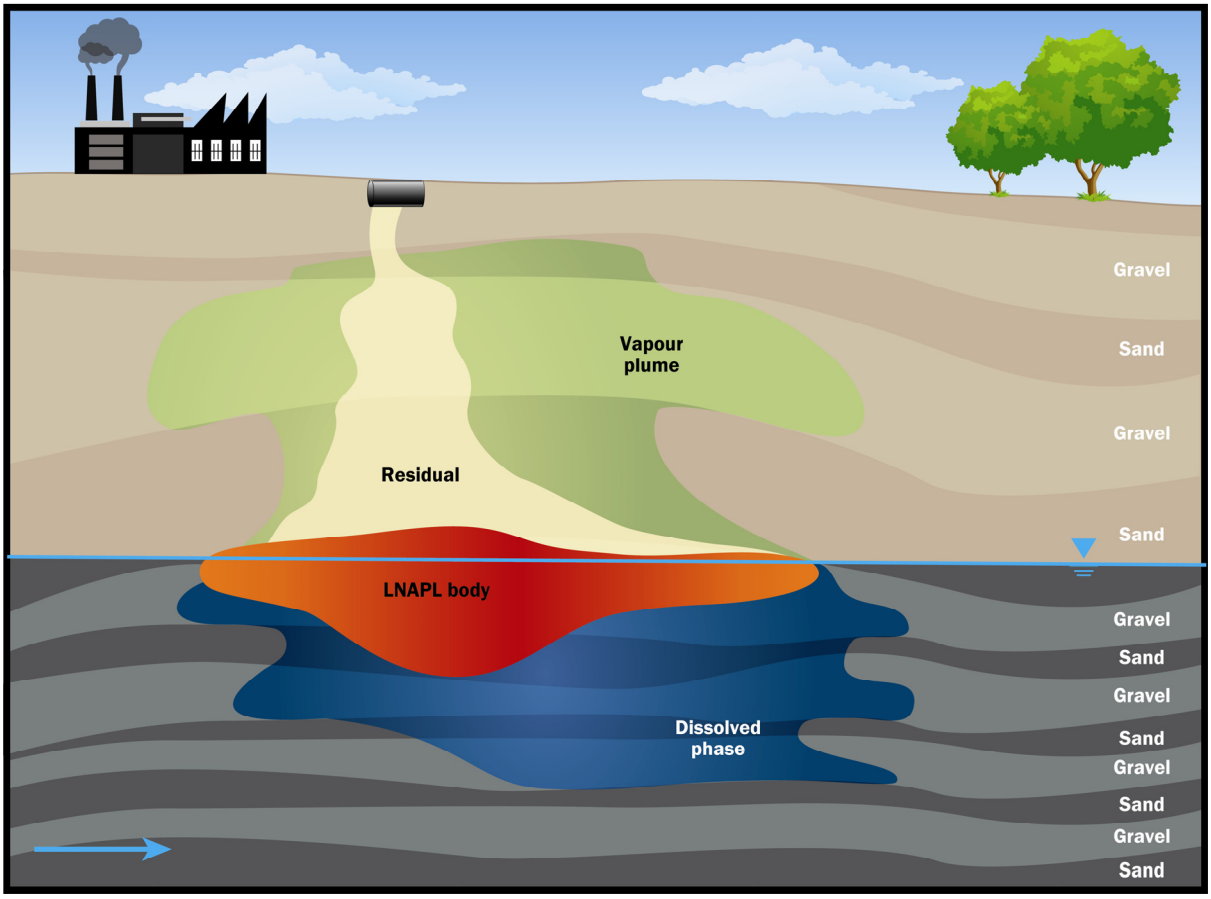

Figure 5.3. LNAPL release into glacio-fluvial sands and gravels.

Given sufficient volume of LNAPL released, the LNAPL will infiltrate to the saturated zone where gravitational head, if sufficient, will allow LNAPL to penetrate through the capillary fringe and below the water table. The bedding structure and stratigraphy aid in limiting the vertical penetration, and the LNAPL may spread radially due to mounding with preferential migration along more permeable and continuous gravels. The LNAPL will continue to spread laterally until there is insufficient gravitational head and gradient to overcome the pore entry pressure of the leading edge of the LNAPL source area. A dissolved-phase plume will form from the LNAPL source area, and will move in the direction of groundwater flow, reaching varying distances due to the variability in the layered deposits, again with potentially greater extent in the more permeable gravels. Given higher velocities within the gravel, plume development tends to dominate in these higher permeability zones but will reach a steady state with aerobic biodegradation at the leading plume edge.

5.6. LNAPL release into glacial till

Fig. 5.4 illustrates a surface release of LNAPL into a thick sequence of clay-rich glacial till. Glacial till is a poorly (or even un-) sorted glacial sediment directly deposited by a glacier. Till varies from clays to mixtures of clay, sand, gravel and boulders. The predominant material is low in permeability and of very high heterogeneity. Some glacial tills, such as

lodgement tills, were deposited in layers and may vary from being laterally extensive to local laterally limited lenses and layers. Given the lower permeability of the strata, the LNAPL within the partially saturated zone tends to spread laterally on the lower permeability layers until vertical pathways through more permeable material within the till are encountered and vertical migration of the LNAPL may ensue. The LNAPL will hence migrate rather tortuously through the till given its lack of structure, with preferential, albeit tortuous migration through the zones of higher permeability that may promote lateral spreading.

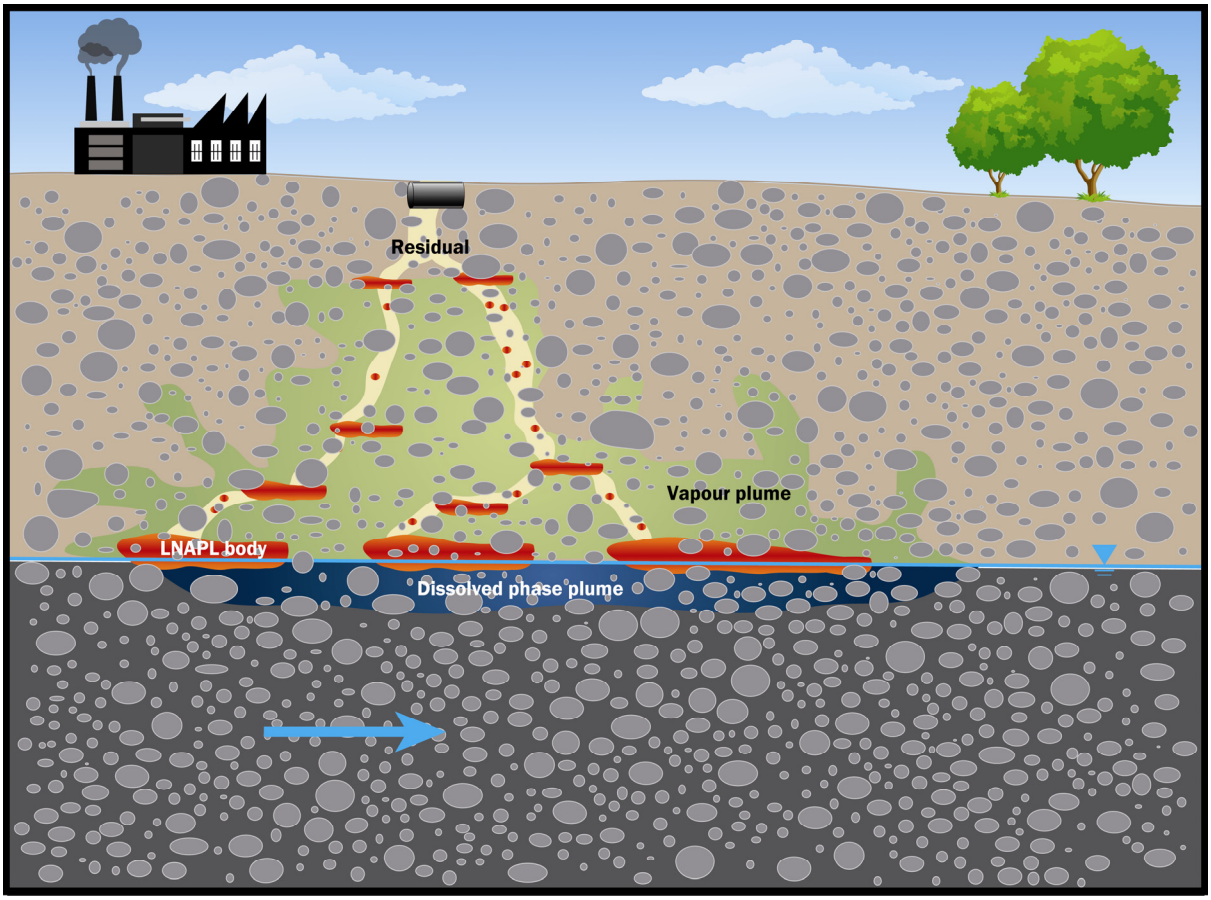

Figure 5.4. LNAPL release into a glacial till.

Once the LNAPL reaches the saturated zone, penetration within and below the water table will be quite limited as the gravitational head is likely disconnected and the LNAPL that has migrated to the water table is often discontinuous to the release point. Mounding of the LNAPL in response to buoyancy forces and the very low permeability of the water-wet clay within the till will enhance lateral spreading within fractures or other higher permeability soils near the water table elevation. LNAPL is unlikely to penetrate till sequences that are exceptionally thick. Residual and mobile LNAPL are retained in any sand horizons that transmitted LNAPL during the release or were later exposed to LNAPL by seasonal water table fluctuations.

Given their sparse nature, LNAPL migration pathways may not be (or sporadically) encountered directly by site characterisation efforts making it difficult to constrain the source LNAPL with confidence. Over time, LNAPL chemicals contacting lower permeability soils

will diffuse into the matrix to become secondary sources of contaminant. Accumulated matrix contaminants may ultimately be released by back diffusion along reversed chemical concentration gradients.

The migration of vapours within the partially saturated zone and dissolved phase within the saturated zone will similarly be tortuous and follow the interface between the clay material and the more porous sands and gravels. The tortuous nature of the till limits the vertical penetration of oxygen within the partially saturated zone, thus the anaerobic degradation zone tends to extend higher above the water table. Dissolved-phase plumes tend to be muted due to the heterogeneity, as oxygen-rich infiltration water will be biased to the more permeable zones of the till and enhance aerobic biodegradation within these zones. Once the oxygen is depleted these higher permeability zones will tend toward anaerobic biodegradation similar to the lower permeability zones, usually with sulphate-reduction predominant.

5.7. LNAPL release into granite / igneous rock

LNAPL migration within granite is fracture-dominant with very limited (if any) migration into the matrix due to its very low (or absent) porosity and permeability; granite typically has a total porosity of ~0.1% and effective porosity of ~0.0005%. Fig. 5.5 shows a LNAPL release within the overburden (i.e., material overlying the bedrock) and migration vertically and preferentially within fractures of the chemically and physically weathered shallower granite saprolite. This material is predominately sand and gravel with lesser amounts of clay. Some lateral LNAPL migration will occur as the rock matrix and clays within this saprolite zone have very low permeability, thus resisting LNAPL penetration; however, the fractures between more competent granite matrices are typically filled with porous sands and gravels, which can allow migration to the water table.

The weathered granite bedrock results mostly from fracturing, with little rock matrix chemical decomposition (and hence porosity). LNAPL migration is predominantly within vertical and sub-vertical fractures. Because of the low fracture porosity and gravitational head from the LNAPL release source, LNAPL can penetrate into the fractures within the water-saturated bedrock. LNAPL penetration can be estimated based upon the balance between the driving force (LNAPL head; distance from source to water table) and the buoyancy of LNAPL and aperture water displacement pressure (i.e., capillary pressure) within a known or estimated aperture width (Section 3.6). Fracture frequency and size decreases with depth and LNAPL will be present as both mobile and residual LNAPL within fractures. Further LNAPL migration is possible within the fracture as water levels vary and/or LNAPL buoyancy influences that can cause upward invasion of overlying fractures.

LNAPL will migrate preferentially in the larger aperture fractures and can spread laterally in all directions, including hydraulically up gradient of the release location. Groundwater flow through the fractures causes LNAPL dissolution and the evolution of a dissolved-phase plume. As granite has extremely low porosity, LNAPL does not enter the matrix as a separate liquid phase, with very little (or any) penetration by the dissolved-phase constituents.

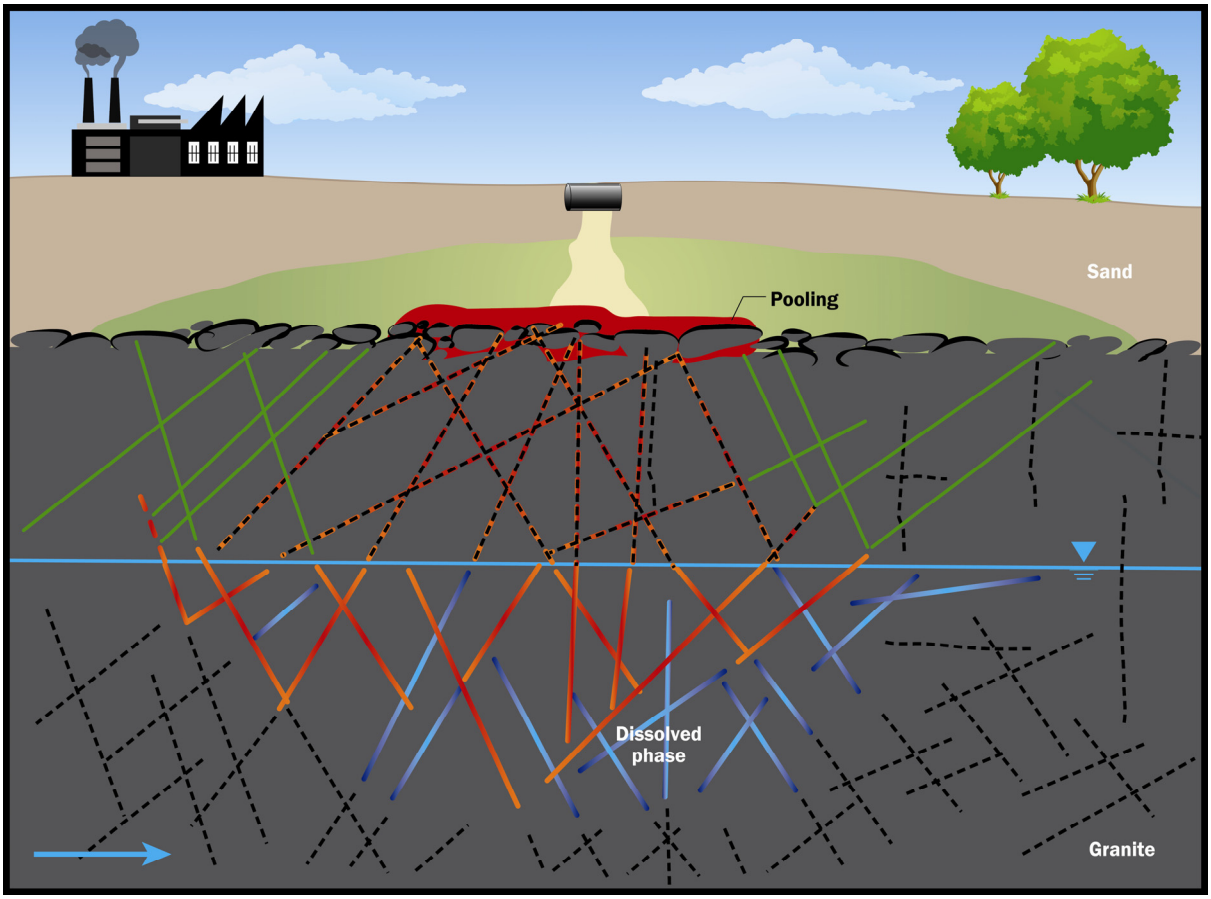

Figure 5.5. LNAPL release into a granite or igneous rock.

The dissolved-phase plume may migrate through the set of interconnected fractures and is subject to advection, dispersion and biodegradation. Diffusion of aqueous-phase contaminants is unable to occur in non-porous granite, but may occur within unconsolidated weathered granite. Biodegradation of plumes is likely limited due to the restricted replenishment of oxygen and nutrients. Also, the typical acidic nature of groundwater in granites will inhibit microbial activity.

5.8. LNAPL release into karst limestone

LNAPL migration within a karst limestone is, like granite, predominantly controlled by the fracture domain, which may often contain predominant sub-vertical and sub-horizontal fissuring. However, fractures are of much greater aperture and connectivity laterally. Limestones often form transmissive aquifer units of high water resource value. Groundwater flow through fissures alongside chemical dissolution of soluble layers of bedrock may lead to major fissure, even cave, (karst) system development.

Figure 5.6 conceptualises a LNAPL release within the overburden of weathered limestone. This consists of a conglomerate similar to glacio-fluvial sands and gravels in which the LNAPL is spread laterally (Section 5.5). As the LNAPL continues to migrate downwards through the partially saturated zone, more competent limestone physically impedes the downward migration and the LNAPL continues to spread laterally within the fractures. Once the LNAPL reaches the saturated zone, the LNAPL will penetrate below the water table if

sufficient gravitational head is present to overcome the buoyancy of the LNAPL and the pore entry pressure of the soil from the decomposed bedrock that may exist within the fractures of the karst limestone.

In some areas, the LNAPL may enter and pool within open dissolution cavities at the water table interface. Given the typically low permeability of the limestone rock matrix and dominance of fracture flow, water table fluctuation on the order of tens of metres is not uncommon. These fluctuations and large fracture apertures give rise to the potential for LNAPL entrapment under confined conditions, i.e., entrapment by an overlying low permeability layer, for example, a marl horizon. With continued water table rise, the confined pressure will continue to increase, resulting in the potential for LNAPL breakthrough and pipe flow of buoyant LNAPL within the overlying fractures.

The open cavities within karst limestone, provide increased surface area of the LNAPL for vapourisation. The conduits within the karst provide preferential pathways for vapour migration and dissolved-phase plume migration. The dissolution of more soluble components within a LNAPL mixture will cause its viscosity and density to increase with time and its mobility to decrease. Where the limestone matrix is more porous, then it may behave in a more chalk-like way (Section 5.10) with, for example, diffusive losses of LNAPL occurring to the matrix pore water.

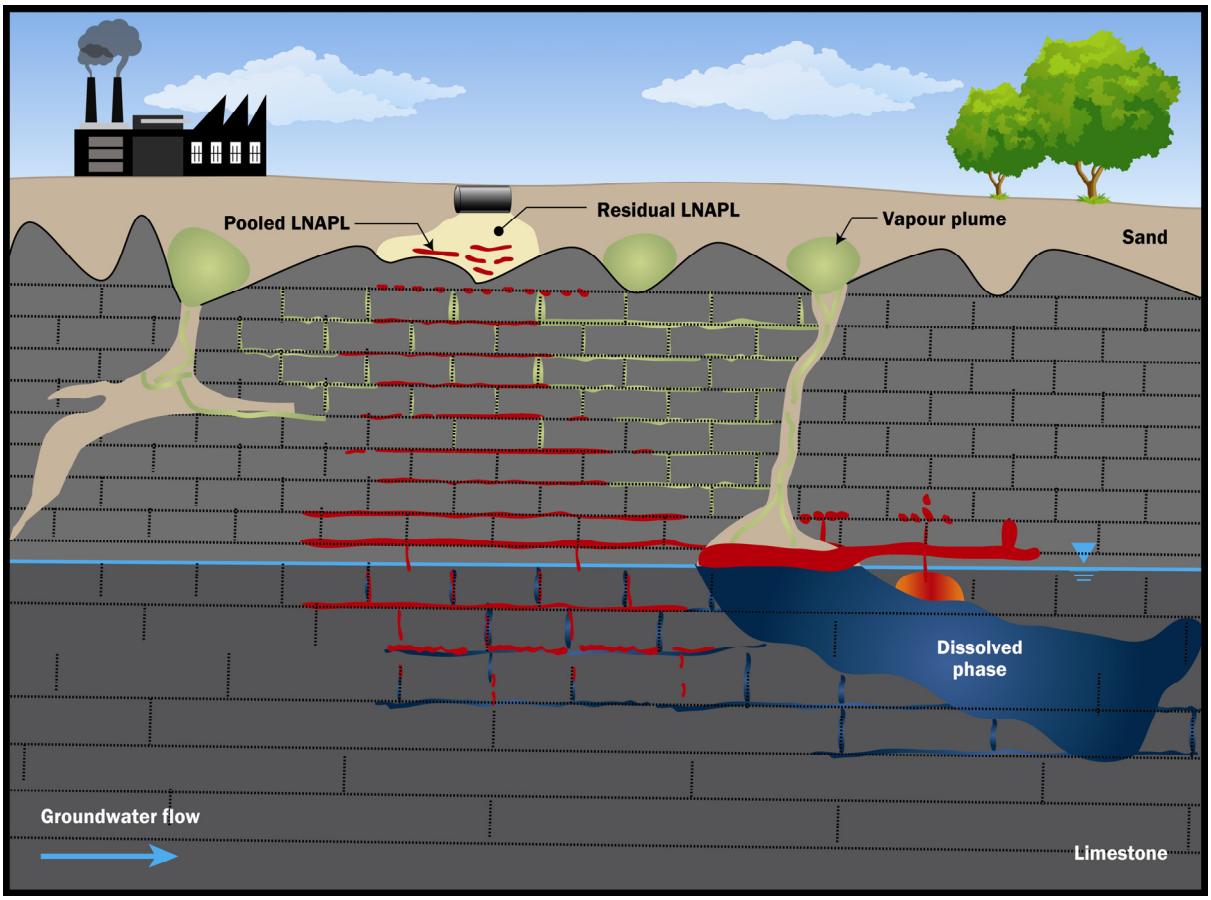

Figure 5.6. LNAPL release into a karst limestone.

5.9. LNAPL release into cemented fractured sandstone

Fig. 5.7 illustrates a release of LNAPL into weakly fractured sandstone or a gritstone that has a low permeability and low porosity matrix due to cementation. The LNAPL will migrate down through the overlying more permeable sands and may pool on the low permeability sandstone matrix. LNAPL migration is predominantly within vertical and sub-vertical fractures under the influence of gravity. With time, LNAPL may penetrate into the matrix if the pore entry pressure is exceeded. There will be preferential entry into the more coarse-grained lithologies. Volatile components will form a vapour plume, which will also preferentially migrate along available fractures and, to a lesser extent, the more permeable sandstone matrix lithologies.

As there is low matrix porosity, given sufficient gravitational head from the LNAPL release source, the LNAPL will penetrate the fracture network below the water table. LNAPL penetration can be estimated from the balance between the driving force or LNAPL head (vertical distance from source to water table) and that of the buoyancy of LNAPL and aperture water displacement (capillary) pressure within an estimated aperture width (Appendix 1). Further migration is possible within the fracture network due to water level fluctuations and LNAPL buoyancy effects. The lateral and vertical migration reduces with time as the higher permeability parts of the matrix may potentially allow some LNAPL invasion and/or diffusive losses into the matrix become significant. With time, the LNAPL becomes more disconnected with less gravitational head to exceed the matrix pore entry pressure.

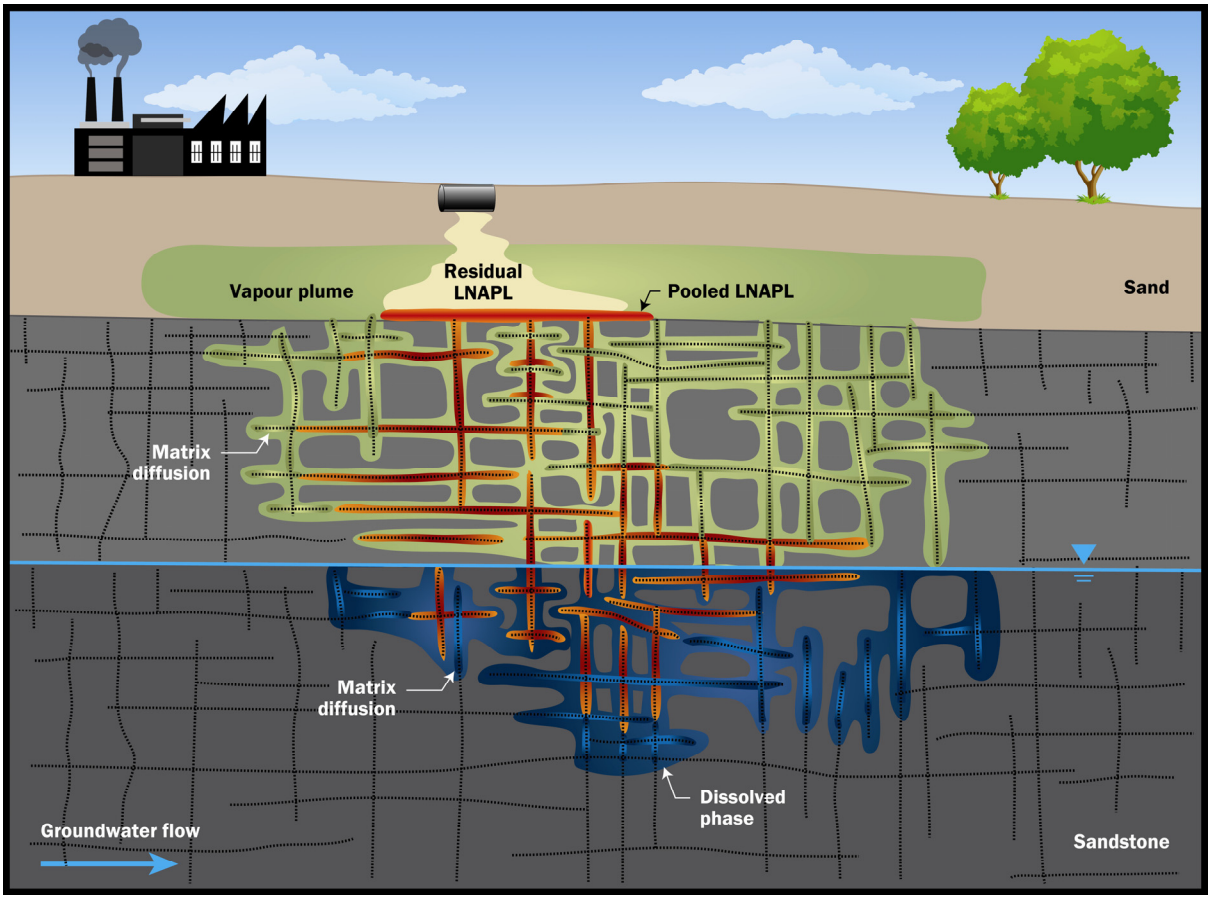

Figure 5.7. LNAPL release into cemented sandstone.

LNAPL will migrate preferentially in the larger aperture fractures and spread laterally in all directions, including up gradient within vertical and sub-vertical fractures. Groundwater flow through the fractures containing residual and mobile LNAPL can lead to the development of a dissolved-phase plume. LNAPL will continue to penetrate into the matrix during the cyclical water table fluctuations with entry into the matrix within the saturated zone limited due to the higher pore entry pressure. However, above the water table some areas of the matrix have very low water saturations and weathering-induced porosity increases, which may allow additional LNAPL migration into the matrix. Groundwater flow within the fractures and matrix may be similar but, as the matrix is water wet, LNAPL flow into the matrix requires sufficient gravitational head or other driving force to exceed the inherent entry pressure. Thus, the LNAPL flow preference is through the fracture network.

The dissolved-phase plume migrates through the interconnected fractures, but not as far as would be predicted by simple groundwater velocity calculations due to diffusion into the adjacent matrix. Through ageing of the LNAPL, the resulting dissolved-phase and vapour-phase plumes will eventually degrade naturally. The leading edges of the plume will normally be aerobic and the core anaerobic.

5.10. LNAPL release into fractured chalk

Fig 5.8 illustrates a release of LNAPL into superficial deposits overlying fractured Cretaceous chalk. Chalk is formed from the mineral remains of tiny marine organisms and is chemically relatively pure calcium carbonate ($CaCO_3$). In the overlying superficial deposits, LNAPL has migrated laterally in all directions in response to the bedding structure present. The LNAPL release volume in this example is sufficient to reach the highly fractured weathered chalk. Within the partially saturated zone, the gravity-driven LNAPL migration is predominantly within vertical and sub-vertical fractures.

The very small pore size of the matrix, means that entry pressure to the water-wet, capillary-saturated, matrix is prohibitively high. Thus, there is limited chance of LNAPL penetrating into the matrix unless weathering-induced porosity increases exist. The low fracture porosity, gravitational head of the LNAPL, coupled with the inability of the LNAPL to penetrate the chalk matrix leads to the LNAPL penetrating the bedrock through the fracture network. In the region of water table fluctuation, the fracture network is enhanced by dissolution weathering. Large, catastrophic releases of LNAPL can lead to significant vertical penetration of LNAPL in fractured chalk (Wealthall *et al*., 2002). Similar to granite, the penetration of LNAPL can be estimated using a balance of the various forces. Likewise, further migration is possible in fractures due to imbibition of groundwater either pushing against the LNAPL within the fractures as water levels vary or due to LNAPL buoyancy, which can cause upward invasion of overlying fractures.

LNAPL migrates preferentially in the larger aperture fractures and spreads laterally in all directions, including hydraulically up gradient. The combination of the gravitational head and the severe water table fluctuations within the chalk further enhance elongation of the LNAPL source zone. Groundwater flow through the highly transmissive fractures containing residual and mobile LNAPL results in LNAPL dissolution and the development of potentially very extensive dissolved-phase plume subject to diffusion losses to the adjacent porous matrix, as well as biodegradation (primarily within the fracture network). Extensive water table fluctuations and the relatively rapid turnover of water in the fracture network will aid the influx

of oxygen to the plume periphery facilitating aerobic degradation, although the source and plume core below the water table can be expected to be predominantly anaerobic.

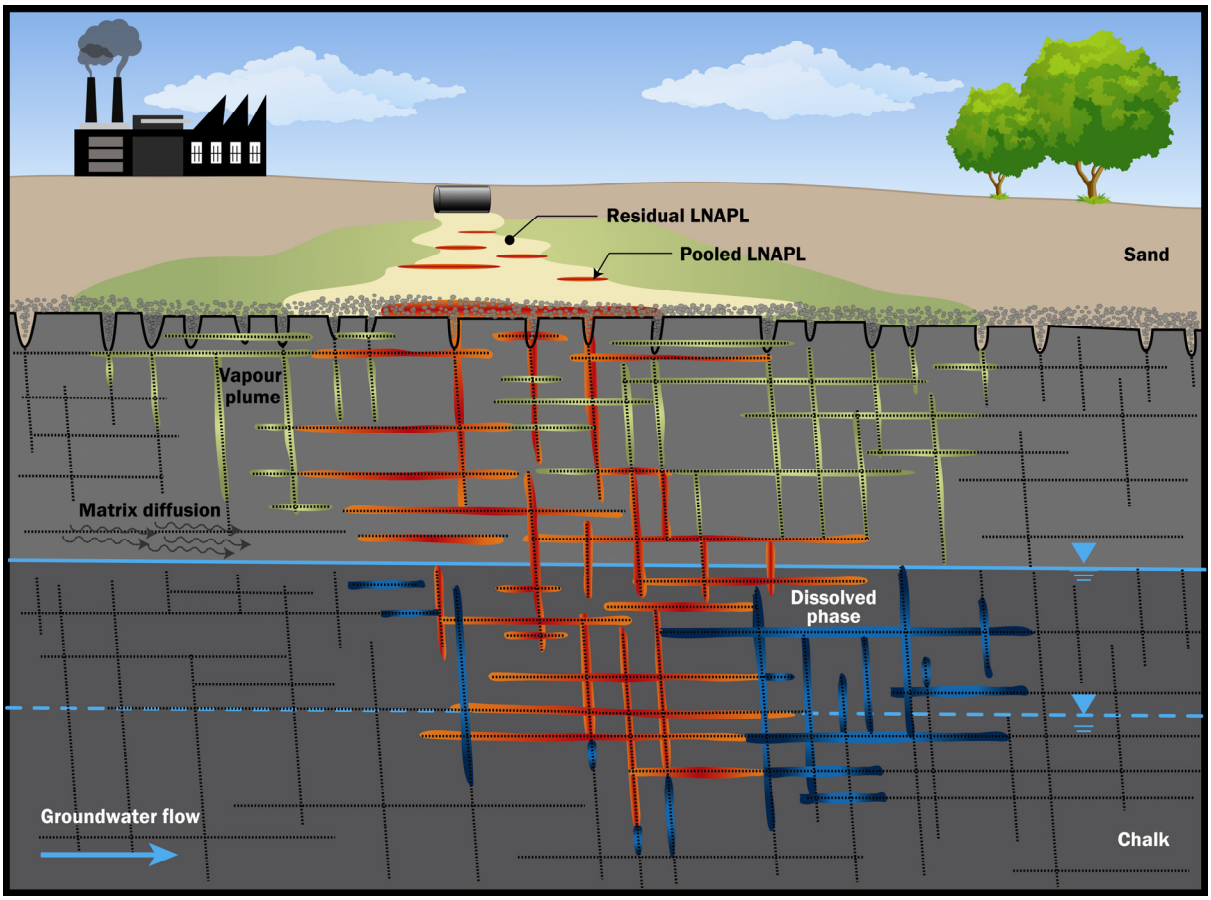

Figure 5.8. LNAPL release into fractured (Cretaceous) chalk.

5.11. LNAPL release into fractured shale or mudstone

Although thick sequences of fine-grained shale and mudstone sedimentary rocks will effectively function as competent aquitards, shallower horizons (exposed to less effective stress) may have some permeability associated with them. This is due to micro-fracturing, the presence of coarser-grained mudstones and/or where bands of soluble minerals such as gypsum may have dissolved away. Fractures associated with faulting in mudstones may also result in preferential LNAPL migration pathways. In the proximity of faults LNAPL migration may be enhanced parallel to the fault and be reduced across the fault due to reduced permeability associated with fault gouge.

In the example CSM (Fig. 5.9), LNAPL has been released into shale or mudstone, which is highly weathered within the partially saturated zone. There is a network of fractures situated along predominantly horizontal and sub-horizontal bedding planes that causes a lateral spread of LNAPL. Weathering within the partially saturated zone may result in near-vertical breaks in the bedding planes that may facilitate migration of the LNAPL to the water table. However, given the predominant fracture array and orientation is near-horizontal it is probable the LNAPL may continue to spread laterally which is further supported by the water table gradient. The density of the fractures and the size of apertures decrease with depth,

and therefore there is increased resistance to vertical penetration of the LNAPL. As the matrix porosity is low, any penetration of LNAPL below the water table will be through fracture flow. A well may observe metres of LNAPL within shale; however, due to the low matrix porosity and small aperture, a measured large LNAPL thickness does not translate to a large recoverable amount of LNAPL.

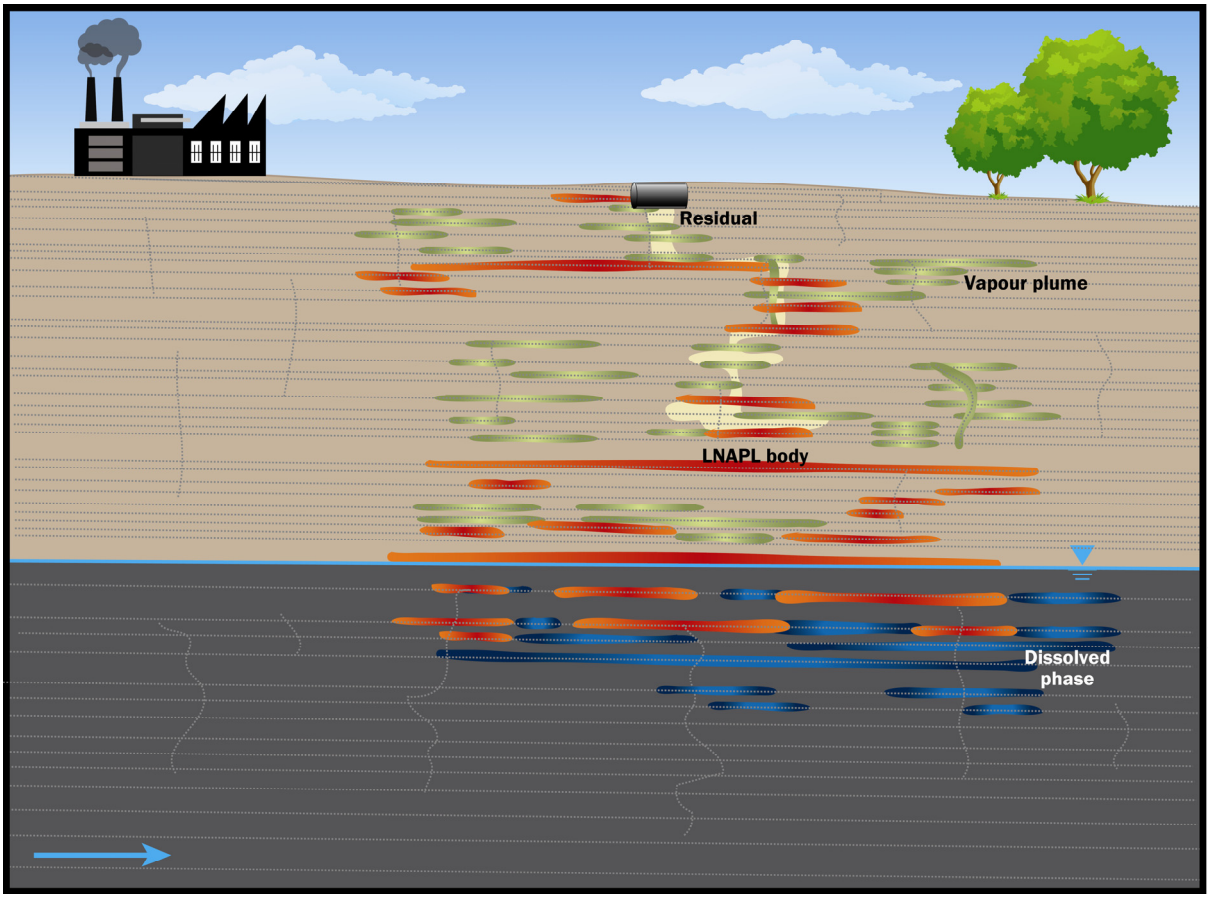

Figure 5.9. LNAPL release into fractured shale or mudstone.

5.12. LNAPL release into fractured porous sandstone

Fig. 5.10 depicts a release of LNAPL into superficial deposits overlying a porous moderately to weakly fractured porous sandstone, for example fluvial or aeolian Permo-Triassic sandstone. The conceptualisation assumes a coarse to medium-grained sandstone that is weakly cemented and of high porosity (~25%), contrasting with a typical fracture porosity of a few percent. Finer grained sandstones and marl / mudstone layers present will act as low permeability barriers. In the overburden, residual and mobile LNAPL can migrate laterally in all directions controlled by clay/sands occurrence, layering, heterogeneity and thickness; this can result in potentially quite attenuated and variable LNAPL footprints reaching the sandstone bedrock. Within the overburden and partially saturated bedrock, a well-defined vapour plume will develop within the partially saturated zone.

The volume of the LNAPL release in the example is sufficient to allow LNAPL to enter the fractured sandstone. Above the water table, LNAPL may enter those regions of the rock matrix that exhibit continuous air pathways and those composed of coarse-grained

sediments. LNAPL is not necessarily restricted to fractures and can enter the sandstone matrix as a separate liquid phase where the matrix is composed of weakly cemented, coarse-grained sediments. Depending upon the severity of fracturing, the LNAPL will have varying penetration into the matrix. Most notably if the sandstone is weakly fractured or predominantly horizontally fractured, then the LNAPL migration (and residual retention) may be highly significant in the porous matrix and distributed in a similar fashion as beach sands (Section 5.3) with uniform LNAPL infiltration with some spread due to the lower porosity from cementation. For more layered heterogeneous sandstone with interbedding of mudstone or shales, the LNAPL will be more laterally spread and similar to glacio-fluvial sands and gravels (Section 5.5).

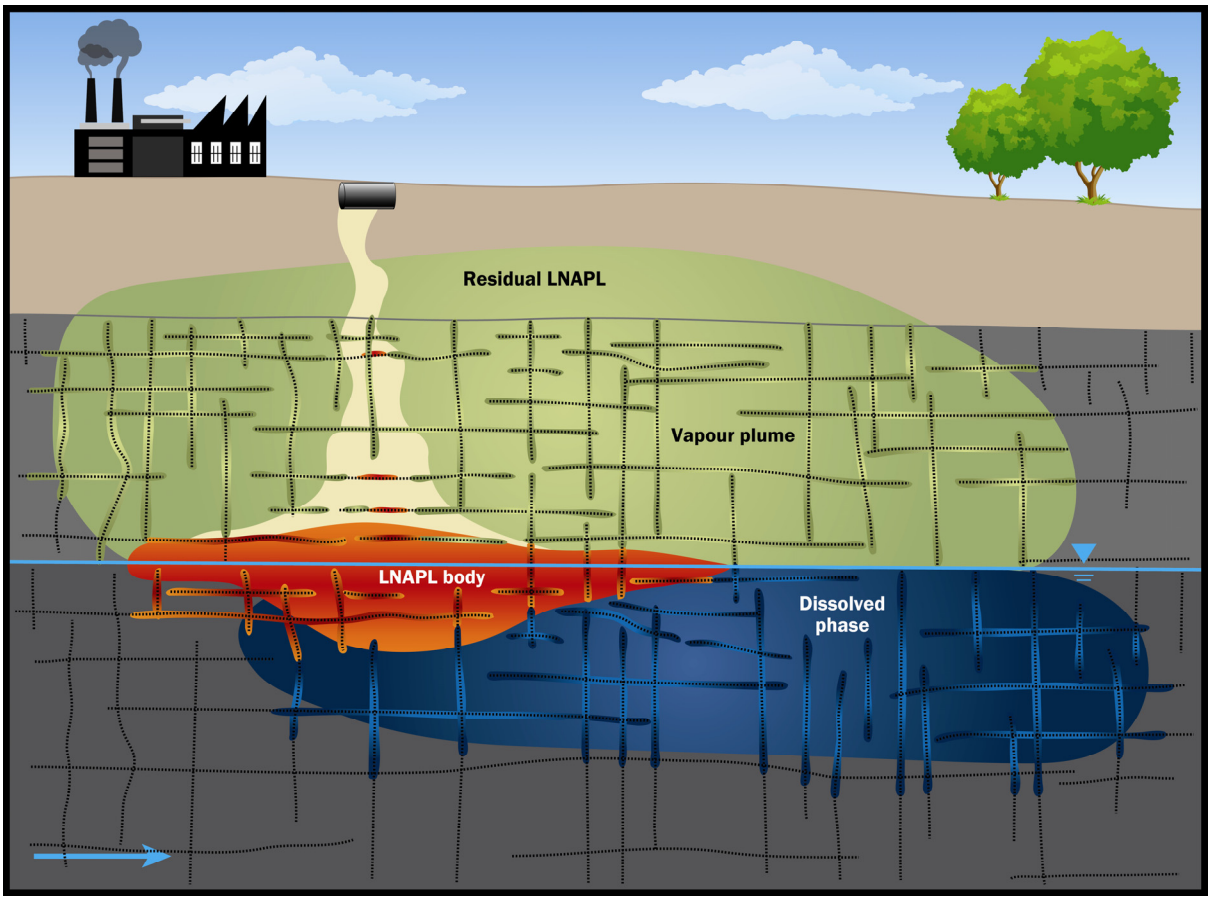

Figure 5.10. LNAPL release into a fractured porous (e.g., Permo-Triassic) sandstone.

Fracture influence on LNAPL migration will depend on the severity of the fracturing, frequency and interconnectivity of fractures. If the fracture array is more vertical to sub-vertical, then the LNAPL will more rapidly migrate under the influence of gravity, predominantly within these fractures, to the saturated zone. Even in highly fractured sandstone, the LNAPL will penetrate the matrix given its high permeability and porosity, with many sandstone sites exhibiting a combination of fracture and porous matrix infiltration of the LNAPL. In some instances, fractures may be sediment filled, which will limit the vertical migration of LNAPL (Wealthall *et al*., 2001).

LNAPL may migrate within both the matrix and fracture network and spread laterally in all directions, with accumulation of LNAPL in horizontal fractures (i.e., bedding plane) near the water table. Due to the high matrix porosity and storativity of sandstone, annual water table fluctuations will likely be low (~ 1-2 m) with the subsequent redistribution of LNAPL being contrastingly less than, for example, a fractured chalk or granite of low matrix permeability. LNAPL penetration depth is similar to an unconsolidated environment, albeit fracture array modified. The depth is still a balance of the various forces and is an average of the fracture distribution and the estimated distribution within an unconsolidated media. Migration of LNAPL will cease rather quickly for a low density and low viscosity LNAPL (petrol / diesel) but for higher viscosity and higher density LNAPL migration may continue for a significantly longer period of time.

Groundwater flow through the fractures and matrix containing residual and mobile LNAPL will bring about transfer of contaminants to, and evolution of, a dissolved-phase plume. The dissolved-phase plume will migrate through both the matrix and interconnected fractures; it is subject to advection, dispersion, biodegradation, and matrix diffusion. NSZD of the LNAPL and natural attenuation of the dissolved- and vapour-phase plumes will typically occur. The predominant bulk flow (at a few tens of metres per year) may be in the sandstone matrix, rather than fractures, particularly when fracture connectivity is limited. The resulting plumes are slow moving, with subsequent slow replacement of dissolved electron acceptors such as oxygen, nitrate and sulphate at the plume edges, resulting in strong redox gradients. Widespread ferric iron and manganese reducing zones are likely in Permo-Triassic sandstones, driven by the dissolution from the sandstone mineralogy.

5.13. LNAPL release into made ground

Made ground of anthropogenic origin is highly variable both in its physical and chemical characteristics, including permeability, grain size, chemical composition and geotechnical properties. It can include reworked natural unconsolidated intergranular sediments, gravel backfill to buildings, granular materials such as clinker, slag and demolition or construction wastes. Many developed urban areas will have made ground and LNAPL will migrate through this into one of the other natural hydrogeological scenarios presented. Backfill material around underground structures (e.g., foundations or utilities) is typically a gravel of higher permeability and/or porosity than the formation and has the ability to transmit the LNAPL preferentially. Reworked made ground, comprised of natural or man-made material, is highly heterogeneous.

Fig. 5.11 illustrates a LNAPL release into made ground containing a variety of subsurface structures. LNAPL has leaked from an underground storage tank and found its way into the gravel backfill of a building footing. Preferential migration of LNAPL takes place along the gravel because of its low capillary resistance. Migration within reworked made ground is likely to be highly complex, but generally follow the more permeable and continuous natural or man-made materials available and may, for example, laterally spread along layers of more permeable and/or poorly packed (higher porosity) materials. Lateral spread and pooling of LNAPL may also be promoted by failure to penetrate low permeability obstacles such as buried concrete slabs and fine-grained waste materials such as ash or sludges.

LNAPL released into made ground may preferentially migrate along abandoned utility corridors which can provide a pathway of low capillary resistance and typically higher

permeability than the surrounding formation, natural or made ground. The presence of residual and mobile LNAPL above the water table supports the potential for vapour diffusion and/or preferential advection along permeable made ground conduits into the interior of, for example, building structures. Fig. 5.11 also illustrates a second LNAPL release that has encountered the gravel backfill surrounding underground piping. The backfill provides a preferential pathway for LNAPL migration that may occur in directions contrary to expectations based on general ground conditions. The LNAPL in this example has also encountered an abandoned borehole that has allowed short-circuiting to the water table.

LNAPL migration laterally will also be influenced by water table depth. Although the true water table may be present within the underlying natural geology, perched groundwater may often be encountered within the made ground where lateral spreading of the LNAPL may hence occur. Historically deep water tables may have risen into, previously dry, reclaimed (filled) or tipped land, especially in valley areas containing (former) industry sites that no longer have requirement to abstract groundwater for industrial use. Rising water tables may also come into contact with abandoned subsurface infrastructure; these notably include tar wells at former gas/coking work plants that may contain significant quantities of LNAPL/DNAPL.

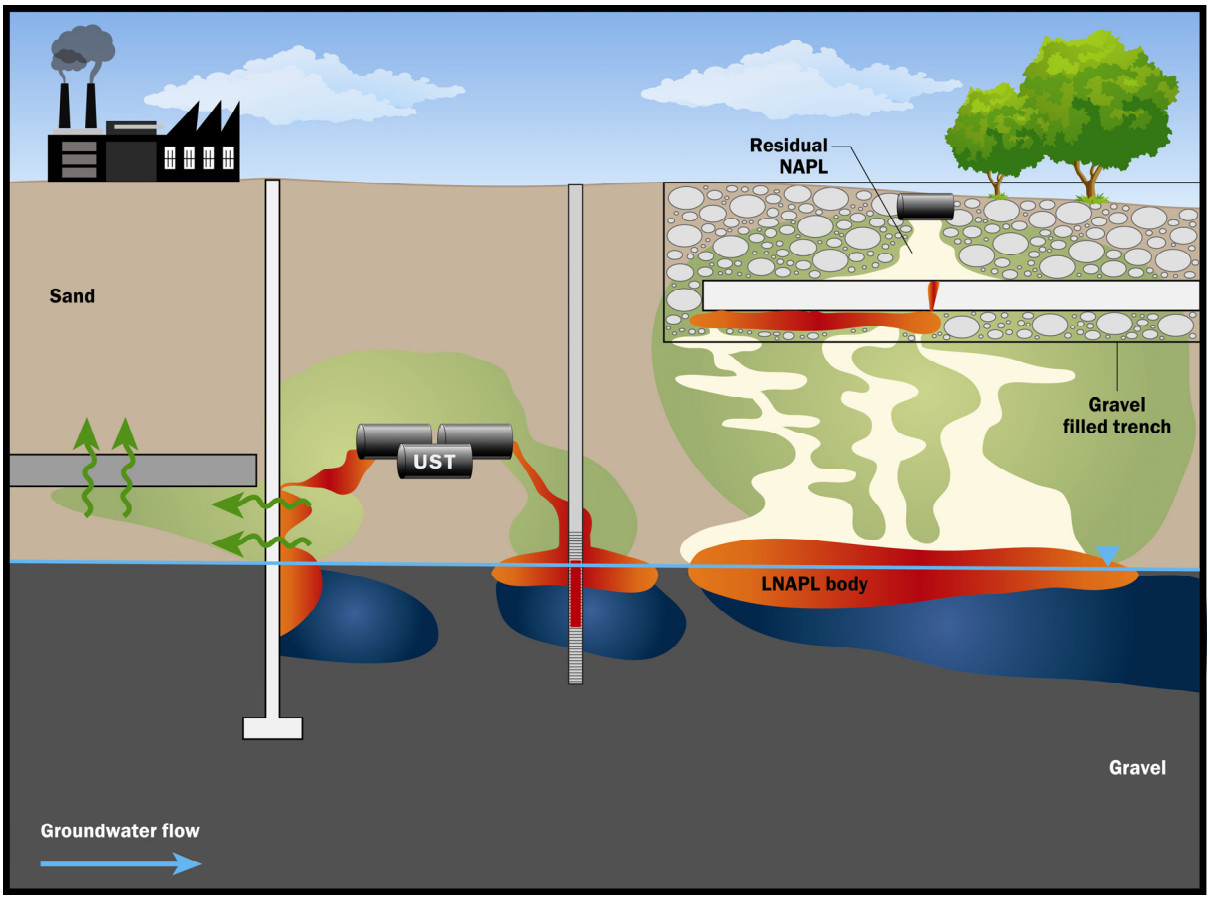

Figure 5.11. LNAPL release into made ground.

6. Characterising LNAPL sites

6.1. Introduction

There are two main drivers in the management of LNAPL-impacted sites that inform site characterisation needs:

- to understand the potential risks posed to receptors by both current and plausible future mobile LNAPL distributions, and the migration of their associated dissolved-phase and vapour-phase plumes; and
- to understand LNAPL constraints on remediation selection, design and operation which often requires more targeted investigation and pilot testing of the system.

A refined, more quantified, CSM is typically a key goal. There has been a general move to risk-based management of LNAPL (EA, 2004; ITRC 2009a,b; USEPA, 2005). Risks posed directly or indirectly to human health and the environment may include:

- accumulation of flammable vapours in subsurface and surface structures;
- chronic risk to human health via long-term exposure to hazardous substances;
- acute risk to human health via short-term exposure to (higher concentrations of, or more) hazardous substances;
- pollution of controlled waters;
- impairment of aesthetic qualities of potable supplies (taste, odour and discolouration);
- detrimental effects on ecosystem structure and function; and
- asphyxiation risk due to confined-space accumulation of vapours and anoxic conditions (although this is unlikely compared to, for example, landfill gas and mine gas scenarios).

If a potential source-pathway-receptor linkage (potential risk) is identified, characterisation is typically focused on the LNAPL source zone: the origin of any potential risk and frequent target for remedial action. Investigation aims to establish source zone distribution and chemical composition, and to identify pathways to potential receptors. Sources, pathways and receptors are identified, and the presence of any linkages between them established, to identify potential risks that need to be estimated and managed (Gormley *et al*., 2011). LNAPL sources pose both saturation-based and composition-based risks (Section 7). Saturation-based risks relate to the amount of LNAPL within the formation and its ability to migrate to a receptor; given sufficient LNAPL volume, it may continue to migrate. Composition-based risks relate to chemicals within the LNAPL that can partition into either dissolved- and vapour-phases, and give rise to plumes that may pose acute, chronic and/or impairment risks to receptors. Investigation will hence focus on assessing these risks which are components of the CSM for LNAPL.

The focus of this section is on LNAPL source term characterisation. This is underpinned by geological and hydrogeological methods that are summarised in Tables 6.1 and 6.2 for porous and fractured media, respectively. Whilst the detail in these tables is not necessary at all sites, the assessment approach needs to be tailored to the site-specific scenario

recognising the potential issues of concern, complexity of the subsurface hydrogeological and contamination scenario and the sensitivity of the site setting. Further, it should be recognised that site characterisation is not just an initial assessment process, but rather an on-going process that may still be very prominent in the remedial programme for a site. For example, passive remediation technologies such as NSZD to evaluate the long-term natural depletion of the LNAPL source zone and MNA to evaluate the long-term stability of the associated dissolved-phase plumes (Sections 4.1.3, 4.3, 7.5.6), both have site assessment guidelines specific to those strategies that extend the initial site characterisation undertaken to address the temporal data needs of those strategies (see, for example, EA (2000), ITRC (2009b)).

Table 6.1. Example geology and hydrogeology investigation methods for unconsolidated and consolidated granular materials (adapted from Davis *et al*., 2006; ITRC, 2009a; Johnston, 2010; Sale, 2001).

Category	Technique	Metrics	Applicability
Regional geology	Aerial-photo, remote sensing	Lineament and trends	Understand structure of the lithology, topography, bedding
	Outcrop mapping	Stratigraphy, porosity, permeability	Understand structure and soil distribution
Local hydrogeology	Surface and combined downhole geophysics	Stratigraphy, porosity, aquifer state (fluid saturation), fluorescence response	Understand formation structure, depth of aquifers, stratigraphy changes, subsurface infrastructure, LNAPL sources – tanks, pipelines, LNAPL distribution.
	Coring/drilling	Stratigraphy, porosity, aquifer state (fluid saturation)	Directly observe soil structure and fluid distribution
	Core analysis	Stratigraphy, porosity, aquifer state (fluid saturation)	Understand formation structure, quantify variation
	Cone penetrometer testing (CPT)	Stratigraphy, porosity, aquifer state (fluid saturation)	CPT determines soils geotechnical engineering properties, stratigraphy
	Wellbore geophysical logging	Stratigraphy, porosity, permeability	Structure of consolidated and unconsolidated geology
	Aquifer testing	Bulk and interval conductivity, permeability, specific yield	Understand aquifer hydraulics, storage, transmissivity

Table 6.2. Example geology and hydrogeology investigation methods in fractured systems (adapted from Davis *et al*., 2006; Hardisty *et al*., 2003; Johnston, 2010; Sale, 2001).

Category	Technique	Metrics	Applicability
Regional geology	Aerial-photo, remote sensing	Major fracture lineament and trends	Understand structure, topography, direction of bedding, strike and dip angle
	Outcrop mapping	Fracture orientation, lengths, connectivity, density, roughness, and character	Understand structure, level of fracturing, distribution of weathering in fracture network
Local hydrogeology	Surface and combined downhole geophysics	Stratigraphy, major fractures, fracture zones, fluorescence response.	Understand formation structure, depth of water-bearing zones, changes in stratigraphy. Locating subsurface infrastructure and LNAPL sources – tanks, pipelines, LNAPL presence
	Coring (vertical and angled)	Fracture orientation, density, roughness and character	Understand structure, mineralogy, level and type of fracturing, changes in stratigraphy
	Core analysis	Rock matrix porosity, permeability and saturation-capillary pressure relationship	Understand matrix structure, storage, and quantify variation in matrix
	Borehole imaging *In situ* fracture casting	Fracture aperture, orientation, density, roughness and character	Understand the formation structure, density of fracturing, size of fractures
	Wellbore geophysical logging	Presence of fractures, fracture zones and in/out flows	Understand formation structure, depth of water bearing zones, density of fracturing, size of fractures.
	Hydraulic packer testing	Bulk and fracture conductivity / permeability	Understand formation hydraulics, depth of water bearing zones, contaminated fractures.
	Downhole video logging	Fracture depths	Understand formation structure, depth of water bearing and potentially LNAPL zones.
	Flexible borehole liners	Bulk and fracture conductivity/ permeability	Understand fracture hydraulics, depth of water bearing zones, LNAPL bearing fractures.

6.2. Planning and optimising site investigation

Defining where the LNAPL source is distributed is typically the first step and is informed through records covering site history and use, site setting (regional geological and hydrogeological information), aerial photographs, and initial site characterisation. These help discern LNAPL composition and related risks, and help an assessor identify areas where investigation is needed to fully understand those risks. This information also helps identify areas to investigate for saturation-based, LNAPL mobility risks.

Presence or absence of LNAPL may be initially unknown, and could remain unknown unless directly measured, or inferred (ASTM, 2007). If potential receptors are confirmed, suspected sources or known releases are investigated initially and a CSM is developed and refined. For large and complex sites, a multiple lines of evidence approach and a variety of integrated multi-discipline techniques may be used to acquire good quality data to underpin management plan development (CL:AIRE, 2002). On smaller and less complex projects the level of investigation may be reduced. In either event, the process continues until a sufficiently robust CSM is developed to ascertain risks and inform management decision making. Further refinement in characterisation may be needed to delineate areas requiring remediation and continue through remediation performance to remediation verification.

6.3. LNAPL distribution - where is the LNAPL?

Establishing where the LNAPL is located within the subsurface, its chemistry, and how it can impact receptors is key to understanding the potential risks it can pose.

6.3.1. Site use/site history

Site investigations begin with a desk study that includes site reconnaissance, discussions with site owners/operators and record searches to establish locations of tanks, conveyance piping and other potential sources, as well as local receptors and potential pathways for migration. Aerial photographs, maps and plans may be examined to determine potential source locations based on distributions of historic operations, above ground piping, storage tanks and fuel transfer stations, as well as local receptors.

6.3.2. Reconnaissance methods for locating sources

Soil-gas surveys of the partially saturated zone can usefully inform on areas for further investigation. They involve passive (sorbent collectors) or active (direct gas) sampling methods to assess the areal extent of vapours, and by inference LNAPL at the water table, or the location of residual LNAPL within the partially saturated zone. This reconnaissance may direct more intensive local investigation of potential source areas. Carbon dioxide (CO_2) respirometry can help to locate the areas of potential LNAPL source areas (Sihota *et al*., 2011) by measuring CO_2-efflux within the soil gas at the ground surface via a dynamic closed chamber. It is sometimes able to delineate the source zone signature at surface and distinguish between the rates of natural soil respiration and contaminant mineralisation. Similarly, oxygen and methane levels can be used to understand degradation potential of plumes (USEPA, 2013). Whilst such reconnaissance methods may in part be confounded by various factors, e.g., complex vapour transport pathways, they may often allow a more targeted and cost-effective subsequent investigation of source areas.

6.3.3. Screening of soil borings and rock cores

Soil borings aim to directly quantify the vertical variation and penetration depths of LNAPL, and its stratigraphic relationship. Vertical investigation should, ideally, continue to the zone of deepest LNAPL penetration, although this may not always be feasible. Although investigation risks are lower than for DNAPL sources, concerns of creating new pathways (e.g., piercing a perched layer of LNAPL on a low permeability unit in the partially saturated zone) must still be considered weighing up benefits of more investigation data versus potential pathway creation and possible liability.

Field-screening methods for soil borings include headspace analysis using a portable photoionisation detector (PID), flame ionisation detection (FID) or fluorescence analysis. Other convenient LNAPL presence screening tools include shaker test, dye shaker test, paint filter test, and paper towel test. Water shake tests are simple tests to look for sheen on water after a soil aliquot is shaken within a vial of water. Dye shaker tests usefully discern LNAPL presence in a sample through use of oleophilic dye (having an affinity for oil) yielding visual colouration upon partitioning to organic-based oils. Such tests, although simple, may achieve reasonable quantification, for example, TPH levels to +/-1000 mg/kg. Other simple approaches include: paint filter test (USEPA SW846 Method 9095B) for free liquids within the soils to assess the presence of LNAPL; the use of a paper towel patted on to a sample and placed under UV light; or, oleophilic pads to assess the presence of LNAPL visually.

Bedrock drilling techniques are typically very aggressive due to high temperatures and high drilling fluid velocities generated in the immediate vicinity. Based on field experience it is now believed that LNAPL can be displaced from fractures by the drilling process before the core is retrieved. It is therefore unreasonable to expect to confirm if LNAPL will be present in the fracture of a rock core, even if drilling within bedrock that is known to have LNAPL present. More viscous heavy fuel and crude oils that coat fracture walls may be an exception. LNAPL or biological activity may have stained the fracture walls and other measures such as PID and FID, or perhaps fluorescence may be used to discern LNAPL presence or if elevated concentrations exist within the fracture and matrix; also, black metal sulphide staining and hydrogen sulphide odours can be markers of LNAPL presence (or this could also manifest from high dissolved-phase plume biological activity). However, absence of staining does not negate LNAPL occurrence prior to core removal. Additional screening techniques include visual inspection of LNAPL within drilling fluids (as iridescent sheens, odours, or LNAPL) and head space analysis of samples that may potentially capture contaminant diffused into the matrix. Use of olfactory techniques (i.e., sniffing samples) is not good practice as it could lead to increased exposure to hazardous chemicals.

6.3.4. Laboratory analysis of soil samples

Soil characterisation typically includes laboratory analysis of soil samples for contaminant composition. This chemical data is useful in defining LNAPL extent and understanding its composition-based risks. NAPL presence in a soil sample (typically provided as mg of oil per kg of (dry or wet) soil) can be evaluated as described in Feenstra *et al*. (1991) and Kueper *et al*. (2003) by considering individual chemical partitioning to the various phases present and use of equilibrium partition coefficients. However, most LNAPLs are mixtures and TPH data are often reported. Ignoring partitioning to other phases (water, air, sorbed) and recognising data availability is a key issue for a multi-component complex LNAPL, the LNAPL saturation may be approximated from TPH data by (Parker *et al*., 1994):

$$S_{NAPL} = \frac{\rho_b \bullet TPH}{\rho_n n(10^6)} \qquad \text{Eq. 6.1}$$

where S_{NAPL} is the NAPL saturation (unitless) of pore space, ρ_b is the soil bulk density (g/cm^3), ρ_n is the NAPL density (g/cm^3), n is porosity (unitless) and TPH units are mg/kg.

Soil cores can also be collected for high-resolution photography under white and UV light. A petroleum laboratory completes this analysis, with the cores collected as an intact core that is flash frozen (dry ice or liquid nitrogen) in the field and shipped frozen (dry ice) to the laboratory (following appropriate safety procedures). This allows for a visual log of the soil conditions, texture, pore structure, and stratigraphy under white light with a comparative photo collected under UV light to aid in visualising LNAPL location and saturation variability with UV light allowing identification of the fluorescent compounds, e.g., PAHs.

6.3.5. Direct push methods

The Membrane Interface Probe (MIP) is a direct push tool used in conjunction with a cone penetrometer-testing (CPT) probe to provide a semi-quantitative estimate of VOC distribution in unconsolidated deposits. VOCs in the subsurface diffuse across the MIP membrane that is in direct contact with the geological formation and partition into a stream of carrier gas analysed at surface by GC based methods (PID, FID, halogen-specific detector). It can rapidly screen areas for further investigation locating VOC-rich source areas and plumes, but does not discern the phase of the contaminant.

Laser-induced fluorescence (LIF) provides real-time, *in situ* field screening of LNAPL source areas. An example log is shown on Fig. 6.1. LIF may provide detailed, qualitative to semi-quantitative information on the subsurface distribution of LNAPL-containing fluorescent components. LIF sensors can be deployed on CPT or percussion direct-push drilling rigs with the former aiding the interpretation of stratigraphic influences. Fuels, oils, creosotes, and coal tars are composed of various amounts of monoaromatic hydrocarbons, PAHs, and aliphatic hydrocarbons leading to varying fluorescent signatures. Being hydrocarbon mixtures, they create overlapping spectra, so it is not possible to identify individual species with *in situ* LIF technology, but it is possible to determine relative concentrations (detection limit of ~50 to 500 mg/kg TPH) and usually the type of LNAPL present (Fig. 6.1).

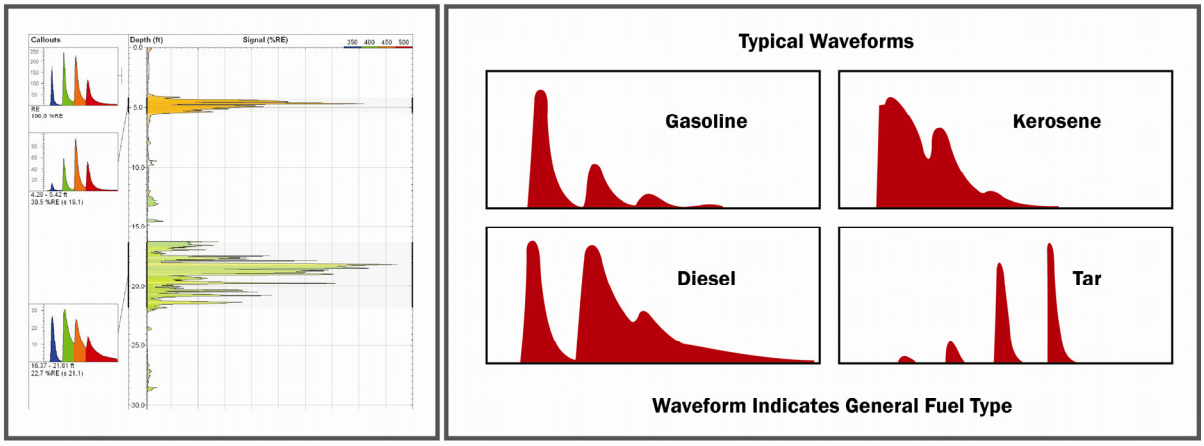

Figure 6.1. Example LIF output showing perched and water table occurrences; observed waveform signatures are compared to known fuel/oil signatures.

6.3.6. Partitioning interwell tracer testing

Partitioning interwell tracer testing (PITT) is an intensive characterisation approach employing injection of multiple tracer chemicals, such as aliphatic alcohols, and monitoring of their migration through an LNAPL source area (Jin *et al*., 1995). Typically, one of the tracers does not partition to the LNAPL, while the others partition into the LNAPL at varying rates. Tracer breakthrough at down-gradient extraction wells is measured and since each tracer has specific partitioning characteristics to the aquifer material and LNAPL, these data can be used to develop an estimate of LNAPL saturation, volume and distribution within the subsurface (USEPA, 2005).

6.3.7. Flexible absorbent borehole liners

Flexible absorbent borehole liners are useful for directly observing LNAPL distributions with depth. A fabric that reacts with the LNAPL is used to produce a very obvious stain on the fabric where it contacts the LNAPL, for instance a contaminated fracture. The liner is deployed and then retrieved, and the depth of observed stains on the inside surface are easily read to infer LNAPL location around the borehole circumference.

6.4. LNAPL mobility

LNAPL in source areas may be mobile with potential to enlarge the footprint of the source zone, or to redistribute mass within the footprint of a stable plume margin. Movement could, however, still be restricted to the existing LNAPL source area if it is predominantly vertical in response to changing water table elevations. LNAPL saturations tend to be highest in the LNAPL source area centre (more mobile) and lessen (lower mobility) towards the LNAPL body perimeter. Understanding such mobility is a concern to regulatory programmes that require removal to a defined level linked to a saturation-based risk or concern. If sufficient drivers and gradients are available, the mobile portions of the LNAPL may migrate and continue to enlarge the LNAPL distribution.

6.4.1. Monitoring well programme

Monitoring wells within the LNAPL source area that are appropriately screened around the zone of water table (LNAPL) vertical fluctuation may help discern the LNAPL distribution.

For bedrock, short-screened multi-level wells can aid in understanding which fractures contain LNAPL as well as depth and areal distribution. Groundwater and LNAPL elevations can be measured with an interface meter that detects the LNAPL-air and LNAPL-water interfaces within a well. Monitoring wells may be designed with large slot size and filter pack size to help convey the LNAPL to the well or benefit from aggressive development to further enhance conveyance.

In-well LNAPL thickness measurements over time may usefully indicate the stability of the LNAPL source area (recognising differences between in-well and in-formation thicknesses). In the early stages of a finite LNAPL release, the LNAPL footprint will continue to expand until the driving forces reach equilibrium (Fig. 6.2). Although LNAPL thicknesses within the LNAPL footprint may change, the areal extent may remain similar between observations. This is because the leading edges of the LNAPL source area are self-containing the LNAPL, as there are insufficient driving forces to significantly extend it at its periphery.

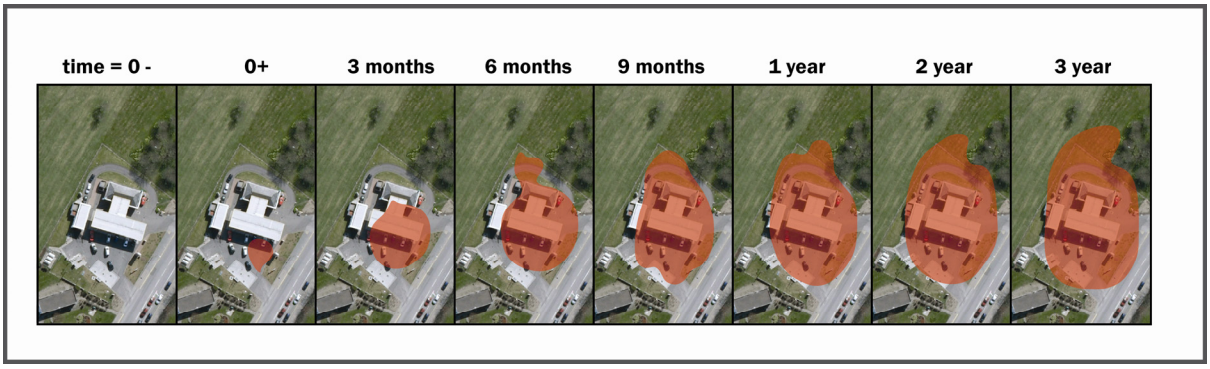

Figure 6.2. LNAPL release of fuel oil observed in monitoring wells showing that lateral stability was largely achieved within the first year of the release with reduced lateral expansion in years two and three. Lighter LNAPLs tend to reach lateral stability quicker (months), whereas heavier more viscous LNAPLs (such as Fuel Oil No.6) may require several years to attain stability (API, 2004). Decreasing saturation, LNAPL gradients and entry pressures retard the growth of the LNAPL source area resulting in its ultimate stabilisation.

If sufficient data exist, LNAPL thicknesses monitoring can be used to assess if the LNAPL is unconfined or confined by low permeability units. Unconfined LNAPL will exhibit the typical response: if the groundwater elevation decreases, the measured LNAPL thickness within the monitoring well will increase (Fig 3.6). The opposite will be the case for confined LNAPL trapped by an overlying low permeability unit due to water table rise after LNAPL release. For confined LNAPL, its thickness will increase with potentiometric surface rise leading to greater LNAPL thickness in wells at equilibrium, and a consistent elevation of the LNAPL-water interface will be observed over time. The perched LNAPL condition will show as an increase in LNAPL thickness with a dropping potentiometric surface with a constant LNAPL-air interface.

In-well LNAPL thickness measurements can help approximate the LNAPL gradient that may be used to calculate a potential LNAPL velocity by Darcy's Law. Steeper LNAPL gradients within the LNAPL source area cause greater LNAPL spreading redistribution without necessarily increasing the LNAPL source area footprint. The key parameter, LNAPL conductivity, may be estimated from bail down tests, or from the measured LNAPL

thickness, soil capillary parameters and a model that assumes static equilibrium (API, 2004). The measured LNAPL thickness can also be used to compare to the calculated threshold minimum LNAPL thickness in a well (h_{NC}) that would be necessary to invade water-wet pores, based upon the displacement entry pressure (Charbeneau *et al*., 1999):

$$h_{NC}=\left(\frac{\sigma_{NW}}{1-\rho_N}-\frac{\sigma_{AN}}{\rho_N}\right)\frac{h_{AW}}{\sigma_{AW}} \qquad \text{Eq. 6.2}$$

Where h_{NC} is the minimum well thickness in a well before LNAPL can move in the ground, σ is the interfacial tension with σ_{NW} as the LNAPL-water interface, σ_{AN} as the as the air-LNAPL interface, and σ_{AW} and the air-water interface; ρ_N is LNAPL density, and h_{AW} is the height of the capillary rise above the air-water interface (also known as capillary fringe thickness). For petrol, the relationship for h_{NC} to h_{AW} is approximately 2.5 to 1. (Charbeneau *et al*., 1999). Examples of LNAPL mobility calculations are provided in Appendix 1.

6.4.2. Laboratory analysis of LNAPL samples

LNAPL fluid properties typically measured include density, viscosity, surface tension and interfacial tension (Sale, 2001). Measurements ideally should be at temperatures close to *in situ* conditions due to parameter temperature dependence (Charbeneau *et al*., 1999). For instances where the remedial approach will include temperature modification (for example, steam injection), analysis of these parameters at a few temperatures is relevant. Estimated LNAPL fluid properties databases are available (Beckett and Joy, 2003) and may preclude the need for (some) site-specific LNAPL measurements at less critical sites.

A LNAPL can be characterised by GC fingerprinting analysis which is a useful tool especially in cases where multiple fuel types or sources are present or suspected. GC fingerprinting obtains a profile and distribution of the component compounds of the LNAPL from which an indication of the compositional mix of the hydrocarbons present can be ascertained. Different fuels/oil types exhibit different characteristic GC fingerprints (Fig. 2.1) which can be used to assess the degree of 'weathering' experienced by the LNAPL. When petroleum products (LNAPLs) are released to the environment they are subjected to many degradation processes which combined are termed "weathering". These weathering processes include volatilisation (evaporation), dissolution and microbial degradation (biodegradation) amongst others. For example, the isoprenoids, pristane and phytane (branched alkanes) are relatively resistant to degradation whereas (similar GC retention time and boiling point / volatility) nC_{17} and nC_{18} (straight-chain n-alkanes) are susceptible to microbial attack. Therefore, if the LNAPL was diesel, it would be possible to obtain an indication of the biodegradation experienced by comparing pristane and phytane with nC_{17} and nC_{18} concentrations. However, more in-depth quantitative analysis, of diagnostic compounds, may be dependent upon the skill and experience of the individual(s) concerned (Wang and Stout, 2007). It is preferable to use longer analytical run times in order to achieve good separation of the compounds present. Otherwise, co-elution of compounds will occur and this will give rise to erroneous and misleading diagnostic ratios being calculated. Laboratories are increasingly reporting carbon banded ranges (e.g., $>nC_8$ to nC_{10}) of aliphatic and aromatic hydrocarbons (TPHCWG, 1999) following solid phase extraction (SPE) of the LNAPL rather than a bulk TPH analysis. This approach allows a more quantitative appraisal of the LNAPL type, chemical composition, properties and its likely environmental behaviour and fate.

6.4.3. Hydrocarbon concentrations in groundwater

Temporal variation in the dissolved-phase plume size and shape may provide insights into the LNAPL source area status (Fig. 6.3). This is similar to (or an extension of) a MNA assessment (EA, 2000; Wiedemeier *et al*., 1999) whereby a lines-of-evidence approach is used to assess the dissolved-phase plume condition, which in turn allows LNAPL source area conditions, (particularly its stability or decline) to be inferred. It may be inferred from a shrinking or stable dissolved-phase plume condition that the LNAPL source area is also shrinking or stable. It is not, however, possible to discern the source status from an expanding groundwater plume condition.

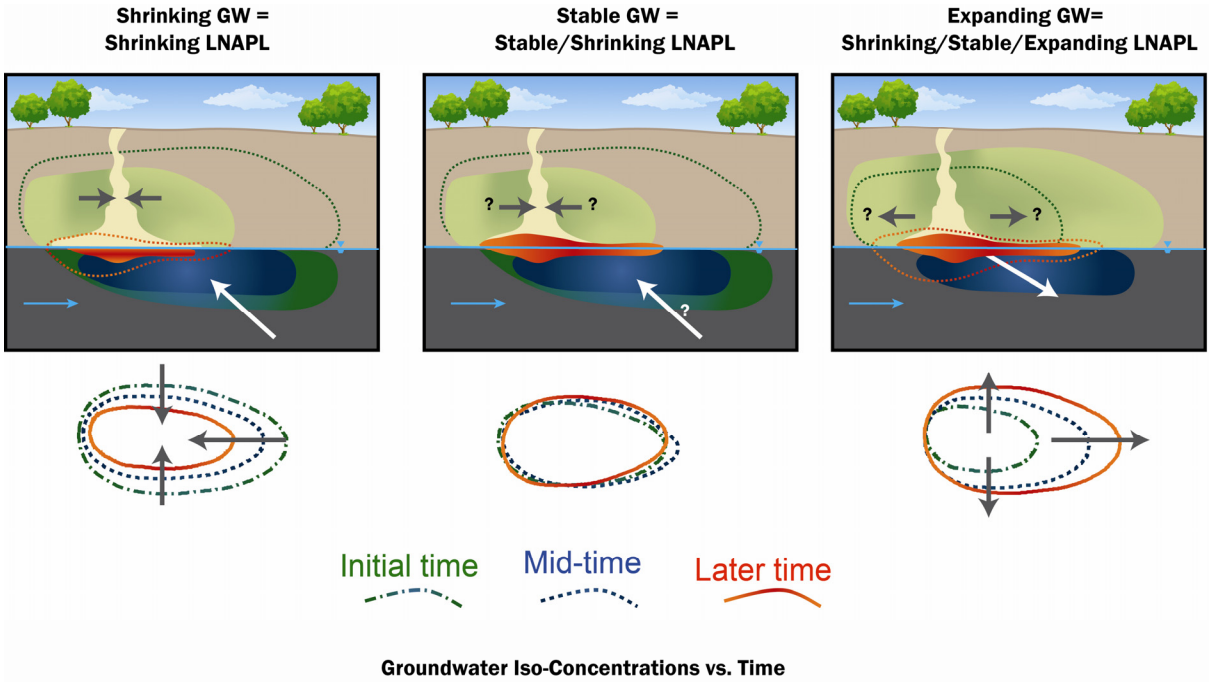

Figure 6.3. Groundwater dissolved-phase plume iso-concentrations versus time as an indicator parameter for LNAPL source area stability.

6.4.4. Undisturbed soil/rock cores for petroleum hydrocarbon laboratory analysis

Intact soil core samples can be collected for specialised petroleum hydrocarbon laboratory analysis; however, this is not typical except for complicated sites, or where a saturation-based risk is a primary concern. These measures aid in quantifying LNAPL and the specifics of the LNAPL distribution and level of saturation, including capillary-held residual maxima and mobility. Cores require field flash freezing by dry ice or liquid nitrogen to encase the LNAPL with frozen formation water. LNAPL saturation is typically measured by sensitive methods such as the Dean Stark Extraction method (API, 1998) at refined intervals to resolve discrete layers of LNAPL presence. Such cores, particularly if taken at different water table elevations over time, offer effective insight into delineating profiles of LNAPL saturation and horizons containing potentially mobile LNAPL, notably avoiding the confusions inherent to use of monitoring well free-phase LNAPL thickness data.

The use of sponge coring, a standard method in the investigation of petroleum reservoirs may have specific application within bedrock source areas. This technique provides a higher quality core than traditional methods and allows for more accurate LNAPL physical characteristic data, LNAPL distribution, and saturation (including residual) levels to be collected. The sponge liner of the core barrel recovers oil escaping from the core. The method reports: the saturation in the core, the saturation in the sponge, and their total. The saturation in the sponge and core are inferred as the mobile and residual fractions of LNAPL although some of the core saturation may be potentially mobile.

Residual saturation is measured in the laboratory by either centrifuge or water drive. The centrifuge method applies ~1,000 times gravity to the sample for 1 hour to demonstrate LNAPL mobility or lack of such. The water drive method drives potentially mobile LNAPL from the sample via water flood. These methods indicate the LNAPL portion that is potentially mobile, and provide a starting estimate for that location and soil type of the residual saturation for further detailed recoverability analysis. Typically, the residual saturation measured using centrifuge method is applied to samples obtained from the partially saturated zone, and water-drive to samples obtained from the saturated zone. Neither method is used routinely, but would have potential to yield valuable data in complex cases.

6.4.5. Field measurement of LNAPL transmissivity

LNAPL transmissivity is an important metric for understanding the hydraulic recovery limits of a given (remedial) technology. Short-term methods cause instantaneous applied stress to the LNAPL body and include baildown, slug and skimmer tests. Long-term methods apply stress to the LNAPL body over a longer period and include recovery data analysis and tracer tests. Test methods are summarised below and calculation of LNAPL transmissivity is detailed within ASTM (2011) (Section 3.8):

- **LNAPL baildown/slug test** consists of either removing the entire LNAPL from the well casing and filter pack or the displacement of a partial volume to induce a head difference (typically a minimum of 15 cm of LNAPL within well). The transmissivity value obtained represents near-well aquifer characteristics. The test offers simplicity and can be used during a hydraulic recovery to monitor the effect on the LNAPL source area. The analysis is similar to a groundwater slug test, but with LNAPL factors incorporated, including LNAPL formation thickness and density (Huntley, 2000).
- **LNAPL skimmer test** is conducted by removing LNAPL at a rate that maintains drawdown in the well until a consistent LNAPL recovery rate is achieved. Being a longer-term test, it provides a greater influence within the LNAPL body and thus more accurate LNAPL transmissivity and recovery estimates.
- **Recovery data-based methods** use information from an oil recovery system. Recovery rate, LNAPL thickness and other information during active LNAPL recovery (via skimmers or active pumping) are used to calculate LNAPL transmissivity. The estimate is often used as a metric to aid in defining when further hydraulic recovery is not warranted.
- **Tracer test methods** (not yet commercially routine) involve spiking wells that have measurable LNAPL with oleophilic fluorescent tracers and observing the rate that LNAPL leaves the well through dilution of the fluorescent tracer by the LNAPL body

within the aquifer; the rate of dilution can be used to calculate LNAPL transmissivity (Mahler *et al*., 2012; Smith *et al*., 2012).

6.5. Data management and visualisation tools

Multiple datasets are often used to develop lines of evidence, both spatially and temporally. Data visualisation tools aid in development of the quantitative CSM, but also help inform where additional site characterisation may be necessary. Shown in Fig. 6.4 is an example of 2-D and 3-D visualisation of collected data. A variety of software tools are available to aid data visualisation, including 2-D and 3-D graphing techniques, which generally adopt spatial data smoothing techniques (e.g., kriging). Other approaches, such as temporal-spatial smoothing of data can be used. An example is the GWSDAT tool that combines spatial and temporal data analysis techniques to help interpret LNAPL and dissolved-phase concentration data. GWSDAT (Jones *et al.,* 2014) was developed by Shell Global Solutions and is freely available at www.claire.co.uk/gwsdat.

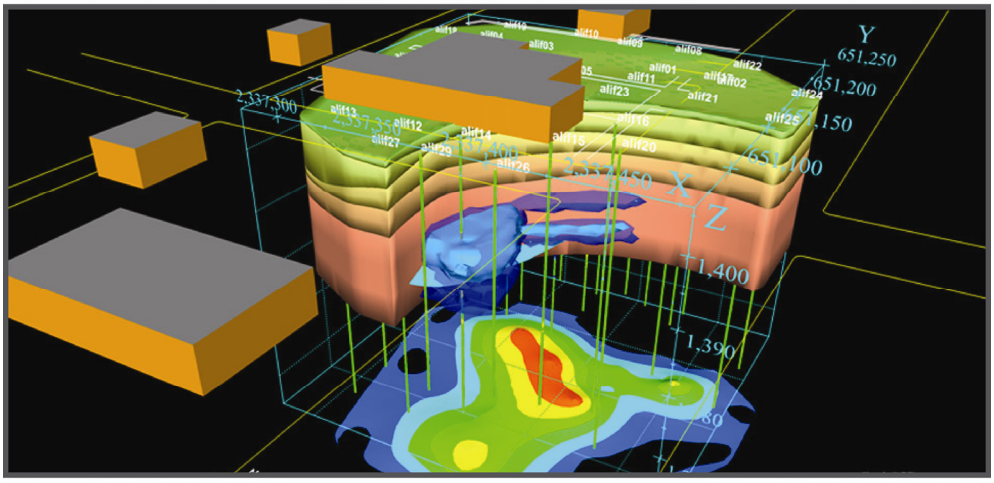

Figure 6.4. Typical 2-D and 3-D data visualisation outputs showing a LNAPL source zone geometry.

7. LNAPL management and remediation

7.1. Introduction – the risk-based context

The management and remediation of contaminated soil and groundwater is increasingly undertaken in the context of sustainable risk-based regulatory frameworks (Defra, 2012; Scott and McInerney, 2012). Whilst the details of each regime vary, the requirement for remediation is typically determined following an appraisal of risks that includes an assessment of contaminant sources, pathways and receptors. Where unacceptable risks are confirmed then the development of a remedial strategy evaluates the options to mitigate the risks. This may include treatment of the source, action to break the pathway and/or protection of the receptor. The identification of a suitable remedial technology is then undertaken via a feasibility study or remedial options appraisal that includes a range of criteria including assessment of technical effectiveness, cost, durability, practicality (EA, 2004; USEPA, 1988) and increasingly, sustainability (ASTM, 2013b; CL:AIRE, 2010).

LNAPL-impacted sites can pose a considerable technical and management challenge (ASTM, 2007). The requirement for remediation may be driven by a range of concerns related to the presence of LNAPL itself and/or associated vapour- and dissolved-phase groundwater plumes and their potential impact to perhaps several receptors (ASTM, 2007; ITRC, 2009a; Johnston, 2010). These varying drivers have been termed composition drivers (i.e., the risk is driven by the presence of hazardous constituents within the LNAPL) or saturation drivers (i.e., the risk is driven by the volumetric presence of LNAPL itself) (ITRC, 2009a). Examples of LNAPL remediation drivers are summarised in Fig. 7.1. The applicability and relative significance of each of these concerns and hence the focus of potential remediation will depend on the regulatory regime, the nature and extent of the LNAPL release, the site setting and the specific circumstances of a given site.

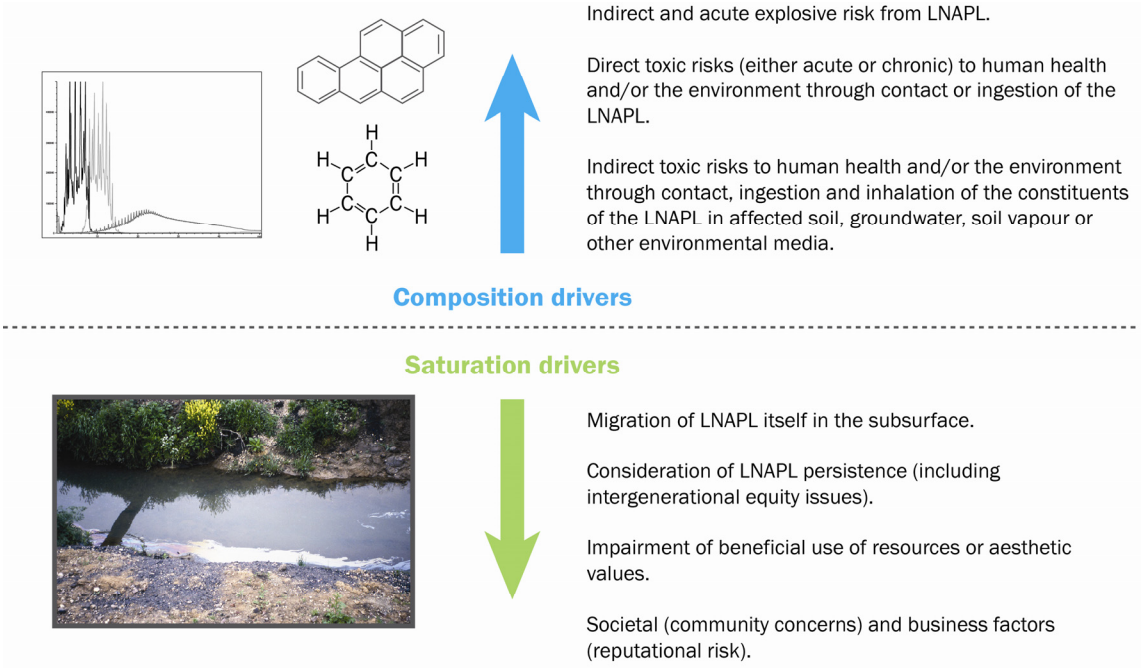

Figure 7.1. Examples of remediation drivers at LNAPL sites (adapted from ITRC (2009a) and Johnston (2010); photograph courtesy of M.O. Rivett).

7.2. Developing a LNAPL management plan

A number of publications have been developed that seek to identify and provide clarity on remediation and management considerations specific to the unique characteristics and challenges posed by LNAPL (ASTM, 2007; ITRC, 2009a; Johnston, 2010; NFEC, 2010; TCEQ, 2008; USEPA, 2004b).

Whilst there are differences in approach, the above publications share many common elements. These include:

- the need to address short-term risks/acute risks/immediate hazards as a priority;
- the development of a detailed CSM (including LNAPL aspects) to serve as the basis for understanding the risks, their uncertainty and feasibility of remediation;
- the need for stakeholder engagement at the outset and throughout the duration of the project;
- development of a clear management strategy or long-term vision at the outset of the project;
- the need to identify clear remedial objectives, remedial goals and metrics that reflect the specific concerns identified in the risk assessment and validation approach;
- recognition of the technical difficulties associated with LNAPL recovery and the requirement to consider cost-benefits in remedial option appraisal and technical impracticality as part of the development of a sustainable remedial closure process;
- a tiered approach to ensure that effort is scaled to site complexity and risk; and
- that an iterative approach is adopted throughout the process.

7.3. LNAPL remediation objectives and metrics

The development of appropriate remedial objectives, goals and metrics is an integral part of a remedial strategy and will underpin remedial process selection.

In the context of LNAPL-impacted sites, remediation objectives are formulated around the abatement of the identified LNAPL concerns identified in Fig. 7.1 and may include both technical risk-based objectives and also non-risk-based objectives that may derive from either regulations or corporate policies, and which may include reputational risk (ASTM, 2007). A summary of concerns and examples of remediation objectives and end points is provided in Fig. 7.2.

Inherent to approaches is the recognition that remedial objectives may be related to the specific nature of concerns posed by the LNAPL (saturation or composition) and can focus on any element of the source-pathway-receptor relationship including source treatment, mitigation along the pathway or institutional controls. Objectives are not solely focused on the recovery of LNAPL either completely or to the maximum extent practicable.

Where the composition of the LNAPL is a key driver, for example from exposure to hazardous constituents such as benzene, then the remedial objective may be to mitigate those components of the LNAPL that are the risk drivers, rather than the bulk of the LNAPL mass. Where saturation is a key driver, for example in LNAPL product migration to a nearby surface water receptor, then LNAPL removal to the extent necessary to reduce LNAPL mobility may be required.

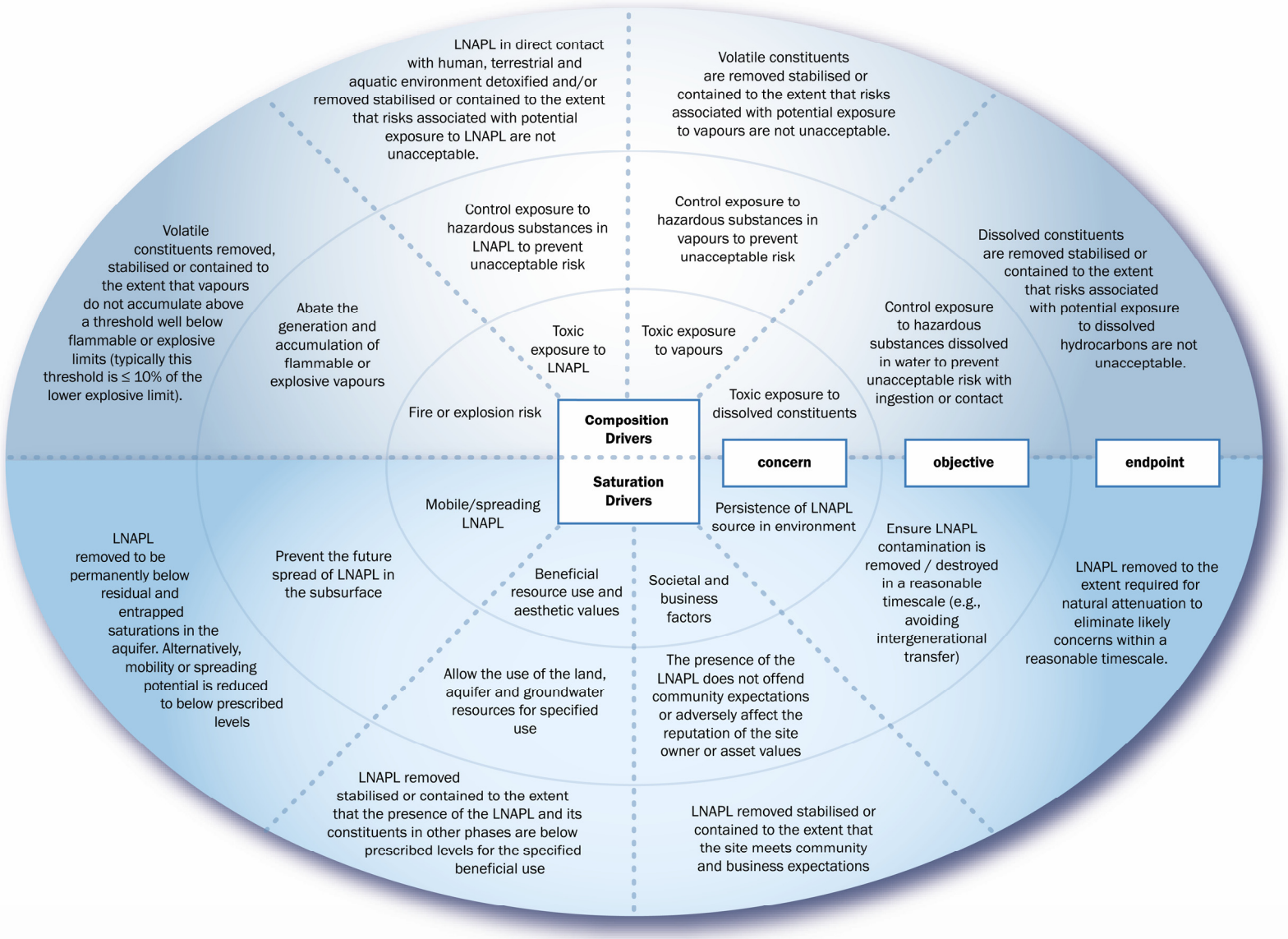

Figure 7.2. Examples of remedial objectives (adapted from Johnston, 2010).

Central to the understanding of these remedial objectives is the relationship between LNAPL mass removal and risk reduction, in particular the expected impact of changing the composition of the LNAPL or removing LNAPL mass on down-gradient dissolved concentrations and plume longevity. This has been explored in ITRC (2009a) and Johnston (2010) and is summarised in Fig. 7.3. Anticipated changes that may occur due to either a reduction in NAPL saturation (timescale) or composition (concentrations) are illustrated and demonstrate the importance of understanding these changes in relation to the remedial objectives.

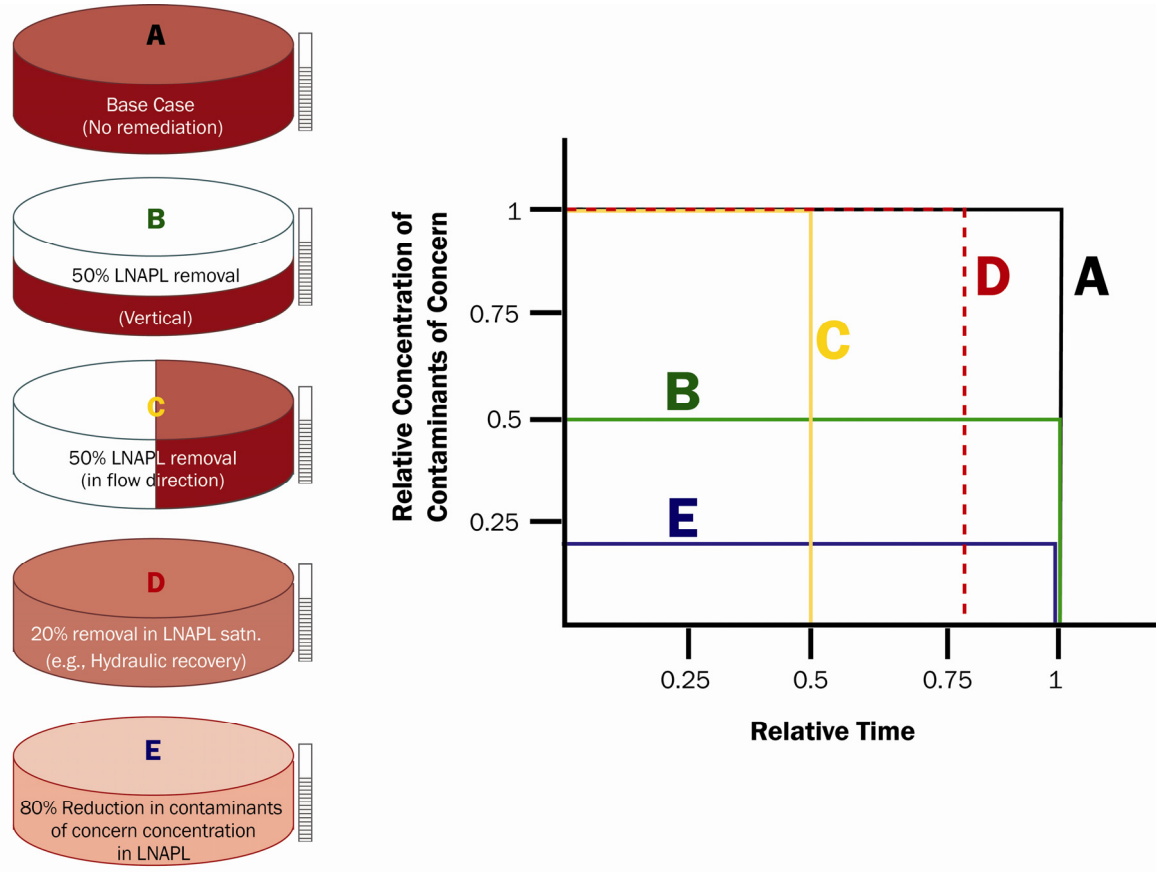

Figure 7.3. Conceptual effect of partial mass removal on LNAPL constituents in a well down gradient in a number of scenarios including a base case (A) and three scenarios (B,C,D) where NAPL recovery is undertaken and a scenario (E) where the composition is changed (adapted from ITRC, 2009a). The figure illustrates that, relative to the base case A, NAPL mass recovery (C,D) may affect remediation timescales but not dissolved-phase concentrations, whilst in other circumstances (B) and where contaminant concentrations are reduced (E), relative individual component concentrations but not remedial timescales are reduced.

Coupled with the development of remedial objectives and goals is the identification of suitable metrics with which to measure progress and ultimately judge when the remedial goal has been met. The nature of these metrics will be specific to the remedial objectives. Examples of metrics associated with a range of composition and saturation based remedial objectives are summarised in Fig. 7.4.

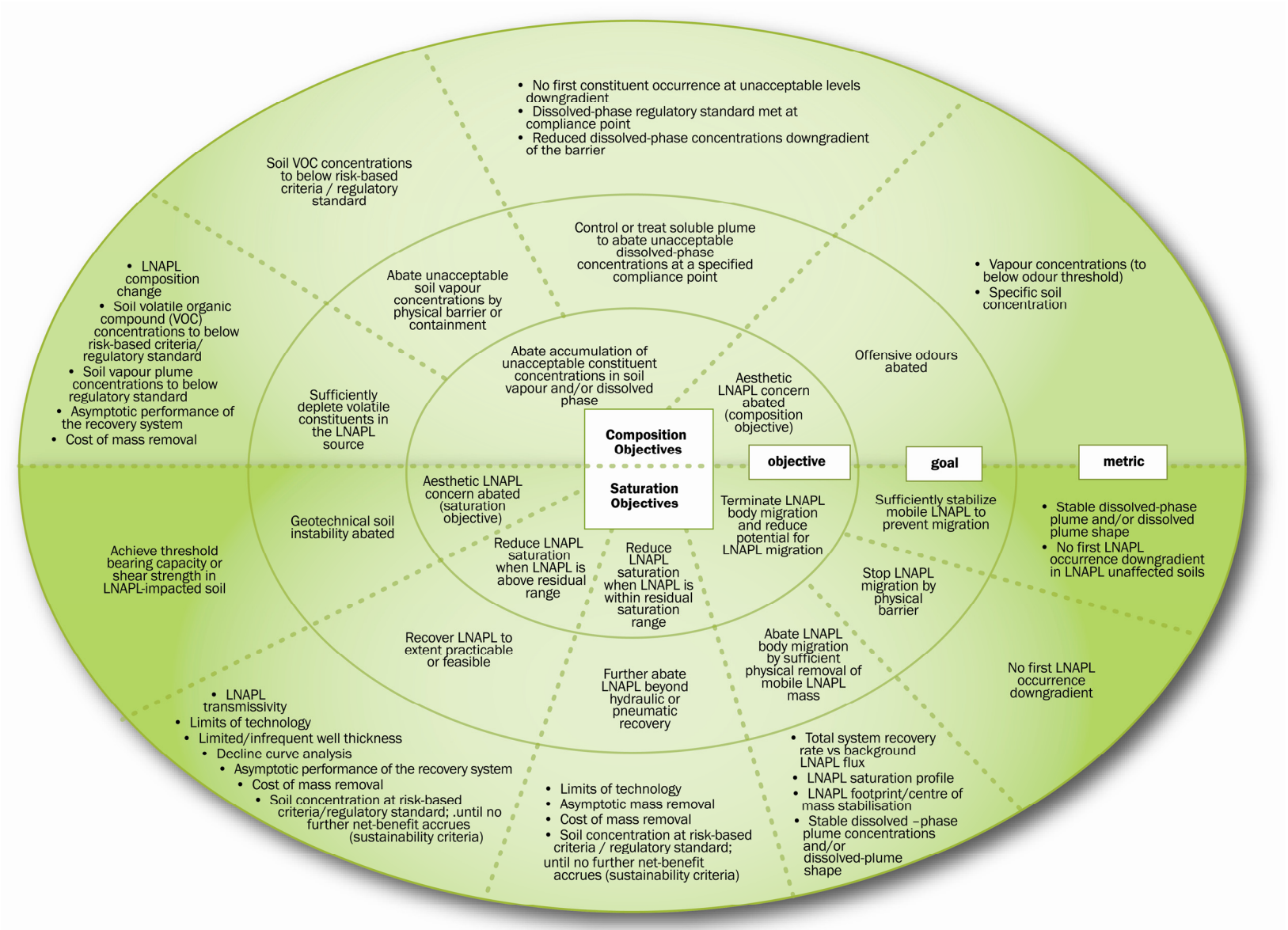

Figure 7.4. Examples of remediation objectives and metrics (adapted from ITRC, 2009a).

Remediation metrics may include the direct environmental benefits of the remediation, such as flux control, risk reduction or source-term reduction. Benefits may also include mitigating direct economic costs associated with LNAPL impacts, as well as costs associated with wider environmentally related issues such as energy use, waste generation and water disposal. This is consistent with the incorporation of principles of sustainability, where the overall net benefit of a system is considered in relation to the primary objective and includes consideration of appropriate and relevant environmental, social and economic indicators (CL:AIRE, 2010).

7.4. Remedial process selection

Where source treatment or pathway interception is considered as part of a remedial strategy there are a wide variety of feasible remedial technologies for managing LNAPL-impacted sites. Such technologies may focus on recovering mobile LNAPL, treating residual LNAPL, managing dissolved-phase and/or vapour-phase plumes. It is paramount that remediation technologies are deployed with a recognised focus (or foci).

Guidance on procedures for the detailed evaluation of options has been summarised elsewhere (API, 2004; EA, 2004; ITRC, 2009a; Johnston, 2010; USEPA, 1988). Separate frameworks and guidance also exist for the appraisal of sustainability considerations during remedial process selection (CL:AIRE, 2010; CL:AIRE, 2011; Holland *et al*., 2011; NICOLE, 2010).

Where mobile NAPL is present, a specific evaluation of the feasibility of LNAPL recovery is usually undertaken. The limitations of product recovery in a variety of hydrogeological settings are well documented and depend upon the nature of the product, the age since release and the geological and hydrogeological setting (API, 2004; ITRC, 2009a). Hydraulic recovery although effective in removing the mobile LNAPL and addressing mobility associated risks, does not address the immobile capillary-held residual (or lower) saturation levels and these may still represent a significant source mass that poses compositional-based risks. Other technologies, for example surfactant flushing, would be necessary to further reduce such mass and associated risks.

Detailed evaluation at the technology screening stage may involve field pilot-scale testing to assess parameters relevant to the proposed metrics and/or the use of NAPL recovery models to predict product recovery (Charbeneau, 2003). The outcome of detailed field-scale evaluation will indicate the extent to which recovery is practical and may inform revision of the CSM and remedial objectives and require a further iteration of the technology selection process.

It is likewise recognised at the outset that some (hydro)geological settings pose a considerable challenge to any *in situ* technology. Fig. 7.5 for instance illustrates the controlling influence of fractures within a clay on NAPL migration and distribution. In this example, after careful field evaluation to determine the practicality of *in situ* treatment, the preferred option was to address shallow impacts through bulk excavation.

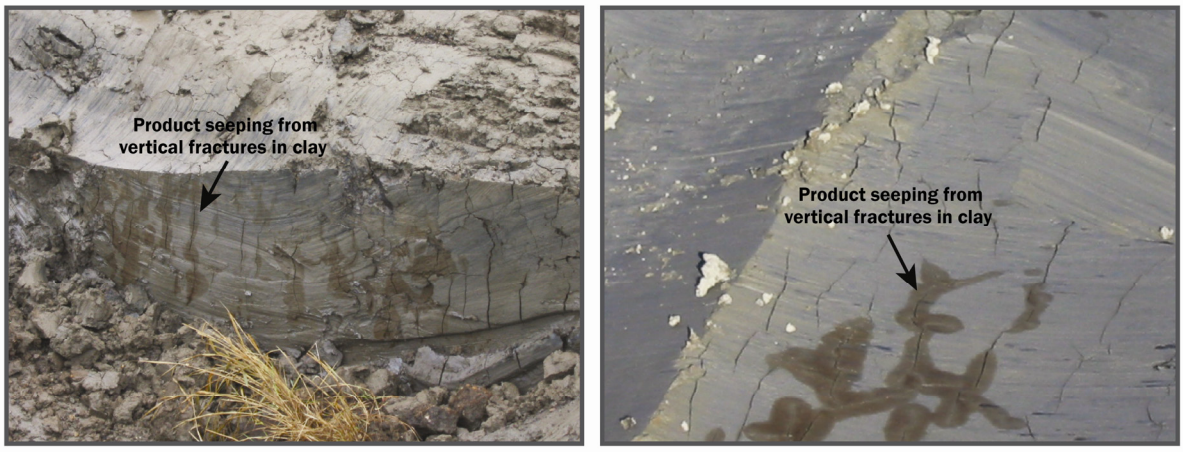

Figure 7.5. During excavation NAPL was seen seeping from fractures in a low permeability geological setting (Photographs courtesy of ERM).

7.5. LNAPL remediation technologies

This handbook is not intended to provide a detailed evaluation of remediation technologies as there is a considerable amount of guidance generally available including LNAPL specific publications (API, 2004; ITRC, 2009a; Johnston, 2010). A general overview of technologies within the categories containment, excavation, mobile LNAPL recovery, residual phase LNAPL recovery, residual phase LNAPL treatment, and, passive treatment is provided within the context of a LNAPL management plan. Fig. 7.6 provides two examples of LNAPL remediation systems.

Figure 7.6. Examples of site remediation systems showing a multi-phase extraction unit (left) and a solar-powered belt skimmer at a Superfund site in the eastern USA (Photographs courtesy of B. Butler, ERM).

7.5.1. Containment

Containment is an intervention approach that breaks the pathway between the LNAPL source and a receptor, and is therefore applicable to either compositional or saturation-based remedial objectives. Techniques based on containment of LNAPL sources include:

- physical containment through the use of vertical cut-off walls and capping layers;
- hydraulic containment through groundwater extraction and/or reinjection; and

- permeable reactive barriers (PRBs) that contain the migration of dissolved-phase plume components from the LNAPL.

None of these technologies is LNAPL-specific. While physical containment can be effective for free-phase LNAPL and dissolved plumes, a key design consideration is the compatibility of the containment material in long-term contact with LNAPL and the need for confident definition of the LNAPL source area to ensure it is fully contained.

Hydraulic containment acts through hydraulic capture or isolation of the LNAPL plume. Hydraulic containment can be maintenance intensive with on-going treatment costs and is often not an ideal long-term solution for LNAPL source zones. It may also result in mobilising or smearing LNAPL from the source area. A key advantage, though, is being able to flexibly increase capture zone extent through increased pumping or additional wells thereby ensuring containment, either close to the source or near a receptor.

PRBs are passive (low management) systems that can intercept the mass flux from a LNAPL zone by *in situ* treatment with a reactive medium placed in a trench or injected in a line perpendicular to the plume. PRBs are not typically designed to treat mobile LNAPL but can be effective in treating the dissolved plume, and PRBs for hydrocarbons use a variety of natural or engineered materials to enhance sorption or stimulate biodegradation.

7.5.2. Excavation

Where residual or free phase LNAPL is present near the ground surface, bulk excavation may be useful and practical as a means of total source removal and can be applicable to either of the main drivers for LNAPL remediation. Excavation remedies need to be carefully designed and executed to minimise potential health and environmental impacts. LNAPL from the excavated materials should be recovered or treated above ground when practical and the materials reused or disposed at an appropriately licensed facility.

7.5.3. Recovery of mobile LNAPL

The recovery of mobile LNAPL is typically a key response to saturation-based remedial objectives and can be undertaken using a variety of approaches (API, 2004).

Interceptor trenches

Interceptor trenches are often applied in heterogeneous geology, at sites where the water table is relatively close to the surface (<3 m) and the LNAPL is mobile and migrating. Construction usually consists of a trench that is orientated perpendicular to the direction of LNAPL migration and is backfilled with a high permeability material. Recovery trenches are often constructed with a membrane on the down gradient side that intersects the water table to act as a barrier to horizontal LNAPL migration, focusing collection of the LNAPL and allowing groundwater to pass below. Recovery of LNAPL from the trench is via a series of sumps or wells that are constructed within the trench and can be undertaken by skimmers or vacuum recovery, as appropriate.

Skimmer wells

Skimmer wells operate using a number of mechanisms that locally recover mobile LNAPL from the surface of the groundwater with little or no recovery of groundwater. There is therefore no hydraulic control of groundwater and the radius of influence of skimming

systems can be low. Skimming is typically more effective in permeable soils and can be useful as a relatively low cost, long-term technique for LNAPL recovery.

Single / dual well total fluids pumping

In single or dual well total fluids pumping, the simultaneous extraction of groundwater with LNAPL is used to create a hydraulic gradient to enhance migration of mobile LNAPL to the point of extraction. The system can therefore also serve as a means of containment of the LNAPL and typically would be expected to have a greater radius of influence than skimming alone. The extracted groundwater usually requires separation of the recovered product from the aqueous phase prior to further treatment. Total fluids pumping may be combined with reinjection of the extracted water to further manipulate the hydraulic gradient and injected water may also be heated to further enhance LNAPL recovery by lowering viscosity, increasing solubility and increasing LNAPL mobility (hot water flooding).

Vacuum enhanced recovery

Vacuum enhanced recovery (VER) is a widely applied technology category that includes dual-phase extraction, multi-phase extraction, high-vacuum extraction and bioslurping (US Army, 2002). The underlying principle in VER is that the application of a vacuum to recovery wells or trenches increases the efficiency and rate of LNAPL and groundwater recovery. If the LNAPL is sufficiently volatile, VER can also recover LNAPL in the vapour phase and encourage *in situ* biodegradation by drawing atmospheric oxygen through the subsurface.

The key technology variants include the use of single or separate pumps for the liquid and vacuum extraction or the use of a drop tube which is placed at the interface of the LNAPL and water table. When a drop tube is used, LNAPL, liquid and vapour are simultaneously removed, though overall water table drawdown and water extraction is minimised. Suitable above ground treatment of all recovered components is required. The use of vacuum tankers (trucks) as mobile VER units has also been undertaken.

High vacuum systems are typically employed in lower permeability or heterogeneous environments with an often high spatial density of extraction points due to their relatively local radius of influence. The efficiency of high vacuum systems can be enhanced further by subsurface heating which can enhance LNAPL recovery due to the increased volatilisation of contaminants.

7.5.4. Recovery of immobile (residual) LNAPL

Where LNAPL is capillary-held in pores at residual or lower saturation (Section 3.1), although immobile, it is still of concern and hence additional enhancements to LNAPL recovery technologies such as chemically or thermally enhanced recovery may be employed to remove this LNAPL mass.

Chemically enhanced recovery of LNAPL

The recovery of LNAPL can be enhanced through the addition of either surfactants or co-solvents to either lower interfacial tension and increase the mobility of LNAPLs or enhance LNAPL solubility. The mobilised or solubilised LNAPL is then typically recovered by groundwater extraction and treated *ex situ*. Each application requires careful selection of surfactants or co-solvents to enhance LNAPL solubilisation adequately. The performance of a surfactant in the subsurface is dependent on temperature, sorption, degradation, the aqueous geochemistry of the injection water and the surface chemistry of aquifer solids. The

efficiency of the process requires good contact between the surfactant and the residual LNAPL.

Thermally enhanced treatment

In situ thermal technologies are designed to primarily enhance mass transfer but in some circumstances may also destroy LNAPL if very high temperatures are applied. Variants of this technology include steam injection, thermal conduction heating, radiofrequency heating and electrical resistance heating. Technology selection is a function of the nature of the contaminants and the site setting.

Thermal technologies often achieve very high mass removal rates in relatively short timeframes, but they are also energy intensive. This should be considered in the context of the overall life cycle of the project on a site-specific basis to assess whether thermal technologies may be more cost-effective or have a lower environmental footprint than conventional technologies that operate over an extended timeframe.

7.5.5. Treatment of residual-phase LNAPL

As an alternative or as a supplement to the recovery of LNAPL, a variety of technologies are available that focus on the *in situ* treatment of residual phase LNAPL through a combination of physical mass transfer, biological degradation and chemical oxidation. These technologies often preferentially remove the more potentially soluble and mobile fractions of a LNAPL and can therefore be used to achieve compositional-oriented remedial objectives.

Soil vapour extraction and bioventing

Soil vapour extraction (SVE) is a well-established technology to address residual VOCs in the partially saturated zone through the application of a vacuum. The applied vacuum draws atmospheric air through the subsurface, volatilising residual VOC mass in the partially saturated zone. SVE systems usually include off-gas treatment to capture or destroy the extracted VOCs. SVE is applicable to those LNAPLs or components that have moderate to high vapour pressures and are hence amenable to volatilisation. SVE is typically most effective in relatively permeable soils. Coincident with physical extraction there is often a contribution to mass removal from enhanced *in situ* bioremediation due to the flow of air introducing oxygen to the subsurface. This latter effect is the focus of bioventing whereby air is injected into the subsurface to encourage *in situ* biodegradation in the partially saturated zone without the need for vacuum extraction or above-ground treatment. This technique is therefore most suited to less volatile LNAPLs and typically has a longer operational time, though lower cost.

Air sparging and biosparging

Air sparging involves the injection of air below the water table and residual LNAPL to stimulate mass transfer to the gaseous phase; this is coupled with the simultaneous capture and extraction by an SVE system. The efficiency of this system is largely controlled by the ability to ensure adequate flow through (rather than bypass of) the residual LNAPL zone and success is therefore usually dictated by geology, with greatest success in homogeneous environments. Biosparging is a less intensive variant of this technology whereby the sparge air is used to introduce oxygen to the subsurface and *in situ* bioremediation, rather than physical stripping, is encouraged. Other variants include the use of either pure oxygen or ozone as the injected gas to achieve higher dissolved oxygen concentrations. Delivery can be via passive or diffusion-based devices as well as active pumping.

In situ bioremediation

In situ bioremediation incorporates a broad range of technology alternatives for residual LNAPL or dissolved-phase treatment. It can be a component of VER and the physical treatment technologies, and is optimised in bioventing and biosparging. *In situ* bioremediation involves creating the appropriate geochemical conditions to enhance microbial activity. These technologies can include systems that utilise aerobic or anaerobic metabolic pathways and typically rely on the addition of electron acceptors (e.g., oxygen, nitrate, sulphate) to the subsurface where these have become rate-limiting. Delivery mechanisms include liquid-phase (through extraction and injection of groundwater mixed with aqueous remedial additives), gas-phase (sparging and venting) and solid-phase (solid oxygen-release compounds) that can be added via wells or through direct mixing with soils.

In situ chemical oxidation

In situ chemical oxidation (ISCO) involves the injection of an oxidising agent into the subsurface to react with residual LNAPL constituents. Some of these agents directly oxidise residual and dissolved-phase hydrocarbons, while others initiate a series of chain reactions that create oxidising free radicals, which in turn react with LNAPL constituents. Common oxidants applied include hydrogen peroxide, Fenton's reagent (hydrogen peroxide and iron catalyst), potassium/sodium permanganate, sodium persulphate and ozone. The application of some oxidants may lead to significant generation of heat and pressure in the subsurface, and hence these, as well as the inherent chemical hazard, need to be carefully managed during an ISCO implementation to ensure a safe working environment.

Oxidants are typically applied to the subsurface through injection but can also be mixed into excavations or trenches. Oxidant selection requires careful analysis of the target compounds and the natural oxidant demand of the soil (e.g., natural organic matter) that may lead to unwanted consumption of oxidant and the geological setting. Oxidants can be effective on the dissolved-phase and can also target residual LNAPL through enhanced dissolution and destruction. ISCO technologies can be effective in relatively short timeframes, though require careful design for safe application and to ensure that the observed decreases in concentrations are sustained to meet remedial objectives. This is important in lower permeability or heterogeneous environments where achieving good contaminant and oxidant contact/mixing can be difficult.

7.5.6. Passive treatment

Passive treatment can be used as a sole approach at low risk sites or more often as a final polishing mechanism in combination with one or more of the active technologies described above.

Monitored natural attenuation

MNA relies on the measurement and quantification of natural processes that mitigate LNAPL constituents over time (Section 4.1.3). The methodology is primarily applied to dissolved-phase contaminants in groundwater, though natural attenuation can also be a significant mechanism for vapours in the partially saturated zone (Section 4.2.3).

The implementation of a MNA programme typically, in more complex cases, requires a 'lines-of-evidence' approach, where contaminant concentrations, aquifer geochemistry and microbiological data are evaluated and integrated to develop a robust understanding of the long-term fate and attenuation of the contaminants of concern, such that remedial objectives

can be met within a reasonable time frame (EA, 2000). MNA has been extensively applied at LNAPL hydrocarbon sites, including sites with oxygenates, principally MTBE and bioalcohols (CONCAWE, 2012). A recent review of long-term plume monitoring data from petrol filling station sites indicates that attenuation of MTBE often occurs with plumes diminishing and/or stabilising at lengths comparable to benzene plumes, and with most sites predicted to achieve remedial goals within timeframes commensurate with, or faster than, benzene plumes (Kamath *et al*., 2012).

Natural source zone depletion

NSZD (Section 4.3) is the assessment of natural mechanisms including volatilisation, leaching and biodegradation on mitigating source zone LNAPL mass rather than the dissolved phase which is the emphasis of MNA. NSZD requires the qualitative and quantitative assessment of the significance of these mechanisms. NSZD is a relatively new concept and is proposed as a basis for benchmarking the performance and relative merit of other remedial options. The quantification of NSZD also is increasingly expected to be important because remedial options rarely remove all residual LNAPL from the subsurface and, also, many hydrocarbon-based LNAPL sources may be vulnerable to natural depletion processes (i.e., many components are relatively biodegradable). It should be recognised that many LNAPL sources are now decades old and will have already undergone potentially significant NSZD. Assessment of NSZD needs to carefully evaluate any decreases in contaminant fluxes from source zones that are typically expected to decline exponentially, where fluxes more gradually reduce with time. Significant temporal data may be required to make reliable predictions of source zone depletion and its significance. The ITRC Technology Overview document (ITRC, 2009b) outlines details of site assessment and evaluation strategies specific to NSZD and provides example case studies.

7.6. Remedial technologies and conceptual model iteration

One of the key considerations of a LNAPL management plan is the requirement to evaluate the CSM and performance of a given remedial technology at key stages throughout the life cycle of the project to ensure that the remedial goals are still achievable and the remedial technology is still appropriate.

Whilst some evolution of the remedial approach can be anticipated prior to the project commencing, this feedback loop is a key mechanism in encouraging the integration of a range of technologies during the course of a project recognising that, as conditions change, the focus of remediation and therefore the most appropriate remediation technique may also change. This integrated remedial strategy approach often includes evolution from a phase of active recovery of mobile free product, through *in situ* treatment of the residual phase to MNA.

Ultimately integrative, progressive and adaptive technology implementation requires multi-disciplinary expertise built around an iterative CSM. This will require the cooperative collaboration of the site problem holder, technical providers and regulators alongside active participation of wider stakeholders, which may range from investing financial institutions to local populations.

Glossary

Advection - Transportation of a substance arising from the bulk movement of a fluid. For example, dissolved-phase contaminant being transported by the moving groundwater.

Biodegradation - The degradation of contaminants as a result of microbiological activity, typically mediated by bacteria resident in the subsurface or perhaps added during bioremediation. The rate of biodegradation depends on factors such as the presence of micro-organisms able to degrade the contaminant(s), availability of electron acceptors, pH, redox and temperature.

Capillary pressure - The pressure difference between the non-wetting fluid (usually the LNAPL oil) and the wetting fluid (usually water). Capillary pressure arises because of interfacial tension and is directly proportional to that tension and inversely proportional to the radius of curvature of the fluid-fluid interface.

Conceptual site model (CSM) - A representation (for example schematic figure) or description (for example an entire report) of the site scenario and the processes that control contaminant transport and fate and is often used as a framework to manage risks posed to receptors.

Electron acceptor (and donor) - A chemical entity that accepts electrons transferred to it from another chemical entity, the '**electron donor**'. The electron acceptor is an oxidising agent as it oxidises the electron donor. By virtue of accepting electrons, the electron acceptor is reduced. Hydrocarbon contaminants typically act as electron donors and are oxidised in the presence of electron acceptors such as oxygen, nitrate, iron (III), manganese (IV), sulphate and carbon dioxide that are reduced - for example, sulphate to sulphide.

Hydrocarbons (Aliphatic, Aromatic, Alicyclic, Polycyclic) - Hydrocarbons are covalently bonded molecules containing just carbon and hydrogen. **Aliphatic hydrocarbons** contain a carbon atom framework of straight or branched carbon chains. **Alicyclic hydrocarbons** contain a ring of carbon atoms in their structure (that may have side chains); **Aromatic hydrocarbons** such as benzene and toluene contain a single planar ring of six carbons with a delocalised aromatic ring of electrons that confers stability on the molecule and persistence in the environment. **Polycyclic aromatic hydrocarbons (PAHs)** (such as benzo[a]pyrene (BaP)) contain multiple adjacent (fused) aromatic rings.

Hydrostatic equilibrium - The pressure at any point in a fluid at rest (i.e., "hydrostatic") is just due to the weight of the overlying fluid.

Hysteresis (Hysteretic behaviour) - Hysteresis is the dependence of a system not only on its current environment but also on its past environment, i.e., its history. Within the context of LNAPL entry and then drainage from an initially water-saturated porous rock, due to the retention of residual LNAPL arising from entrapment processes due to capillary forces, the capillary pressure curves for the primary drainage curve and for primary imbibition curves follow different pathways. A further cycle of water drainage with accompanying LNAPL invasion, would likewise produce a secondary drainage curve non-coincident with the primary due to the differing starting position – it is hysteretic.

Imbibition - occurs when a wetting fluid displaces a non-wetting (immiscible) fluid, contrary to **drainage** where a non-wetting phase displaces the wetting fluid. Typically within the porous media context, water will be the wetting fluid and the LNAPL, the non-wetting fluid.

Interfacial tension - A tensile force that exists in the interface between **immiscible fluids** (fluids that do not mix and form separate phases, for example water and LNAPL). Without interfacial tension, LNAPLs would be fully miscible (infinitely soluble) in water. Interfacial tension exists between any pair of immiscible fluids such as air and water, LNAPL and water, and LNAPL and air.

LNAPL (light non-aqueous phase liquid) - A liquid that is less dense than water and immiscible (does not mix) with the water thus forming a separate (floating) liquid phase when in contact. Chemical constituents of the LNAPL may still have some solubility in the adjacent water and form a dissolved-phase (plume) in that aqueous-phase liquid. Likewise, some constituents may be volatile and form a vapour phase (plume) in the adjacent gas (air) phase. LNAPL examples include hydrocarbon fuels and oils.

Plume - A contiguous region of groundwater containing dissolved-phase contaminants. So-called **dissolved-phase plumes** are typically formed by the dissolution (solubilisation) of LNAPL into groundwater and therefore occur hydraulically down gradient of the source zone. Vapour plumes may similarly arise that comprise volatilised contaminant in the air-phase surrounding a LNAPL.

Pore (or fracture) entry pressure - The threshold capillary pressure required for a non-wetting fluid to enter a wetting-fluid saturated rock pore (or fracture). Pore or (fracture) entry pressures are directly proportional to the interfacial tension and wettability, and inversely proportional to the fracture aperture.

Residual LNAPL - Disconnected blobs and **ganglia** (blobs joined over several pore bodies) of organic liquid (LNAPL) trapped by capillary forces in either porous or fractured media. Residual LNAPL forms at the trailing end of a migrating LNAPL body as a result of pore-scale hydrodynamic instabilities leading to snap-off of the LNAPL as isolated entities, i.e., blobs and ganglia of LNAPL left behind held as a result of capillary forces. As it is held by capillary forces, residual LNAPL is difficult to mobilise.

Sorption - The transfer (or partitioning) of contaminants dissolved in water to the solid phase – typically fracture walls, the surfaces of sand/silt/clay grains or the surfaces of the solid portion of the rock matrix. For organic contaminants, (sedimentary) organic matter / carbon present in the geological media, although typically present in low amounts, represents the most attractive sorption site. Sorption hence increases with greater fraction of organic carbon (f_{oc}) content of the geological material – measuring f_{oc} contents is hence important.

Surfactants - Compounds that lower the interfacial tension between two liquids or between a liquid and a solid. Surfactant molecules accumulate at the interface as they have a dual polar – non-polar component nature and hence the ‘polar head’ of the molecule would have an affinity for the polar aqueous-phase and the non-polar tail an affinity for the hydrophobic organic contaminant. Surfactants will lead to enhanced aqueous-phase solubility of LNAPL components and also modify the interfacial tension of a LNAPL that may result in potential mobilisation of capillary-held previously immobile (residual) LNAPL. Surfactants may hence, with appropriate care, be used in the remediation of sites.

Transmissivity - describes the ability of an aquifer (porous rock containing groundwater) to transmit groundwater horizontally throughout its entire saturated thickness. It is the product of the aquifer hydraulic conductivity and saturated aquifer thickness. A related concept, LNAPL transmissivity, may be applied to LNAPL to quantify LNAPL flow through a formation, typically to a recovery well (Section 3.8).

Vapourisation - The transfer of chemical mass from the LNAPL phase to the adjacent air phase. The rate of vapourisation is proportional to the LNAPL vapour pressure that is temperature dependent.

Viscosity - The shear resistance to flow of a fluid. Higher viscosity (thicker) fluids such as viscous oils migrate more slowly in the subsurface than lower viscosity (thinner) fluids such as petrol.

Volatilisation - The transfer of chemical contaminants dissolved in water to the air phase. Volatilisation is characterised by the Henry's law constant of the dissolved contaminant of interest that is the ratio of concentrations (or vapour pressures) in the air phase and aqueous phase.

Wettability - The affinity of one fluid for a solid surface in the presence of a second fluid, for example water in the presence of LNAPL. The fluid that preferentially wets the solid surface is referred to as the **wetting fluid** and the other as the **non-wetting fluid**. Within the geological subsurface, water is normally wetting (spreading preferentially across the mineral surface) with respect to LNAPL which in turn is wetting with respect to air. Repeated exposure may potentially cause a surface to gradually become LNAPL wetting with time.

References

Abdul, A.S., Kia, S.F., Gibson, T.L., 1989. Limitations of monitoring wells for the detection and quantification of petroleum products in soil and aquifers. *Groundwater Monit. R.*, 9(2), 90-99. http://dx.doi.org/10.1111/j.1745-6592.1989.tb01144.x

Abreu, L.D., Johnson, P.C., 2005. Effect of vapor source, building separation and building construction on soil vapor intrusion as studied with a three-dimensional numerical model. *Environ. Sci. Technol.*, 39, 4550-4561. http://dx.doi.org/10.1021/es049781k

Abreu, L.D., Johnson, P.C., 2006. Modeling the effect of aerobic biodegradation on soil vapor intrusion into buildings - influence of degradation rate, source concentration and depth. *Environ. Sci. Technol.*, 40, 2304-2315. http://dx.doi.org/10.1021/es051335p

Adamski, M., Kremesec, V., Kolhatkar, R., Pearson, C. Rowan, B., 2005. LNAPL in fine-grained soils: conceptualization of saturation, distribution, recovery, and their modeling. *Groundwater Monit. R.*, 25(1), 100-112. http://dx.doi.org/10.1111/j.1745-6592.2005.0005.x

API (American Petroleum Institute), 1998. Recommended practices for core analysis (2nd Ed.), API RP-40. http://publications.api.org/

API, 2004. API interactive LNAPL guide. Version 2.04. Soil and Groundwater Technical Task Force. http://www.api.org/environment-health-and-safety/clean-water/ground-water/lnapl/api-interactive-lnapl-guide

API, 2006a. Interactive LNAPL guide, http://www.api.org/environment-health-and-safety/clean-water/ground-water/lnapl/api-interactive-lnapl-guide

API, 2006b. API parameters database http://www.api.org/~/link.aspx?_id=6C87D80236C64655A4E88DB8FA835EEB&_z=z

ASTM (American Society for Testing and Materials), 1998. ASTM guide for remediation by natural attenuation at petroleum release sites. ASTM E1943. http://dx.doi.org/10.1520/E1943-98R10

ASTM, 2006. Standard guide for development of conceptual site models and remediation strategies for light nonaqueous-phase liquids released to the subsurface. ASTM E2531-06e1. http://dx.doi.org/10.1520/E2531-06E01

ASTM, 2007. Standard guide for development of conceptual site models and remediation strategies for light nonaqueous-phase liquids released to the subsurface. *ASTM E2531-06*. http://dx.doi.org/10.1520/E2531-06

ASTM, 2011. Standard guide for estimation of LNAPL transmissivity, *ASTM* E2856-11. http://dx.doi.org/10.1520/E2856-13

ASTM, 2013a. Standard guide for estimation of LNAPL transmissivity, ASTM E2856-13 http://dx.doi.org/10.1520/E2856-13

ASTM, 2013b. Standard guide for integrating sustainable objectives into cleanup. ASTM E2876-13. http://dx.doi.org/10.1520/E2876

Beckett, G.D., Joy, S., 2003. Light non-aqueous phase liquid (LNAPL) parameters database, Version 2.0. *API Publ.* 4731. http://www.api.org/environment-health-and-safety/clean-water/ground-water/lnapl/lnapl-params-db

Beckett, G.D., Lundegard, P.D., 1997. Practically impractical - The limits of LNAPL recovery and relationship to risk. Conference Proceedings of the 1997 Petroleum Hydrocarbons & Organic Chemicals in Ground Water. Houston, Texas, National Ground Water Association & American Petroleum Institute.

Benbow, S.J., Rivett, M.O., Chittenden, N., Herbert, A.W., Watson, S, Williams, S.J., Norris, S., 2014. Potential migration of buoyant LNAPL from Intermediate Level Waste (ILW) emplaced in a Geological Disposal Facility (GDF) for UK radioactive waste. *J. Contam. Hydrol.*, 167, 1-22. . http://dx.doi.org/10.1016/j.jconhyd.2014.07.011

Bowers, R.L., Smith J.W.N., 2014. Constituents of potential concern for human health risk assessment of petroleum fuel releases. *Q. J. Eng. Geol. Hydroge.* 47, 363-372. http://dx.doi.org/10.1144/qjegh2014-005

Charbeneau, R.J., 2003. Models for design of free-product recovery systems for petroleum hydrocarbon liquids. API Publ. No. 4729. http://publications.api.org/

Charbeneau, R.J., Johns, R.T., Lake, L.W., McAdams, M.J., 1999. Free-product recovery of petroleum hydrocarbon liquid. API Publ. No. 4682. http://publications.api.org/

Christophersen, M., Broholm, M.M., Mosbæk, H., Karapanagioti, H.K., Burganos, V.N., Kjeldsen, P., 2005. Transport of hydrocarbons from an emplaced fuel source experiment in the vadose zone at Airbase Værløse, Denmark. *J. Contam. Hydrol.*, 81, 1-33. http://dx.doi.org/10.1016/j.jconhyd.2005.06.011

CL:AIRE, 2002. Site characterisation in support of monitored natural attenuation of fuel hydrocarbons and MTBE in a chalk aquifer in Southern England. CL:AIRE Case Study Bulletin, CSB 1. http://www.claire.co.uk/index.php?option=com_cobalt&view=record&id=16:site-characterisation-in-support-of-monitored-natural-attenuation-of-fuel-hydrocarbons-and-mtbe-in-a-chalk-aquifer-in-southern-england&Itemid=61

CL:AIRE, 2010. A framework for assessing the sustainability of soil and groundwater remediation. SuRF-UK Report. CL:AIRE, London. http://www.claire.co.uk/index.php?option=com_phocadownload&view=file&id=61:initiatives&Itemid=78

CL:AIRE, 2011. A framework for assessing the sustainability of soil and groundwater remediation: Annex 1 - The SuRF-UK indicator set for sustainable remediation assessment. SuRF-UK Report. CL:AIRE, London. http://www.claire.co.uk/index.php?option=com_phocadownload&view=file&id=262:initiatives&Itemid=78

Clements, L., Palala, T., Davis, J., 2009. Characterisation of sites impacted by petroleum hydrocarbons. CRC CARE Technical Report No. 11. http://www.crccare.com/publications/technical-reports

CONCAWE, 2012. Gasoline ether oxygenate occurrence in Europe, and a review of their fate and transport characteristics in the environment. CONCAWE report 4/12, CONCAWE, Brussels. https://www.concawe.eu/DocShareNoFrame/docs/1/PPJNPADCAEGGMDCJBMKIPPFCVEVCWY9K9YBYP3BY7DG3/CEnet/docs/DLS/Rpt_12-4-2012-02904-01-E.pdf

Corey, A.T., 1990. Mechanics of immiscible fluids in porous media. Water Resources Publications, Littleton, Colorado.

Davis, G.B., Merrick, N., McLaughlan, R., 2006. Protocols and techniques for characterizing sites with subsurface petroleum hydrocarbons – a review. CRC CARE Technical Report No. 2, http://www.crccare.com/files/dmfile/CRCCARETechReport2-Protocolsandtechniquesforcharacterisingsiteswithsubsurfacepetroleumhydrocarbons2.pdf

Davis, G.B., Patterson, B.M., Trefry, M.G., 2009. Biodegradation of petroleum hydrocarbon vapours. *CRC CARE Tech. Rep.* No. 12. http://www.crccare.com/publications/technical-reports

Davis, G.B., Rayner, J.L., Trefry, M.G., Fisher, S.J., Patterson, B.M., 2005. Measurement and modelling of temporal variations in hydrocarbon vapor behavior in a layered soil profile. *Vadose Zone J.*, 4, 225-239. http://dx.doi.org/10.2136/vzj2004.0029

Davis, G.B., Trefry, M.G., Patterson, B.M., 2004. Petroleum and solvent vapours: quantifying their behaviour, assessment and exposure. CSIRO Land and Water Report. http://www.clw.csiro.au/publications/consultancy/2004/WA_DoE_Vapour_Review.pdf

Defra. 2012. Environmental Protection Act 1990: Part 2A. Contaminated land statutory guidance. https://www.gov.uk/government/uploads/system/uploads/attachment_data/file/223705/pb13735cont-land-guidance.pdf

DeVaull, G.E., 2007. Indoor vapor intrusion with oxygen-limited biodegradation for a subsurface gasoline source. *Environ. Sci. Technol.*, 41(9), 3241-3248. http://dx.doi.org/10.1021/es060672a

DeVaull, G.E., 2011. Biodegradation rates for petroleum hydrocarbons in aerobic soils: A summary of measured data. International Symposium on Bioremediation and Sustainable Environmental Technologies, June 27-30, 2011, Reno, Nevada.

EA (Environment Agency), 2000. Guidance on the assessment and monitoring of natural attentuation of contaminants in groundwater. Environment Agency R&D Publication 95. https://www.gov.uk/government/uploads/system/uploads/attachment_data/file/297675/sr-dpub95-e-e.pdf

EA, 2001. Guide to good practice for the development of conceptual models and the selection and application of mathematical models of contaminant transport processes in the subsurface. EA NGWCLC Rep. NC/99/38/2. https://www.gov.uk/government/uploads/system/uploads/attachment_data/file/290422/scho0701bitr-e-e.pdf

EA, 2002. Vapour transfer of soil contaminants. Environment Agency R&D Technical Report P5-018/TR. https://www.gov.uk/government/uploads/system/uploads/attachment_data/file/290400/sp5-018-ts-e-e.pdf

EA, 2004. Model procedures for the management of land contamination, Defra and Environment Agency, Contaminated Land Report 11, Environment Agency. https://www.gov.uk/government/publications/managing-land-contamination

Efroymson, R. A., Alexander, M., 1994a. Biodegradation in soil of hydrophobic pollutants in nonaqueous-phase liquids (NAPLs). *Environ. Toxicol. Chem.,* 13(3), 405-11. http://dx.doi.org/10.1002/etc.5620130307

Efroymson, R. A., Alexander, M., 1994b. Role of partitioning in biodegradation of phenanthrene dissolved in nonaqueous-phase liquids. *Environ. Sci. Technol.*, 28(6), 1172-79. http://dx.doi.org/10.1021/es00055a031

Farr, A.M., Houghtalen, R.J., McWhorter, D.B., 1990. Volume estimation of light nonaqueous phase liquids in porous media. *Groundwater* 28(1), 48-56. http://dx.doi.org/10.1111/j.1745-6584.1990.tb02228.x

Feenstra, S., Mackay, D.M., Cherry, J.A., 1991. A method for assessing residual NAPL based on organic chemical concentrations in soil samples. *Ground Water Monit. Remed.*, 11,128-136. http://dx.doi.org/10.1111/j.1745-6592.1991.tb00374.x .

Garg, S., Rixey, W.G., 1999. The dissolution of benzene, toluene, m-xylene and naphthalene from a residually trapped non-aqueous phase liquid under mass transfer limited conditions. *J. Contam. Hydrol.*, 36, 311-329. http://dx.doi.org/10.1016/S0169-7722(98)00149-1

Gormley, A., Pollard, S., Rocks, S., 2011. Defra - Guidelines for environmental risk assessment and management: Green Leaves III. https://www.gov.uk/government/publications/guidelines-for-environmental-risk-assessment-and-management-green-leaves-iii

Grathwohl, P., Klenk, I.D., Maier, U. Reckhorn, S.B.F., 2002. Natural attenuation of volatile hydrocarbons in the unsaturated zone and shallow groundwater plumes: Scenario-specific modeling and laboratory experiments. In GQ2001: Natural and Enhanced Restoration of Groundwater Pollution, Sheffield, U.K., 16-21 June 2001. (eds, Thornton, S.F & Oswald, S.O.), IAHS Publ. No. 275, 141-146.

Hardisty, P.E., Wheater, H.S., Birks, D., Dottridge, J., 2003. Characterization of LNAPL in fractured rock. *Q. J. Eng. Geo. Hydroge*., 36, 343-354. http://dx.doi.org/10.1144/1470-9236/03-019

Hardisty, P.E., Wheater, H.S., Johnston, P.M., Bracken, R.A., 1998. Behaviour of light immiscible liquid contaminants in fractured aquifers. *Geotechnique*, 48, 747-760. http://dx.doi.org/10.1680/geot.1998.48.6.747

Hardisty, P.E., Wheater, H.S., Johnston, P.M., Dabrowski, T.L., 1994. Mobility of LNAPL in fractured sedimentary rocks: Implications for remediation. Proceedings. API / NGWA Conference on Hydrocarbons and Organic Chemicals in Groundwater, Houston, 1994.

Holland, K. S., Lewis, R.E., Tipton, K., Karnis, S., Dona, C., Petrovskis, E., Bull, L.P., Taege, D., Hook, C., 2011. Framework for integrating sustainability into remediation projects. *Remediation*, 21 (3), 7-38. http://ww.sustainableremediation.org/library/guidance-tools-and-other-resources/

Huntley, D., 2000. Analytic determination of hydrocarbon transmissivity from baildown tests. *Groundwater*, 38(1), 46-52. http://dx.doi.org/10.1111/j.1745-6584.2000.tb00201.x

Huntley, D., Beckett, G.D., 2002. Persistence of LNAPL sources: relationship between risk reduction and LNAPL recovery. *J. Contam. Hydrol.*, 59, 3-26. http://dx.doi.org/10.1016/S0169-7722(02)00073-6

Huntley, D., Hawk, R.N., Corley, H.P., 1994a. Nonaqueous phase hydrocarbon in a fine-grained sandstone: 1. Comparison between measured and predicted saturations and mobility. *Groundwater*, 32: 626-634. http://dx.doi.org/10.1111/j.1745-6584.1994.tb00898.x

Huntley, D., Wallace, J.W., Hawk, R.N., 1994b. Nonaqueous phase hydrocarbon in a fine-grained sandstone: 2. Effect of local sediment variability on the estimation of hydrocarbon volumes. *Groundwater*, 32: 778-783. http://dx.doi.org/10.1111/j.1745-6584.1994.tb00919.x

ITRC (Interstate Technology & Regulatory Council), 2009a. Evaluating LNAPL remedial technologies for achieving project goals. *Interstate Technology and Regulatory Council, LNAPLs Team*. http://www.itrcweb.org/guidance/getdocument?documentid=48

ITRC, 2009b. Evaluating natural source zone depletion at sites with LNAPL. *Interstate Technology and Regulatory Council.* http://www.itrcweb.org/GuidanceDocuments/LNAPL-1.pdf

ITRC, 2011. Green and sustainable remediation: A practical framework. ITRC Report GSR-2. http://www.itrcweb.org/GuidanceDocuments/GSR-2.pdf

ITRC, 2014. Petroleum vapor intrusion: Fundamentals of screening, investigation, and management. PVI-1. Washington, D.C.: Interstate Technology and Regulatory Council, Petroleum Vapor Intrusion Team. http://www.itrcweb.org/PetroleumVI-Guidance.

Jin, M., Delshad, M., Dwarakanath, V., McKinney, D.C., Pope, G.A., Sepehrnoori, K., Tillburg, C., Jackson, R.E., 1995. Partitioning tracer test for detection, estimation and remediation performance assessment of subsurface nonaqueous phase liquids. *Water Resour. Res.*, 31(5), 1201-1211. http://dx.doi.org/10.1029/95WR00174

Johnson, P.C., Ettinger, R.A., 1991. Heuristic model for predicting the intrusion rate of contaminant vapors into buildings. *Environ. Sci. Technol.*, 25, 1445-1452. http://dx.doi.org/10.1021/es00020a013

Johnson, P.C., Lundegard, P., Liu. Z., 2006. Source zone natural attenuation at petroleum hydrocarbon spill sites: I. Site-Specific Assessment Approach. *Groundwater Monit. R.*, 26(4), 82-92. http://dx.doi.org/10.1111/j.1745-6592.2006.00114.x

Johnston, C.D., 2010. Selecting and assessing strategies for remediating LNAPL in soils and aquifers. CRC for contamination assessment and remediation of the environment, CRC Care Technical Report No.18. http://www.crccare.com/publications/technical-reports/technical-reports

Jones, W.R., Spence, M.J., Bowman, A.W., Evers, L., Molinari, D.A., 2014. A software tool for the spatiotemporal analysis and reporting of groundwater monitoring data. *Environ. Modell. Softw.*, 55, 242-249. http://dx.doi.org/10.1016/j.envsoft.2014.01.020

Kamath, R., Connor, J., McHugh, T., Nemir, A., Le, M., Ryan, A., 2012. Use of long-term monitoring data to evaluate benzene, MTBE, and TBA plume behavior in groundwater at retail gasoline sites. *J. Environ. Eng.*, 138(4), 458-469. http://dx.doi.org/10.1061/(ASCE)EE.1943-7870.0000488

Keller, A.A., Chen, M., 2003. Effect of spreading coefficient on three-phase relative permeability of nonaqueous phase liquids. *Water Resour. Res.* 39(10), 1288, http://dx.doi.org/10.1029/2003WR002071

Kemblowski, M.W., Chiang, C.Y., 1990. Hydrocarbon thickness fluctuations in monitoring wells. *Groundwater* 28(2), 244-252. http://dx.doi.org/10.1111/j.1745-6584.1990.tb02252.x

Kirkman, A.J., Adamski, M., Hawthorne, J.M., 2012. Identification and assessment of confined and perched LNAPL conditions. *Groundwater Monit. R.*, 33(1), 75-86. http://dx.doi.org/10.1111/j.1745-6592.2012.01412.x

Knight, J.H, Davis, G.B., 2013. A conservative vapour intrusion screening model of oxygen-limited hydrocarbon vapour biodegradation accounting for building footprint size. *J. Contam. Hydrol.*, 155, 46-53. http://dx.doi.org/10.1016/j.jconhyd.2013.09.005

Kueper, B.H., McWhorter, D. B., 1991. The behavior of dense, nonaqueous phase liquids in fractured clay and rock. *Groundwater*, 29: 716-728. http://dx.doi.org/10.1111/j.1745-6584.1991.tb00563.x

Kueper, B.H., Redman, D., Starr, R.C., Reitsma, S., Mah, M., 1993. A field experiment to study the behavior of tetrachloroethylene below the water table: spatial distribution of residual and pooled DNAPL. *Groundwater*, 31: 756-766. http://dx.doi.org/10.1111/j.1745-6584.1993.tb00848.x

Kueper, B.H., Wealthall, G.P., Smith, J.W.N., Leharne, S.A., Lerner, D.N., 2003. An illustrated handbook of DNAPL transport and fate in the subsurface. Environment Agency R&D Publication 133, Bristol, UK. https://www.gov.uk/government/publications/an-illustrated-handbook-of-dense-non-aqueous-phase-liquids-dnapl-transport-and-fate-in-the-subsurface

Lahvis, M.A., 2005. Evaluation of potential vapor transport to indoor air associated with small-volume releases of oxygenated gasoline in the vadose zone. *API Bulletin* 21. http://publications.api.org/

Lahvis, M.A., Hers, I., Davis, R.V., Wright, J. DeVaull, G.E., 2013. Vapor Intrusion Screening at Petroleum UST Sites. *Groundwater Monit. R.*, 33, 53-67. http://dx.doi.org/10.1111/gwmr.12005

Lenhard, R.J., Parker, J.C., 1987. Measurement and prediction of saturation-pressure relationship in three phase porous media systems. *J. Contam. Hydrol.*, 1, 407-424. http://dx.doi.org/10.1016/0169-7722(87)90017-9

Lenhard, R.J., Parker, J.C., 1988. Experimental validation of the theory of extending two phase saturation-pressure relations to three fluid phase systems for monotonic drainage paths. *Water Resour. Rev.*, 24, 373-380. http://dx.doi.org/10.1016/0169-7722(87)90017-9

Lenhard, R.J., Parker, J.C., 1990a. Estimation of free hydrocarbon volume from fluid levels in monitoring wells. *Groundwater* 28(1), 57-67. http://dx.doi.org/10.1111/j.1745-6584.1990.tb02229.x

Lenhard, R.J. Parker, J.C., 1990b. Discussion of estimation of free hydrocarbon volume from fluid levels in monitoring wells. *Groundwater* 18(5), 800-801. http://dx.doi.org/10.1111/j.1745-6584.1990.tb01994.x

Lundegard, P.D., Johnson, P.C., 2006. Source zone natural attenuation at petroleum hydrocarbon spill sites: II. Application to a former oil field. *Groundwater Monit. R.*, 26(4), 93-106. http://dx.doi.org/10.1111/j.1745-6592.2006.00115.x

Ma, J., Rixey, W.G., DeVaull, G.E., Stafford, B.P., Alvarez, P.J.J., 2012. Methane bioattenuation and implications for explosion risk reduction along the groundwater to soil surface pathway above a plume of dissolved ethanol. *Environ. Sci. Technol.*, 46, 6013-6019. http://dx.doi.org/10.1021/es300715f

Mahler, N., Sale, T., Smith, T., Lyverse, M., 2012. Use of single-well tracer dilution tests to evaluate LNAPL flux at seven field sites. *Groundwater*, 50, 851-860. http://dx.doi.org/10.1111/j.1745-6584.2011.00902.x

Marinelli, F., Durnford, D.S., 1996. LNAPL thickness in monitoring wells considering hysteresis and entrapment. *Groundwater,* 34(3), 405-414. http://dx.doi.org/10.1111/j.1745-6584.1996.tb02021.x

McHugh, T.E., Kamath, R. Kulkarni, P.R., Newell, C.J., Connor, J.A., Garg., S., 2012. Remediation progress at California LUFT sites: insights from the Geotracker Database. API Technical Bulletin #25: http://api.org/~/media/Files/EHS/Clean_Water/Bulletins/25_Bull.ashx

Mercer, J.W., Cohen, R.M., 1990. A review of immiscible fluids in the subsurface: properties, models, characterization and remediation. J. *Contam. Hydrol*., 6(2), 107-163. http://dx.doi.org/10.1016/0169-7722(90)90043-G

Molins, S., Mayer, K.U., Amos, R.T., Bekins, B.A., 2010. Vadose zone attenuation of organic compounds at a crude oil spill site – interactions between biogeochemical reactions and multicomponent gas transport. *J. Contam. Hydrol.*, 112, 15-29. http://dx.doi.org/10.1016/j.jconhyd.2009.09.002

Naval Facilities Engineering Command (NFEC), 2010. LNAPL site management handbook, https://portal.navfac.navy.mil

NICOLE (Network of Industrially Contaminated Land in Europe), 2010. NICOLE roadmap for sustainable remediation. http://www.nicole.org/uploadedfiles/2010-wg-sustainable-remediation-roadmap.pdf

Oostrom M., Hofstee, C., Wietsma, T.W., 2006. Behavior of a viscous LNAPL under variable water table conditions. *Soil Sediment Contam*. 15(6):543-564. http://doi:10.1080/15320380600958976

Parker, J.C., Waddill, D.W., Johnson, J.A., 1994. UST corrective action technologies: Engineering design of free product recovery systems, prepared for Superfund Technology Demonstration Division, Risk Reduction Engineering Laboratory, Edison, NJ, Environmental Systems & Technologies, Inc., Blacksburg, VA. http://nepis.epa.gov

Rao, P.S.C., Lee, L.S., Wood, A.L., 1991. Solubility, sorption and transport of hydrophobic organic chemicals in complex mixtures. USEPA Environmental Research Brief, EPA/600/M-91/009, Robert S Kerr Environmental Research Laboratory, Ada, Oklahoma. http://nepis.epa.gov

Rivett, M.O., Thornton, S.F., 2008. Monitored natural attenuation of organic contaminants in groundwater: principles and application. *Water Management*, 161(6), 381-392. http://dx.doi.org/10.1680/wama.2008.161.6381

Rivett, M.O., Wealthall, G.P., Dearden, R.A., McAlary, T.A., 2011. Review of unsaturated-zone transport and attenuation of volatile organic compound (VOC) plumes leached from shallow source zones. *J. Contam. Hydrol.*, 123, 130-156. http://dx.doi.org/10.1016/j.jconhyd.2010.12.013

Roggemans, S., Bruce, C.L., Johnson, P.C., Johnson, R.L., 2001. Vadose zone natural attenuation of hydrocarbon vapors: an empirical assessment of soil gas vertical profile data. API Bull. no. 15. http://publications.api.org/

Sale, T., 2001. Methods for determining inputs to environmental petroleum hydrocarbon mobility and recovery models. API Publ. No. 4711. http://publications.api.org/

Scott, K., McInerney, M., 2012. Developing a national guidance framework for Australian remediation and management of site contamination: Review of Australian and international frameworks for remediation. CRC for contamination assessment and remediation of the environment, CRC Care Technical Report No. 22. http://www.crccare.com/publications/technical-reports/technical-reports

Shah, N.W., Thornton, S.F., Bottrell, S.H., Spence, M.J., 2009. Biodegradation potential of MTBE in a fractured chalk aquifer under aerobic conditions in long-term uncontaminated and contaminated aquifer microcosms. *J. Contam. Hydrol.*, 103, 119-133. http://dx.doi.org/10.1016/j.jconhyd.2008.09.022

Sihota, N.J., Singurindy, O., Mayer, K.U., 2011. CO_2-efflux measurements for evaluating source zone natural attenuation rates in a petroleum hydrocarbon contaminated aquifer. *Environ. Sci. Technol.*, 45(2), 482-488. http://dx.doi.org/10.1021/es1032585

Smith, T., Sale, T., Lyverse, M., 2012. Measurement of LNAPL flux using single-well intermittent mixing tracer dilution tests. *Groundwater*, 50, 840-850. http://dx.doi.org/10.1111/j.1745-6584.2012.00931.x

Spence, M.J., Bottrell, S.H., Thornton, S.F., Richnow, H., Spence, K.H., 2005. Hydrochemical and isotopic effects associated with fuel biodegradation pathways in a chalk aquifer. *J. Contam. Hydrol.,* 79, 67-88. http://dx.doi.org/10.1016/j.jconhyd.2005.06.003

TCEQ (Texas Commission on Environmental Quality), 2008. Risk-based NAPL management. TCEQ Regulatory Guidance Remediation Division. RG-366/TRRP-32. http://tceq.texas.gov/publications

Thornton S.F., Bottrell, S.H., Spence, K.H., Pickup, R., Spence, M.J., Shah, N., Mallinson, H.E.H. Richnow, H.H., 2011. Assessment of MTBE biodegradation in contaminated groundwater using 13C and 14C analysis: Field and laboratory microcosm studies. *Applied Geochemistry,* 26(5), 828-837. http://dx.doi.org/10.1016/j.apgeochem.2011.02.004

Thornton, S.F., Quigley, S., Spence, M., Banwart, S.A. Bottrell, S., Lerner, D.N., 2001. Processes controlling the distribution and natural attenuation of dissolved phenolic compounds in a deep sandstone aquifer. *J. Contam. Hydrol.*, 53, 233-267. http://dx.doi.org/10.1016/S0169-7722(01)00168-1

Thornton, S.F., Tobin, K., Smith, J.W.N., 2013. Comparison of constant and transient-source zones on simulated contaminant plume evolution in groundwater: Implications for hydrogeological risk assessment. *Groundwater Monit. R.*, *http://dx.doi.org/10.1111/gwmr.12008*

Tillman, F.D., Weaver, J.W., 2005. Review of recent research on vapor intrusion. USEPA Office of Research and Development, Washington DC, EPA/600/R-05/106. http://www.epa.gov/athens/publications/reports/Weaver600R05106ReviewRecentResearch.pdf

TPHCWG (Total Petroleum Hydrocarbon Criteria Working Group), 1999. Total Petroleum Hydrocarbons Working Group Series, Volumes 1-5. Association for Environmental Health and Sciences. https://www.scribd.com/fullscreen/42789364?access_key=key-29jwkkdylyk663co8v6w

US Army, 2002. Soil vapor extraction and bioventing. Engineering Manual, US Army Corps of Engineers, EM 1110-1-4001 http://140.194.76.129/publications/eng-manuals/index.html

USEPA (United States Environmental Protection Agency), 1988. Guidance for conducting remedial investigations and feasibility studies under CERCLA. EPA/540/G-89/004 http://www.epa.gov/superfund/policy/remedy/sfremedy/rifs/overview.htm

USEPA, 2004a. Performance monitoring of MNA remedies for VOCs in ground water. EPA-600-R-04-027. http://nepis.epa.gov/Adobe/PDF/10004FKY.pdf

USEPA. 2004b. A decision-making framework for cleanup of sites impacted with light non-aqueous phase liquids (LNAPL). EPA-542-R-04-011. EPA Remediation Technologies Development Forum, NAPL Cleanup Alliance. http://clu-in.org/download/rtdf/napl/decisionframework.pdf

USEPA, 2005. Cost and performance report for LNAPL characterization and remediation partition interwell tracer testing (PITT) and rapid optical screening tool (ROSTTM). Characterization and evaluation of the feasibility of surfactant enhanced aquifer remediation (SEAR) at the Chevron Cincinnati Facility, Hooven, OH. EPA 542-R-05-017. http://clu-in.org/download/rtdf/napl/cpchevron.pdf

USEPA, 2009. Underground storage tank program – 25 years of protecting our land and water. EPA-510-B-09-001. http://www.epa.gov/swerust1/pubs/25annrpt.htm

USEPA, 2011. Groundwater road map - Recommended process for restoring contaminated groundwater at Superfund Sites. OSWER 9283.1-34 http://www.epa.gov/superfund/health/conmedia/gwdocs/pdfs/gwroadmapfinal.pdf

USEPA, 2012. Petroleum hydrocarbons and chlorinated hydrocarbons differ in their potential for vapor intrusion. USEPA Office of Underground Storage Tanks, Washington, D.C. http://www.epa.gov/oust/cat/pvi/pvicvi.pdf

USEPA, 2013. Evaluation of empirical data to support soil vapor intrusion screening criteria for petroleum hydrocarbon compounds, EPA-510-R-13-001. http://www.epa.gov/oust/cat/pvi/PVI_Database_Report.pdf

USGS (United States Geological Survey), 1998. Ground water contamination by crude oil near Bemidji, Minnesota. USGS Fact Sheet 084-98. http://mn.water.usgs.gov/projects/bemidji/results/fact-sheet.pdf

Vadas, G.G., MacIntyre, W.G., Burris, D.R., 1991. Aqueous solubility of liquid hydrocarbon mixtures containing dissolved solid components. *Environ. Toxicol. Chem.*, 10(5), 633-639. http://dx.doi.org/10.1002/etc.5620100509

Verginelli, I., Baciocchi, R., 2011. Modeling of vapor intrusion from hydrocarbon-contaminated sources accounting for aerobic and anaerobic biodegradation. *J. Contam. Hydrol.*,126 (3-4),167-180. http://dx.doi.org/10.1016/j.jconhyd.2011.08.010

Wang, Z., Stout, S.A., 2007. Oil spill environmental forensics: Fingerprinting and source identification. Elsevier Inc. Burlington, MA. http://www.sciencedirect.com/science/book/9780123695239

Wealthall, G.P., 2002. Migration of NAPLs in the geosphere: implications for repository performance. BGS Report CR/02/284, available from http://www.nda.gov.uk/documents/biblio/.

Wealthall, G.P., Steele, A., Bloomfield, J.P., Moss, R.H. and Lerner, D.N., 2001. Sediment filled fractures in the Permo-Triassic sandstones of the Cheshire Basin: observations and implications for pollutant transport. *J. Contam. Hydrol.*, 50(1-2): 41-51. http://dx.doi.org/10.1016/S0169-7722(01)00104-8

Wealthall, G.P., Thornton, S.F., Lerner, D.N., 2002. Assessing the transport and fate of MTBE-amended petroleum hydrocarbons in the Chalk aquifer, UK. IAHS Publication, v. 275, p. 205-212.

Werner, D., Höhener, P., 2001. The influence of water table fluctuations on the volatilisation of contaminants from groundwater. In: Natural and enhanced restoration of groundwater pollution. IAHS Publ. 275, 213-218. http://ks360352.kimsufi.com/redbooks/a275/iahs_275_213.pdf

White, R.A., Rivett, M.O., Tellam, J.H., 2008. Paleo-roothole facilitated transport of aromatic hydrocarbons through a Holocene clay bed. *Environ. Sci. Technol.,* 42(19), 7118-7124. http://dx.doi.org/10.1021/es800797u

Wiedemeier, T.H., Rifai, H.S., Newell, C.J., Wilson, J.T., 1999. Natural attenuation of fuels and chlorinated solvents in the subsurface. John Wiley & Sons, Inc., New York. ISBN 0 471 19749 1. http://eu.wiley.com/WileyCDA/WileyTitle/productCd-0471197491.html

Wiedemeier, T.H., Swanson, M.A., Moutoux, D.E., Wilson, J.T., Kampbell, D.H., Hansen, J.E., Haas, P., 1997. Overview of technical protocol for the natural attenuation of chlorinated aliphatic hydrocarbons in ground water under development for the U.S. Air Force Center for Environmental Excellence. Proc. Symposium on Natural Attenuation of Chlorinated Organics in Ground Water, 37-61. U.S. EPA/540/R-97/504.

Wiedemeier, T.H., Wilson, J.T., Kampbell, D.H., Miller, R.N. Hansen, J.E., 1995. Technical protocol for implementing intrinsic remediation with long term monitoring for natural attenuation of fuel contamination dissolved in groundwater. U.S. Air Force Center for Environmental Excellence. http://www.lm.doe.gov/cercla/documents/rockyflats_docs/SW/SW-A-005904.pdf

Wilson, R.D., Thornton, S.F. Mackay, D.M., 2004. Challenges in monitoring the natural attenuation of spatially variable plumes. *Biodegradation* 15, 359-369. http://dx.doi.org/10.1023/B:BIOD.0000044591.45542.a9

Appendix 1. LNAPL penetration below the water table and potential lateral spread

LNAPL during a release will migrate downwards under the influence of gravity and, given sufficient spill volume, will continue to push below the water table, until resisted by buoyancy forces and pore-entry pressures. These will cause the LNAPL to spread laterally until there is a balance of forces. Example scoping calculations of LNAPL penetration depth and potential for lateral spread are provided below to estimate the horizontal and vertical distribution of the LNAPL within (a) porous media and (b) fractured bedrock settings.

a. Porous media

i. Depth of LNAPL penetration below the water table

The depth of LNAPL penetration into a porous media aquifer system is controlled by a balance of forces below the water table. For a continuous leakage release of LNAPL into an unconsolidated unconfined aquifer (or a release of sufficient volume to reach steady state), the maximum LNAPL-penetration depth below the water table occurs at the point where the pressure due to gravitational forces arising from the height of LNAPL release are resisted by the upward buoyancy force of the LNAPL and the force required to enter the pore (i.e., overcome the pore-entry pressure). This can be conservatively estimated from the following:

$$h_p = \frac{\rho_n g h_n - \left(\frac{2\sigma \cos\theta}{r}\right)}{\rho_w g} \qquad \text{Eq. A1.1}$$

where:

- h_p = penetration depth of LNAPL
- h_n = LNAPL height above water table
- ρ_n = density of LNAPL
- ρ_w = density of groundwater
- θ = interface contact angle through the wetting phase
- σ = interfacial tension between LNAPL and water
- r = average pore throat radius
- g = gravitational force

Example: An underground storage tank failed and released a sufficient volume of petrol into the glacio-fluvial sand and gravel aquifer to reach the water table. The unconfined aquifer water table is approximately 10 m below ground surface, with the depth of the leak suspected at 2 m below ground surface. The petrol has a density, viscosity, and interfacial tension of 0.729 g/cm^3, 0.6 cP, and 18 mN/m, respectively. The density of the groundwater was measured as 0.998 g/cm^3. The pore throat radius is assumed to be an average of 100 µm, with an advancing contact angle of 30 degrees:

The depth of LNAPL penetration is 5.82 m as calculated below (noting unit conversions to achieve consistency in units):

$$h_p = \frac{729\,\frac{kg}{m^3} \times 9.81\,\frac{m}{s^2} \times (10\text{ m} - 2\text{ m}) - \left(\frac{2 \times 0.018\,\frac{N}{m} \times \cos 30^o}{100\ \mu m \times 10^{-6}} \right)}{998\,\frac{kg}{m^2} \times 9.81\,\frac{m}{s^2}} = 5.82\text{ m}$$

ii. Lateral spread

LNAPL will continue to spread laterally during a continuous release or a release of sufficient volume adding to the LNAPL body to exceed laterally confining forces. If no more LNAPL is being released, the LNAPL will eventually come to a quasi-static equilibrium position. LNAPL thicknesses within monitoring wells can be used to understand the potential for LNAPL to continue to spread laterally. A critical thickness is the minimum LNAPL thickness in a well before it can move in the ground, and if the thickness is greater the LNAPL has sufficient drive to exceed the confining pressures, which is defined as follows: (modified from Charbeneau *et al*., 1999):

$$h_{n,\,critical} = \left(\frac{\sigma_{nw}}{1 - \frac{\rho_n}{\rho_w}} - \frac{\sigma_{an}}{\frac{\rho_n}{\rho_w}} \right) \frac{h_d}{\sigma_{aw}} \qquad \text{Eq. A1.2}$$

where:

$h_{n,critical}$ = thickness of LNAPL in a well to exceed pore entry pressure
σ_{nw} = interfacial tension between LNAPL and groundwater
σ_{an} = surface tension of LNAPL
σ_{aw} = surface tension of groundwater
ρ_n = density of LNAPL
ρ_w = density of groundwater
h_d = displacement pressure head (i.e., height of capillary fringe)

The flow of fluids within the subsurface porous media is based upon Darcy's Law for each individual fluid, with LNAPL as follows:

$$q_n = K_n i_n \qquad \text{Eq. A1.3}$$

where:

q_n = Darcy flux for LNAPL
K_n = LNAPL hydraulic conductivity
i_n = LNAPL gradient

The LNAPL gradient (i_n) will vary significantly during a release and will be typically steeper than the gradient of the groundwater surface. The LNAPL gradient will be pseudo radial from where the release point connects with the aquifer. Over time, the LNAPL gradient will become closer to that of groundwater. At the early stages of LNAPL release the LNAPL will mound on the water table, and as the LNAPL spreads the slope of the mound also decreases and approaches the same gradient of the water table.

The hydraulic conductivity of the LNAPL is based upon an understanding of the groundwater hydraulic conductivity. The addition of LNAPL causes an interplay of the two fluids which causes the permeability relative to each fluid to be reduced due to the presence of the other

fluid. The greater the quantity (saturation), the lower the LNAPL conductivity (and vice versa). The LNAPL hydraulic conductivity is calculated as follows:

$$K_n = K_{w,sat} \frac{\rho_n}{\rho_w} \frac{\mu_w}{\mu_n} k_{rn} \qquad \text{Eq. A1.4}$$

where:

K_n = LNAPL hydraulic conductivity
$K_{w,sat}$ = Groundwater hydraulic conductivity for fully saturated condition
ρ_n = density of LNAPL
ρ_w = density of water
μ_n = dynamic viscosity of LNAPL
μ_w = dynamic viscosity of groundwater
k_{rn} = LNAPL relative permeability

Thus the ability of LNAPL to flow (q_n) and migrate is directly proportional to the amount of LNAPL present as this will increase the LNAPL relative permeability, and the heavier the LNAPL the higher the LNAPL conductivity, whereas the more viscous the LNAPL the less the propensity for the LNAPL to flow and be mobile. The velocity of the LNAPL is derived from Darcy's flux but accounts for the effective porosity as follows:

$$v_n = \frac{q_n}{\varphi_{eff}} = \frac{q_n}{\varphi S_n} \qquad \text{Eq. A1.5}$$

where:

v_n = velocity of LNAPL
q_n = Darcy flux for LNAPL
φ_{eff} = effective soil porosity
φ = total soil porosity
S_n = LNAPL saturation of pore space

LNAPL mobility should be evaluated using a lines of evidence approach including, but not limited to, stability of the areal extent of the LNAPL body, stability or shrinking of the resulting dissolved-phase groundwater plume concentrations from a LNAPL body, reduction in LNAPL recovery rates, low LNAPL transmissivity, low LNAPL saturation levels based upon laboratory testing of saturation levels and flushing methods (i.e., centrifuge or water flood) that do not see a reduction in LNAPL saturation, and very low LNAPL velocity.

Example: A large release of toluene from a chemical manufacture facility above ground tank (ground surface of 25 m above mean sea level) has occurred and the resulting LNAPL body has migrated through the partially saturated zone, penetrated the water table and has continued to spread laterally within the porous media aquifer unit. In two down-gradient wells, 100 cm of LNAPL has been measured in the well near the release (Well 1), and 60 cm in the well 12 m down-gradient (Well 2) with depth to LNAPL elevations of 5 m and 5.5 m, respectively. Confirm if the LNAPL is still migrating and at what rate within the fine sand unconsolidated aquifer with a groundwater hydraulic conductivity of 10^{-2} cm/s, 40-percent porosity, 40 cm capillary fringe. The elevation of the top of LNAPL in Well 1 and Well 2 were measured as 5.5 m and 5.4 m above mean sea level, respectively.

The density, viscosity, surface tension, and interfacial tension for toluene were measured as 866.7 kg/m^3, 0.590 cP, 28.5 mN/m, and 18.0 mN/m, respectively. The density, viscosity and surface tension of water was measured as 998 kg/m^3, 1.002 cP, and 72.8 mN/m. Based upon analysis of soil results for total recoverable petroleum hydrocarbons, a maximum LNAPL saturation was calculated as 30% of pore space, with an estimated LNAPL relative permeability of 0.1. [Note, 1 cP = 0.001 N s/m^2 = 0.001 Pa s]

The critical thickness to indicate if the LNAPL body still has the potential to migrate is as follows:

$$h_{n,\,critical}=\left(\frac{0.018\frac{\mathrm{N}}{\mathrm{m}}-\frac{0.0285\frac{\mathrm{N}}{\mathrm{m}}}{\frac{866.7\frac{\mathrm{kg}}{\mathrm{m}^3}}{998\frac{\mathrm{kg}}{\mathrm{m}^3}}}}{1-\frac{866.7\frac{\mathrm{kg}}{\mathrm{m}^3}}{998\frac{\mathrm{kg}}{\mathrm{m}^3}}}\right)\frac{0.4\ \mathrm{m}}{0.0728\frac{\mathrm{N}}{\mathrm{m}}}=0.571\ \mathrm{m}=57.1\ \mathrm{cm}\ll 60\ \mathrm{cm}$$

Therefore, the down gradient Well 2 has a measurable thickness greater than the critical thickness indicating that the LNAPL may still be migrating; however, other lines of evidence should also be used. Given the LNAPL is potentially migrating, an estimate of the rate of migration is provided by:

$$v_n=\frac{q_n}{\varphi S_n}=\frac{K_n i_n}{\varphi S_n}=\frac{\left(K_{w,sat}\frac{\rho_n}{\rho_w}\frac{\mu_w}{\mu_n}k_{rn}\right)i_n}{\varphi S_n}$$

$$v_n=\frac{\left(0.0001\frac{\mathrm{m}}{\mathrm{s}}\times\frac{866.7\frac{\mathrm{kg}}{\mathrm{m}^3}}{998\frac{\mathrm{kg}}{\mathrm{m}^3}}\times\frac{0.590\mathrm{x}10^{-3}\ \frac{\mathrm{N\cdot s}}{\mathrm{m}^2}}{1.002\mathrm{x}10^{-3}\frac{\mathrm{N\cdot s}}{\mathrm{m}^2}}\times 0.1\right)\times\left(\frac{5.5\ \mathrm{m}-5.4\ \mathrm{m}}{12\ \mathrm{m}}\right)}{0.40\times 0.30}=3.551\mathrm{x}10^{-7}\frac{\mathrm{m}}{\mathrm{s}}$$

Therefore the velocity of the LNAPL is moving at 11.2 m per year in the down-gradient direction from Well 2. This is the measure at this current moment in time. As the LNAPL continues to migrate laterally, the LNAPL gradient will become progressively less steep and thus the lateral flow velocity of the LNAPL will likewise decline with time.

b. Fractured bedrock

i. Depth of LNAPL penetration below the water table

As presented on Figure 3.8, the depth of LNAPL within a fractured-bedrock setting (where fracture transport of the LNAPL is dominant compared to the matrix) is similarly based upon a balance of forces as within the porous media unconsolidated aquifer examples above and can be estimated from the following:

$$h_p=\frac{\rho_n g h_n-\left(\frac{2\sigma\cos\theta}{b}\right)}{\rho_w g}$$ Eq. A1.6

where:

h_p = penetration depth of LNAPL below the water table

h_n = LNAPL height above water table

ρ_n = density of LNAPL
ρ_w = density of water
θ = interface contact angle through the wetting phase
σ = interfacial tension between LNAPL and water
b = aperture thickness
g = gravitational force

Example: A diesel fuel was released of sufficient volume to migrate through the fractured granite to the water table and continue to cause lateral spread of LNAPL. The source of the release was believed to be from a pipe in the subsurface 5 m above the water table. The diesel has a density of 824.5 kg/m^3, interfacial tension for LNAPL and water of 29.4 mN/m, and a contact angle of 10^o of the advancing LNAPL. The granite has an average aperture thickness of 5 microns (µm). This equates to a penetration of approximately 2.94 m as calculated below.

$$h_p = \frac{824.5\,\frac{\text{kg}}{\text{m}^3} \times 9.81\,\frac{\text{m}}{\text{s}^2} \times 5\text{ m} - \left(\frac{2 \times 0.0294\,\frac{\text{N}}{\text{m}} \times \cos 10^o}{5\ \mu\text{m} \times 10^{-6}}\right)}{1000\,\frac{\text{kg}}{\text{m}^3} \times 9.81\,\frac{\text{m}}{\text{s}^2}} = 2.94\text{ m}$$

ii. Lateral spread

LNAPL within fractured rock can continue to spread laterally with fluctuating water table elevations within the fracture network. The flow of LNAPL will depend upon if the water table is rising or falling, and the size and orientation (i.e., dip) of the fractures, as well as the permeability of the matrix. In the fractured aquifer case, LNAPL can also become trapped below the water table, and during a subsequent change in water table elevation this water will add to the hydrodynamic pressure. In the case of the falling and rising water table, the balance of hydrodynamic, buoyancy and pore entry pressure is expressed as follows (Hardisty *et al.,* 1994):

Falling water table: $P_n = P_e + P_b$ Eq. A1.7

Rising water table: $P_n = P_e - P_b$ Eq. A1.8

where:
P_n = hydrodynamic pressure of LNAPL
P_e = pore entry pressure
P_b = buoyancy pressure

When expanded, the critical hydrodynamic pressures of LNAPL for lateral up-dip and down-dip flow of trapped LNAPL are expressed as follows:

Falling water table:

$$h_{n,\,critical} = \frac{2\sigma_{nw}\cos\theta\left(\frac{1}{b_2} - \frac{1}{b_1}\right) + Lg(\rho_w - \rho_n)\sin\omega}{(\rho_w - \rho_n)g}$$ Eq. A1.9

Rising water table:

$$h_{n,\,critical} = \frac{2\sigma_{nw}\cos\theta\left(\frac{1}{b_2} - \frac{1}{b_1}\right) - Lg(\rho_w - \rho_n)\sin\omega}{(\rho_w - \rho_n)g}$$ Eq. A1.10

where:

$h_{n,critical}$ = critical LNAPL thickness as observed in well
σ_{nw} = interfacial tension between LNAPL and groundwater
b_1 = aperture of fracture with LNAPL
b_2 = aperture of fracture to be invaded
L = length of trapped LNAPL within fracture
ρ_n = density of LNAPL
ρ_w = density of water
ω = fracture dip angle

The fracture will have a width known as the aperture (b), and a tilt relative to horizontal which is commonly referred to as the dip angle (ω).

Example: A release of petrol (interfacial tension of 18 mN/m; density of 729 kg/m^3; viscosity of 0.6 cP; contact angle of 30^o) occurred into a chalk aquifer (dip angle of ~35^o, fracture aperture size of ~100 µm) of sufficient volume that the LNAPL is likely still migrating laterally. The water table within the chalk has historically been measured to fluctuate up to 5 m each season. The footprint area of the LNAPL based upon the last round of gauging was approximately 20 m^2 in a near radial distribution, with LNAPL thickness observed within the down-gradient direction of 2 m during a low water table condition and 0.2 m during the water table high. The calculation below aims to confirm if the LNAPL is still moving laterally, as the aperture size continues to decrease laterally (aperture size ~50 µm). The calculation assumes a groundwater density at 15^{o}C of 999.1 kg/m^3. A fracture-based calculation is appropriate as the chalk matrix pores are sub-micron sized and LNAPL transport will be restricted to the fractures.

The critical LNAPL thickness necessary for continued lateral flow would be as follows for the falling and rising water table condition:

Length of LNAPL is the diameter of the circular LNAPL body: $L = 2\sqrt{\frac{20\text{m}^2}{\pi}} = 5.05\text{m}$

Falling head condition:

$$h_{n,\ critical} = \frac{2\times 0.018\frac{\text{N}}{\text{m}}\times\cos 30^o\left(\frac{1}{50\text{x}10^{-6}\text{m}}-\frac{1}{100\text{x}10^{-6}\text{m}}\right)+5.05\text{m}\times 9.81\frac{\text{m}}{\text{s}^2}\times\left(999.1\frac{\text{kg}}{\text{m}^3}-729\frac{\text{kg}}{\text{m}^3}\right)\sin 35^o}{\left(999.1\frac{\text{kg}}{\text{m}^3}-729\frac{\text{kg}}{\text{m}^3}\right)\times 9.81\frac{\text{m}}{\text{s}^2}}$$

$h_{n,critical}$ = 3.01 m > 0.2 m; therefore not migrating during falling head.

Rising head condition:

$$h_{n,critical} = \frac{2\times 0.018\frac{\text{N}}{\text{m}}\times\cos 30^o\left(\frac{1}{50\text{x}10^{-6}\text{m}}-\frac{1}{100\text{x}10^{-6}\text{m}}\right)-5.05\text{m}\times 9.81\frac{\text{m}}{\text{s}^2}\times\left(999.1\frac{\text{kg}}{\text{m}^3}-729\frac{\text{kg}}{\text{m}^3}\right)\sin 35^o}{\left(999.1\frac{\text{kg}}{\text{m}^3}-729\frac{\text{kg}}{\text{m}^3}\right)\times 9.81\frac{\text{m}}{\text{s}^2}}$$

$h_{n,critical}$ = -2.78 m < 0 m < 2 m; therefore potentially migrating during rising head.

A negative value of $h_{n,critical}$ indicates that the LNAPL will migrate upwards in this fractured rock environment and the LNAPL will migrate during a rising head condition.

Appendix 2. Estimation of vapour-phase mass flux in the partially saturated (vadose) zone due to volatilisation

The mass flux (loss) of VOCs due to volatilisation of LNAPL components can be estimated using Fick's Law for steady-state vapour diffusion (Huntley and Beckett, 2002):

$$J_v = -D_e \, dC/dZ \qquad \text{Eq. A2.1}$$

where J_v is the vapour flux from the top of the LNAPL source at depth (e.g., on a water table) to ground surface (units of mass/area/time), D_e is the effective vapour diffusion coefficient, and dC/dZ is the vapour concentration gradient. The vapour-phase concentration of component i in the LNAPL is estimated using Raoult's Law (assuming the ideal gas law applies):

$$C_{veff} = X_i \, P_i^o \, M_i / RT \qquad \text{Eq. A2.2}$$

where C_{veff} is the effective vapour concentration (mg/L) for mole fraction X_i in the LNAPL, P_i^o is the pure phase vapour pressure of that component, M_i is the molar mass of the pure component, R is the ideal gas constant, and T is temperature (K). Concentration at ground surface is assumed to be zero (although biodegradation often decreases the vapour-phase concentration to zero below ground surface). The air diffusion coefficient can be approximated by the Millington-Quirk relationship:

$$D_e = D_a \theta_\alpha^{3.33} / \theta_t^2 \qquad \text{Eq. A2.3}$$

where D_a is the free-air diffusion coefficient, θ_α is the air-filled porosity, and θ_t is the total porosity. The effective vapour diffusion coefficient is a function of the air-filled porosity, which varies with LNAPL and water saturation; D_e therefore varies with height above the LNAPL. An average vertical effective vapour diffusion coefficient is therefore used. This coefficient can be calculated similarly to the average vertical hydraulic conductivity of a vertically stratified sediment:

$$D_e = \frac{\sum Z_i}{\sum Z_i / D_i} \qquad \text{Eq. A2.4}$$

where D_i is the diffusion coefficient of the i^{th} interval above the top of the LNAPL and Z_i is the thickness of the i^{th} interval. The use of an average effective vapour diffusion coefficient, calculated as above, conserves mass by maintaining a constant vapour flux over the vertical interval.

Example: The following calculation illustrates the use of the above equations to estimate the vapour-phase diffusive mass flux of hydrocarbon compounds to the ground surface from a LNAPL petrol fuel source at the water table. Benzene is used as a model compound, the parameter values taken from fuel release sites and the literature (Table A2.1) and the calculation performed for an ambient temperature of 20°C and partially saturated (vadose) zone thickness of 3 m.

Table A2.1. Parameter values used for example calculation of vapour-phase mass flux.

Parameter	Description	Units	Value
$D_{free\ oxygen}$	Free diffusion coefficient of oxygen in air	m^2/sec	2.01 x 10^{-5}
$D_{free\ benzene}$	Free diffusion coefficient of benzene in air	m^2/sec	8.68 x 10^{-6}
θ_t	Total porosity of vadose zone media	fraction	0.51
θ_α	Air-filled porosity of vadose zone media	fraction	0.34
$X_{benzene}$	Mole fraction of benzene in LNAPL	unitless	0.005
$P_{benzene}$	Pure phase vapour pressure of benzene	mm Hg	76
$M_{benzene}$	Molar mass of benzene	g/mol	78.11
R	Ideal gas constant	atm.L/mol.K	8.21 x 10^{-2}

In Eq. A2.2 the pure phase vapour pressure of benzene must be converted into atmospheres. This is done knowing that 1 atmosphere has a pressure of 760 mm Hg. The temperature in Kelvin (K), corresponding to 20°C, is 293.15. Therefore from Eq. A2.2:

$$C_{veff\ benzene} = 0.005 \times 76\ \text{mmHg} \times \frac{1\ \text{atm.}}{760\ \text{mmHg}} \times 78.11 \frac{\text{g}}{\text{mol}} \times \frac{1}{8.21 \times 10^2} \frac{\text{mol.K}}{\text{atm.L}} \times \frac{1}{293.15\text{K}} \times 1000 \frac{\text{mg}}{\text{g}}$$

$C_{veff\ benzene}$ = 1.62 mg/L

From Equation A2.3

$$D_{e\ benzene} = 8.68 \times 10^{-6} \frac{\text{m}^2}{\text{s}} \times \frac{0.34^{3.33}}{0.51^2}$$

$D_{e\ benzene}$ = 9.15 x 10^{-7} m^2/s

Substituting in Equation A2.1, with a vadose zone thickness, z, of 3 m and assuming concentration at ground surface is zero gives:

$$J_{v\ benzene} = 9.15 \times 10^{-7} \frac{\text{m}^2}{\text{s}} \times 1.62 \frac{\text{mg}}{\text{L}} \times \frac{1}{3\text{m}} \times \frac{1000\text{L}}{\text{m}^3}$$

$J_{v\ benzene}$ = 4.94 x 10^{-4} mg/m^2/s

or, 42.7 mg/m^2/day

Appendix 3. Estimation of subsurface oxygen penetration for vapour plume aerobic biodegradation

Davis *et al.* (2009) present a simple model to estimate subsurface oxygen penetration for aerobic biodegradation of vapour-plume contaminants. The model balances oxygen diffusion into a soil profile open at ground level with the efflux of LNAPL vapours. It can be used to predict the oxygen migration into the subsurface and the zone of expected aerobic biodegradation near a building.

Consider: (i) steady-state vapour diffusion from a constant concentration source $C_{vap,max}$ at a depth $z = L_{max}$ at the base of a soil profile; and, (ii) oxygen diffusion from a constant maximum concentration $C_{oxygen,max}$ at the ground surface, $z = 0$. It is assumed that the vapours react (biodegrade aerobically) instantaneously with the oxygen at the depth $z = L$ and decrease to zero at this point. For these assumptions the equations for oxygen, $C_{O2}(z)$, and vapour, $C_{vap}(z)$, concentrations are:

$$C_{O2}(z) = C_{O2,max}\,(1\text{-}z/L) \qquad \text{Eq. A3.1}$$

$$C_{vap}(z) = C_{vap,max}\,[1\text{-}(L_{max}\text{-}z)/(L_{max}\text{-}L)] \qquad \text{Eq. A3.2}$$

Balancing the steady-state fluxes (Fick's Law – Eq. A2.1 in Appendix 2) at $z = L$ gives:

$$D_{O2}\,.\,C_{O2,max}/L = \gamma D_{vap}\,.\,C_{vap,max}/(L_{max}\text{-}L) \qquad \text{Eq. A3.3}$$

Where D_{O2} is the effective oxygen diffusion coefficient, D_{vap} is the effective vapour diffusion coefficient and γ is the stoichiometric mass of oxygen consumed per mass of vapour-phase organic chemical aerobically consumed. Rearranging gives:

$$L = L_{max}/(1+1/\eta) \qquad \text{Eq. A3.4}$$

where $\eta = D_{O2}\,.\,C_{O2,max}/(\gamma D_{vap}\,.\,C_{vap,max})$ measures the undersupply of oxygen flux (η <1, $L/L_{max} \rightarrow 0$), or oversupply of oxygen flux ($\eta > 1$, $L/L_{max} \rightarrow 1$), with respect to the vapour-phase flux.

The model only requires *a priori* knowledge of the maximum oxygen and vapour-phase contaminant concentration, their diffusion coefficients and the biodegradation reaction stoichiometry. $C_{vap,max}$ can be obtained directly from field gas measurements or partitioning calculations.

Example: The following calculation illustrates the use of the equations above to estimate the penetration of oxygen into the subsurface for aerobic biodegradation of hydrocarbon vapours originating from a LNAPL petrol fuel source at the water table. The example uses relevant results and equations from the calculation completed in Appendix 2. The calculation is done for an ambient temperature of 20°C and vadose zone thickness (L_{max}) of 3 m. A value of 279 mg/L is used for $C_{O2,max}$ and 19 mg/L for the concentration of TPH (Davis *et al.,* 2009), which represents $C_{vap\,max}$. The corresponding free diffusion coefficient for the vapour-phase hydrocarbons is 8.0 x 10^{-6} m^2/sec (Davis *et al.,* 2009). Following Eq. A2.3 and using the same values for θ_t and θ_α, the effective diffusion coefficients for oxygen and the hydrocarbons are calculated to be 2.11 x 10^{-6} m^2/sec and 8.44 x 10^{-7} m^2/sec, respectively.

From Eq. A3.4:

$$\eta = 2.11\times10^{-6}\,\frac{m^2}{sec}\times279\,\frac{mg}{L} / \left(3.46\times8.44\times10^{-7}\,\frac{m^2}{sec}\times19\,\frac{mg}{L}\right)$$

$\eta = 10.61$

In the above equation, the stoichiometric coefficient of 3.46 is the mass of oxygen consumed per unit mass of benzene consumed by aerobic biodegradation, according to the reaction:

$C_6H_6 + 7.5O_2 = 6CO_2 + 3H_2O$

where 270 g of oxygen are required to biodegrade 78 g of benzene, i.e., 270/78 = 3.46. This is specific for aerobic biodegradation of benzene and is used for illustration. An approximate value of this coefficient for aerobic biodegradation of TPH is 3.5.

Substituting relevant terms in Eq. A3.4 gives

$$L = 3\text{ m} / \left[1+\left(\frac{1}{10.61}\right)\right]$$

$L = 2.74$ m

Hence, under these conditions the penetration of air into the vadose zone restricts the vertical migration of the vapour plume, by aerobic biodegradation, to 2.74 m below ground level, i.e., the vapour plume migrates only 26 cm from the water table. The positive value of η and ratio of 0.91 for L/L_{max} indicates that the supply of oxygen into the vadose zone is in excess of that required for aerobic biodegradation of the hydrocarbons.